FUNDAMENTAL STUDY OF THE BREAKAGE CHARACTERISTICS OF SILICA BED PARTICLES UNDER MULTIPLE IMPACTS

DONALD TSHIDISO LEGODI

A dissertation submitted to the Faculty of Engineering and the Built Environment, University of the Witwatersrand, Johannesburg, in fulfillment of the requirements for the degree of Master of Science.

Johannesburg, 2012

DECLARATION

I declare that this thesis is my own, unaided work, unless otherwise stated. It is being submitted for the degree of Master of Science in the University of the Witwatersrand, Johannesburg. It has not been submitted before for any degree or examination in any other University.

_____

Donald Tshidiso Legodi

_____ day of _____ 2012

ABSTRACT

Fundamental tools of breakage were applied to investigate the breakage behaviour of a bed of silica particles which were subjected to multiple impacts. Experiments aimed at determining the effect of the grinding media diameter, drop height, bed height, input energy and specific energy on the resultant particle size distributions (PSDs) were performed using drop tests. The Attainable Region analysis tool was applied to determine the optimum production of an intermediate size class. In this context the AR is used more like a maximizing yield tool, as the goal is to determine the operating conditions that produce the most of an intermediate sized product, and mixing does not offer any advantage to milling alone. It was shown that different grinding media diameters produce different PSDs. The results show that there is a minimum amount of impact energy that needs to be reached in order for breakage to occur and an optimum impact energy in order to avoid overbreakage. It was proved that the specific energy is an extremely valuable parameter in analysing the breakage process and that for the same energy intensity, the resultant PSD is different. The results suggest that in a ball mill, one needs to use large grinding media (30 mm) and small grinding media (10 mm) in order to obtain more breakage and production of fines, respectively.

DEDICATION

In Memory of my late

Grandfather Jacob Thobane Legodi and Uncle Lesiba Michael Legodi.

ACKNOWLEDGEMENTS

I would like to express gratitude to my supervisors, Professor Diane Hildebrandt and Professor David Glasser for their motivation and guidance over the past two years. Their encouragement, advice, insight and creativity have been invaluable. I am indebted to both of them for all their contributions to my studies and beyond. I would also like to thank everyone at the COMPS group.

I would also like to express my gratitude to all my colleagues, especially all the guys in COMPS Post Grad Offices (RW 309) for their support, pleasant conversations and for making the last two year so memorable.

I want to acknowledge the contributions and involvement Matt Metzger. He provided the motivation for this project but gave me complete liberty in developing, and executing, my research approach. He provided constant support along the way and was always available as a sounding board for ideas and suggestions.

To my family; especially my grandmother, my mother; I am grateful for their unconditional support and help throughout the years. I would also like to thank my friends (and fellow chemical engineers): Rhulani, Leonard, Thabo and Fulufhelo; it has been a pleasure sharing these last few years of campus with all of you. Special thanks to Makgotso for being there for me in this journey.

I acknowledge the financial assistance from COMPS, NRF, and the University of the Witwatersrand.

Above all, I thank the Lord Almighty for his grace, love and mercy.

TABLE OF CONTENTS

LIST OF FIGURES

LIST OF TABLES

CHAPTER 1

1 INTRODUCTION

1.1 INTRODUCTION

Comminution is a process carried out either on dry materials or slurries where by a material is gradually reduced in size to produce material of the desired size class. This can be done to free the freshly excavated material from gangue material; here a large surface area is generated to enable the successful leaching of the impurities. Crushing and grinding are the chief processes carried out in comminution where ball mill grinding has found industrial preference over the years. “Comminution theory is concerned with the relationship between energy input and the particle size made from the given feed size and all the comminution theories assume that the material is brittle, so that no energy is adsorbed in processes such as elongation or contraction which is not finally utilised in breakage.” (Wills et al., 2006).

The greatest challenge in comminution is the optimization of the energy input to the crushing and grinding machines, where it has been observed that only a small percentage of the total energy input really does the breaking while the rest is consumed by the machine concerned and lost to contacts that do not result in breakage. The optimization part enters the picture in trying to specify the conditions to ensure a minimum energy use for achieving desired size class (Austin et al., 1984).

Drop weight test have been used by previous researchers to investigate the breakage characteristics of single particles. However, most industrial mills contain many particles, and thus breakage normally occurs on a bed of particles, not a single particle. Therefore, the aim of this research is to investigate breakage characteristics of a bed of particles under multiple impacts.

1.2 AIM OF THE STUDY

This research aims at determining the breakage characteristics of silica bed particles subjected under multiple impacts. The Attainable Region (AR) tool is then used to optimize mass fraction of size class two for a minimal energy input.

1.3 THESIS OUTLINE

Chapter 2

This chapter explains the literature survey that was used as a background for this thesis.

Chapter 3

This chapter provides an overview of the experimental apparatus that was used to obtain data.

Chapter 4

The key issue emphasized in this chapter is the results obtained based on the experimental work.

Chapter 5

This chapter includes the discussion and interpretation of the results.

Chapter 6

The chapter concludes the thesis by summarizing the conclusions drawn from chapter 4 and 5.

Chapter 7

In this chapter, further work and possible areas of future research to study are proposed.

Chapter 8

This chapter provides references that were cited in the thesis.

Chapter 9

This chapter provides raw experimental data and additional results which were not presented in the results section.

CHAPTER 2

2 LITERATURE REVIEW

Comminution is any process where particles are crushed, ground, or otherwise broken to reduce their particle size. Crushing and grinding of various feedstocks is a critical operation in mining, as well as in a range of other industries. It is necessary to liberate valuable minerals from waste constituents so that they can be separated, and for producing products with the correct particle sizes for use. However, comminution is both energy-intensive and expensive, with tremendous room for improvement.

Crushing and grinding are the chief processes carried out in comminution where ball mill grinding has found industrial preference over the years. “Comminution theory is concerned with the relationship between energy input and the particle size made from the given feed size and all the comminution theories assume that the material is brittle, so that no energy is adsorbed in processes such as elongation or contraction which is not finally utilised in breakage.” (Wills et al., 2006). The greatest challenge in comminution is the optimization of the energy input to the crushing and grinding machines, where it has been observed that only a small percentage of the total energy in put really does the breaking while the rest is consumed by the machine concerned. The optimization part enters the picture in trying to specify the conditions to ensure a minimum energy use for achieving desired size class (Austin et al., 1984).

Grinding is an energy intensive operation with some of the energy being lost in the form of heat, sound, and friction in the bearings, particle to particle interactions and ball to ball interactions. “It has been estimated that 1.5 % of electrical energy in USA is consumed in comminution processes while in mineral processing plants 30-50% of power draw is used by comminution (and for hard ores up to 70 %)” (Remes et al., 2007). Grinding is the last stage of comminution after crushing, often carried in tumbling ball mills following their affordability, controllably, reliability, etc (Austin., 1984).

Another important aspect of comminution is that particles of the correct size distribution must be produced in the comminution process. Pulverized coal fired into large steam generators burns satisfactory when it is mainly less than 75μm and contains no more than 5% weight greater than 300 μm (Austin et al., 1984). Both undersized as well as oversized particles may lead to losses in the recovery efficiency of downstream extraction processes, in industries such as classification, flotation and gravity concentration just to mention a few. As a result, the control of the particle size distribution (PSD) from a comminution process is very important.

For the coarser material breakage is assumed to be a combination of chipping, abrasion and self-breakage. The term self-breakage is used loosely and refers to breakage that occurs when a falling big rock breaks due its own weight (Bwalya 2005). Milling is believed to be a combination of abrasion and fracture. Three size reduction mechanisms as identified by Austin et al., (1984) are; disintegrative fracture, chipping of fragments from the surface and abrasion. Abrasion can be assumed to be the dominant mechanism for larger particles which is normally preceded by a short period of chipping while the rough edges get smoothed off. Disintegrative fracture refers to breakage resulting from the propagation of cracks within the body of the particle Bwalya (2005).

In his 2005 thesis, Bwalya performed drop weight test experiments to establish the relationship between energy input and probability of fracture. It was found that both the number of impacts and the energy input have an effect on the probability of breakage. It was then concluded that when the energy input is low, each extra impact steadily increased the probability of breakage while for the higher energy inputs, the change in probability is substantial for the first few attempts before asymptoting.

The amount of powder fed in a ball mill has a significant effect on the grindability of the material, hence the power consumed. Filling the mill with less powder can cause an increase in ball to ball interactions resulting in low breakage rates whereas filling the mill with more powder might cause cushioning, also resulting in a decrease in breakage rates. This has influenced much research to find a suitable fractional fill so as to avoid the mentioned setbacks. N.S Lamesck et al. (2006) did another study on the effects of media shape milling kinetics on quartz where spherical balls and worn balls were used. It was found that for the two media shapes, breakage followed a first order behaviour. The findings showed that

breakage rate is directly proportional to the particle size and the breakage rate is inversely proportional to the fractional filling.

Bwalya (2005) also performed experiments to determine the effect of specific energy on the product size distribution where two different size fractions were subject to impacts. It was shown that the higher the energy input the finer the product. However, to achieve the similar levels of size reduction, the finer sample required higher specific energy. Sahoo et al (2004) measured the breakage characteristics of coal at different specific comminution energy levels. The breakage products of coal particles revealed that the fineness of the products increases with the specific comminution energy.

Kelly et al., (1990) state that there have been a number of papers which have described fracture in terms of mechanisms such as cleavage, shatter, abrasion, and chipping. Interpretation of this work is complicated by two factors; different authors have used different terms for what may be the same mechanism, but, more significantly, some have been considering single fracture events, while others were considering multi-fracture events. Kelly et al., (1990) introduced the concept that the fracture mechanism, and the resulting size distribution, were dependent on the energy intensity applied to the particle.

The other factor of significance regarding energy intensity is the rate at which the energy is applied (which must of course be dependent on particle size). If the energy is applied slowly to a single (relatively large) particle, then primary facture can occur just after the weakest flaw is overloaded. The resulting fracture will cause unloading of the product particles, and the size distribution will be a few particles of size close to that of the original particle. Such fracture is best described as *cleavage. (Chipping* can then be thought of as a special case of cleavage whereby a relatively small piece is cleaved off the particle, leaving a particle of essentially the original size.) (Kelly et al., 1990).

Particle size analysis plays a critical role in evaluating the grindabilty of the machine and the extent of grinding sustained by the material. There are several methods of particle size analysis i.e. test sieving covering particle size range of 100 000 - 10 µm, elutriation with 40 - 5 µm range, microscopy (optical) methods with range of 50 - 0.25 µm, sedimentation (gravity) covering range of 40 - 1µm, sedimentation (centrifugal) covering range of 5 - 0.05 µm and electron microscopy covering range of 1 - 0.005 µm. Test sieving is the widely used

method for particle size analysis due to its simplicity, cheapness and ease of interpretation (Wills et al., 2006). The effectiveness of the sieving test depends on the amount of the sample to be sieved and the amount of movement imposed on the sample by the shaker. The challenge concerned with the method is the irregularity of particles and the obstruction of the sieve apertures by the particles. The technique is time consuming and this has led to the adoption of the laser diffraction technique by some researchers when analysing the particle sizes. Laser diffraction is a particle sizing technique where light scattering behaviour of particles is predicted while the quality of this prediction determines the accuracy of the particle size analysis.

Austin et al., (1984) did a study on the effects of ball size and particle size on the specific rate of breakage for dry grinding of quartz where he discovered that the breakage rate increases with increased particle size for a given ball size, which can be attributed to the collision spaces between the balls being filled with the material (V. Deniz et al 2002) while specific rate of breakage increases with decrease in ball size for a given feed size. Austin's findings were supported by Bozkurt et al., (2007) where dry grinding kinetics of colemanite was studied in a stainless steel laboratory ball mill. The results showed that as the colemanite feed particle size increased, there was an increase in the specific rate of breakage with quartz breaking slower than colemanite when compared under the same experimental conditions in terms of the specific rate of breakage. Investigations published (Stehr, 1988; Mankosaet al., 1986; Stadler et al., 1990; Bunge, 1992; Bunge and Schwedes, 1990; Thiel and Schwedes, 1990) show that besides the specific energy input the size of grinding media greatly affects the product fineness.

A study was done for fine grinding in a horizontal ball mill where the aim was to study the effect of ball size on the feed and product size distributions. It was discovered that small balls are most suited for fine feeds, while larger balls are suited for coarse feeds. The smaller media sizes were very ineffective and inefficient for grinding of the coarse feeds (Yan et al., 2006). Yashima (1986) investigated the relationships between particle size and fracture energy required to fracture as estimated from single particle crushing. The results found support most researcher's findings that the specific fracture energy is a function of particle size where it increases with decrease in particle size and it was observed with natural materials that when the particle size was less than 500 μm the specific fracture energy

increased quickly, which meant that larger amounts of energy are necessary for fine grinding or ultra-fine grinding.

An understanding of single particle fracture, which is the fundamental process of comminution, is of great benefit. Additionally it provides a means to separate a material's fracture behaviour from the operating conditions of comminution machines. Impact tests on single particles and/or particle populations are used to determine the fracture characteristics of particles (Khumalo et al., 2006).

Drop test experiments were performed by Krogh (1980) where he subjected individual particles to impact by a falling object. From this testing method, three basic milling characteristics were quantified, i.e. crushing probability, energy function and breakage function. Particles of the same material with the same size do not necessarily have the same strength; hence the crushing probability function as stated by Krogh (1980) is a measure of the strength distribution of particles for a given size. The energy required to break a particle of a given size is calculated from the height and the mass of the falling object.

During the process of milling, excessive impact energy may result in extreme particle size reduction. However, if the impact energy is too low, the stress generated in a particle may not be sufficient to cause particle fragmentation. Somewhere between these two extreme cases lies an optimum level of impact energy (Pauw et al., 1988). By using a testing device similar to that of Krogh (1980), Pauw et al., (1988) conducted impact testing on four size ranges of ore samples at different energy levels. Each size range of particles is impacted with a known load until all the particles are broken to smaller than their feed size. Experiments were performed with the same feed but at different impact energy levels and a correlation between the specific breakage energy with respect to the input energy per impact was established. By plotting the two, optimum impact energy for particle breakage was obtained (Pauw et al., 1988). According to Tavarez (1998), the drop weight test is the simplest method in investigating the behaviour of material breakage characteristics. This has the advantage of flexibility, simple operation, extended input energy range and the possibility of testing particle beds.

There are mainly three types of single particle tests; single impact, double impact and slow compression as shown in the figure below:

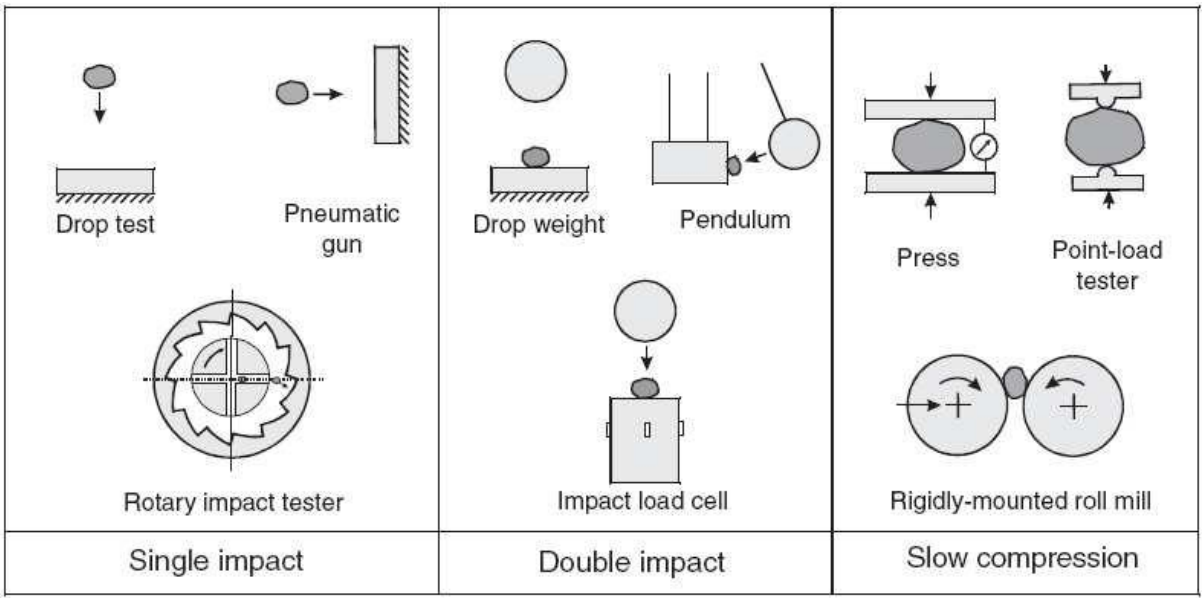

Figure 1: Different types of single particle tests (Tavares, 2007).

Single impact

This can be performed by drop tests or using a pneumatic gun on a particle propelled against a surface, in both cases the specific impact energy is given by half of the square of the particle velocity at the instant of the collision.

Double impact

A test specimen is crushed between two hard surfaces as can be seen in Figure 1 above.

(i) Drop-weight tests: Here a particle is resting on a hard surface is crushed by a free falling weight. This method can be used to estimate the minimum energy to comminute materials. It is a useful tool to determine the energy-size relationship for the breakage of particulate material; however it does not allow the direct measurement of the fraction of the input energy that is used to break particles, called comminution energy (Tavarez, 1998). Drop weight tests can be used to determine the breakage and energy utilization parameters for the comminution model for single particles, as well as beds of particles.

(ii) The pendulum test: This is also used to establish the relationship between energy and size. Furthermore it can overcome the limitation of the drop weight test. The JKMRC drop-weight tester and the Ultra-Fast-Load-Cell developed at Utah University are examples of double impact tests and using them, it has been possible to study how energy input affects progeny size distribution. From the breakage of single particles, models have been developed to estimate the breakage functions (Napier-Munn et al 1996, King and Bourgeios 1993).

Khumalo et al., (2006) showed that specific energy of particles is an important fundamental property. Investigations of Stehr (1982), Stehr and Schweded (1982), Weit (1987), Wet and Schwedes (1987) and Weit et al. (1986) have shown that the specific energy input is the main parameter influencing the comminution result for a wide range of operating parameters. When a particle is impacted by a falling weight, the impact and specific energy can be established by selecting the appropriate combination of weight and height from which the falling weight is dropped by gravity. The minimum input energy required for the breakage of a particle can be calculated from the experimental data by using equation 1 as follows:

$$E_b = m_b g h \quad (1)$$

where m_b is the mass of the drop weight (ball) in kg

g is the gravitational accelerations in m/s^2 and

h is the drop height in m.

The total impact energy (J) and the specific energy (J/g) are calculated according to equation 2 and 3 respectively as shown below

$$E_T = N E_b \quad (2)$$

$$E_s = \frac{E_T}{M_p} \quad (3)$$

where N is the number of impacts and M_p is the mass of the particles in g.

One can see from the above equations that it is possible to change the specific energy of breakage in four ways: (i) the number of drops (N), (ii) the mass of the grinding media (adjusted here by changing the grinding media diameter, d_m), (iii) the drop height (h) and (iv) the mass of the particle bed (M_p). If the impact energy applied in a given breakage event is not properly selected for the size of the particle being broken, inefficiency will result, in the form of either overgrinding where a product particle size smaller than that desired is produced, or in no breakage, where the particle absorbs the energy, but does not break.

According to Krogh (1980) particles of the same sieve size will not break by the same energy input due to the difference in factors such as shape, size and pre existing crack distribution. The probability of breakage is a function of the energy input. When there is total regularity in

the physical properties of particles, no particles will break below a certain energy level, whereas all the particles will break at an energy input at about the same level. However, with increasing irregularity in material physical properties, the energy range for breakage will widen. Furthermore, according to Khumalo et al. (2006) the same net input energy consumed in a grinding process can produce different product particle size distribution (PSD) and therefore it is advisable that comminution circuits should be controlled using specific energy instead of net or total input energy. According to Herbst and Fuerstenau (1980), as cited in Khumalo et al. (2006), using specific energy for mill design and scale-up allows mills of different sizes to yield the same product size distribution for the same specific energy when fed with almost identical material.

Many different techniques have been adopted in comminution to find a way of energy optimization in milling situations. "Attainable Region (AR) analysis is a method that allows us to solve process synthesis and other optimization problems by providing guidelines for the construction of an Attainable Region as well as providing some necessary conditions to check the results. The Attainable Region is defined as the set of all possible outcomes, for the system under consideration, that can be achieved using fundamental processes operating within the system, and that satisfy all constraints placed on the system" (http://web.wits.ac.za/Academic/Centres/COMPS/Research/AR/ARTheory/Introduction.htm)

Khumalo et al., (2006) applied the Attainable Region approach to comminution where he represented the PSDs as a single point in space allowing connectivity of the points rather than using the traditional approach of representing PSDs in terms of cumulative plots as shown in Figure 2 (a) below. He claimed using the approach that the PSDs discharged were dependent on the specific energy from the grinding mill and later experimentally validated his assumption using silica and quartz feeds in (Khumalo et al., 2007), where he showed that the experimental Attainable Region is convex as shown in Figure 3 below where the PSDs are now plotted as single points and joined together.

Metzger et al., (2009) applied the Attainable Region analysis to optimize the comminution of silica sand particles in a bench top laboratory ball mill and showed that it's a useful tool in determining optimal policies to reduce milling processing times. A system where the attainable region was non-convex was examined and that led to a strategy where mixing the product stream with the feed material was optimal. When constructing the AR plots, the boundary curve should be convex. If the region is not convex, it would be possible to extend

it by mixing, namely drawing a straight line between the appropriate points to fill in the concavity (Metzger et al., 2009).

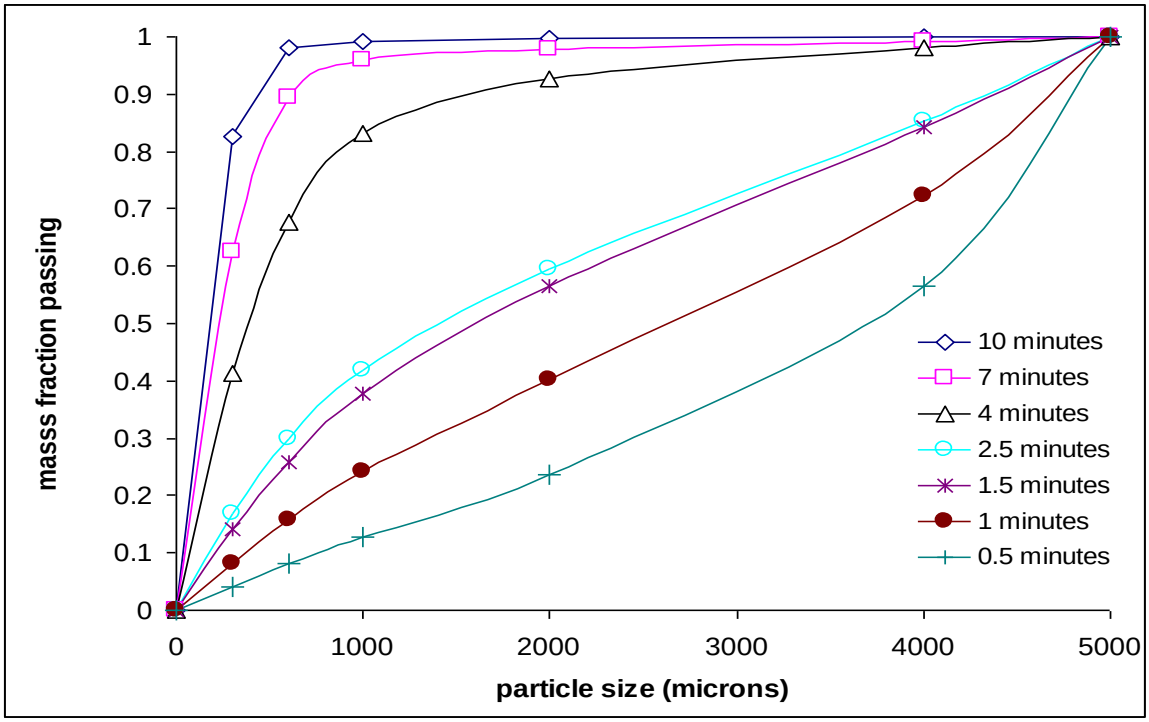

Figure 2: Cumulative particle size distributions as one increase the grinding time for a laboratory ball mill at 92 rotations per minute and 20 % ball loading (Khumalo et al., 2007).

Figure 3 is the proposed method of representing the particle size distributions in Figure 2 as single points in space. The three size classes chosen in this investigation were (Khumalo et al., 2007):

i) Size class 1: Everything greater than 4000 µm,

ii) Size class 2: Between 4000 µm and 2000 µm,

iii) Size class 3: Everything less than 2000 µm.

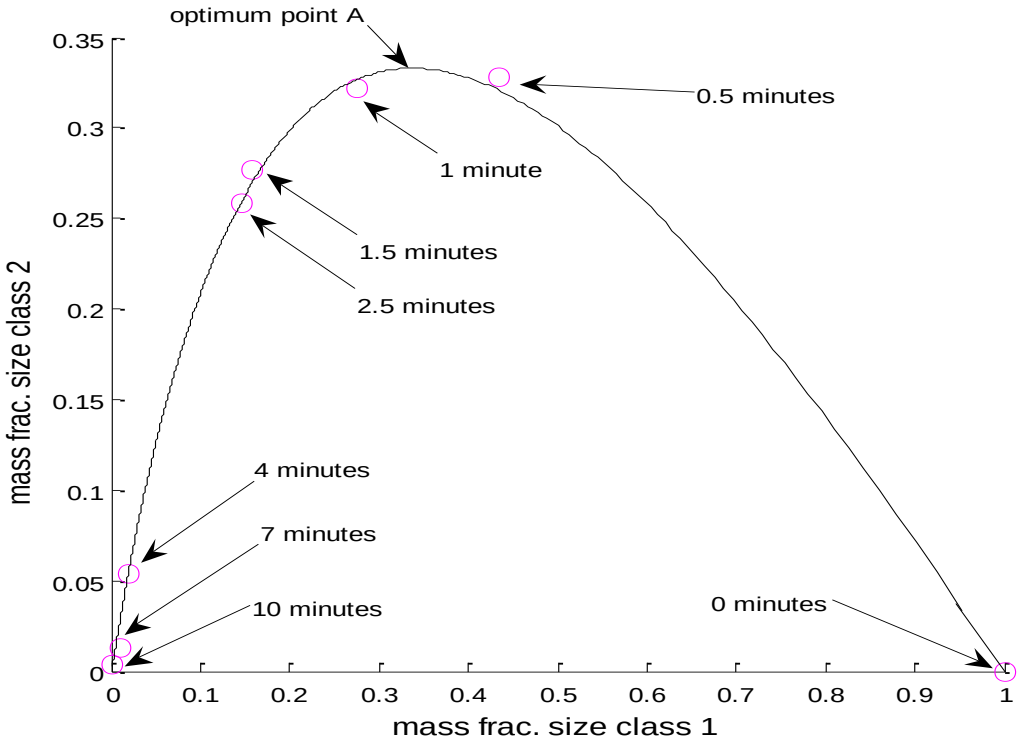

Figure 3: Our new proposed method for representing the eight product particle size distributions in Figure 2 as a single trajectory (Khumalo et al, 2007).

CHAPTER 3

3 EXPERIMENTAL SECTION

3.1 Introduction

This chapter outlines the way in which experimental data was collected and also explains the apparatus that was used to perform the experiments.

3.2 Description of the equipment

Experiments were carried out using the drop weight test as shown in Figure 4 below. The apparatus consists of an anvil as a crushing surface of hardened mild steel and a cylinder with an inside diameter of 4.8 cm. The anvil was used as a surface of impact while the cylinder was used to restrict the breakage area and to prevent losing broken fragments during the tests. The silica particles to be tested were poured manually through the tube to make a bed on the anvil. After each impact, the fragments from the crushed or uncrushed particles were removed from the anvil into a stainless steel container to mix the particles together and then subjected to more breakage until the required impacts.

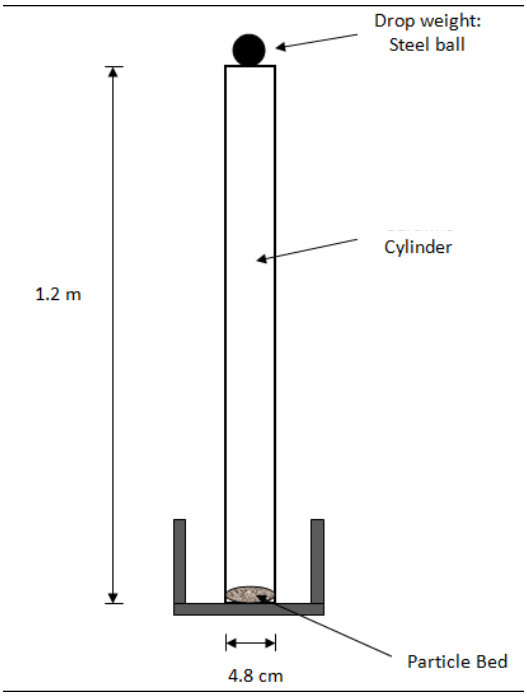

Figure 4: Schematic of the drop weight apparatus.

3.3 Experimental procedure

3.3.1 Experimental method

Experiments were conducted to investigate the effect of grinding media diameter on the resultant particle size distributions (PSDs) of silica bed particles. The main aim was to determine the grinding media size that produced the most breakage. Two spherical steel grinding media sizes 10 mm and 30 mm were initially used as drop weights. The choice of the media range was based on the fact that we needed a ball size which is just above the feed size and another ball size which is bigger than the feed size but won't crush the particles at once. For this set of experiments, the number of impacts (N) was varied from 50 to 600 impacts while the drop height (h) and the bed height or mass of the silica bed particles (M_p) were kept constant at 1.2 m and 10 g respectively. Based on the experimental results, more experiments were conducted using the intermediate grinding media (20 mm). Due to time constraints, breakage experiments using the 20 mm ball size were investigated by varying the number of impacts (N) from 50 to 300 at drop height (h) of 1.2 m and bed height of 10 g.

To investigate the effect of input energy and specific energy on the resultant particle size distributions (PSDs), mass of particles (M_p) and number of drops (N) were kept constant at 10 g and 50 drops, respectively. The drop height (h) and the grinding media sizes were varied from 0.55 m, 1.2 m, 1.75 m high and 10 mm, 20 mm, 30 mm, respectively. The drop weight was allowed to free fall from the drop height of choice onto silica bed particles which is positioned on the anvil. Experiments aimed at investigating the energy intensity effect on the breakage characteristics of silica bed particles were conducted for two cases. The grinding media sizes used were 10 mm and 30 mm ball sizes. In the first case, the drop height was kept constant while changing the number of impacts. For the second case, the number of impacts was kept constant and the drop height was varied. Both cases the bed height (mass of the particles) was kept constant at 10 g.

Multiple impact tests were also conducted to determine the effect of the mass of the particles (bed height) on the resultant PSDs. The number of impacts (N) and drop height (h) were fixed at 50 drops and 0.55 m respectively. The grinding media size was varied from 10 mm, 20 mm and 30 mm as well as the mass of the particles (M_p) were varied from 10 g, 20 g and 30 g. After performing all sets of experiments, the broken products were collected and using the laser diffraction method, the particle size distributions (PSDs) were determined.

Figure 5 below shows the Mastersizer 2000 used for analysing dry samples, the Hydro 2000G used for analysing wet samples and the optical cell where the laser diffraction occurs when samples are analysed. The optical cell is only applicable to the Mastersizer 2000.

Figure 5: Malvern Equipment for particle size analysis.

CHAPTER 4

4 RESULTS

4.1 Effect of increasing the number of impacts

Figure 6a and 6b illustrate the effect of energy input on the resultant product size distribution. The above mentioned figures shows the cumulative distribution representation for smaller media (10mm) of a sample of bed particles tested for increasing the number of impacts from 0 - 300 drops. Both figures are the same except that the Gaudin-Schumann plot (Figure 6b) depicts a clear picture as to what exactly happens in the fine size region. As can be seen from the figure, at low energy input, insufficient energy was provided to the particles and no breakage was observed. It can be seen that when the number of impact ranged from 0-200 the four curves lie on top of each other meaning that there's no effect on the breakage within that range. As one increases the number of impacts to 250 to 300 there is evidence of breakage taking place by forming fines.

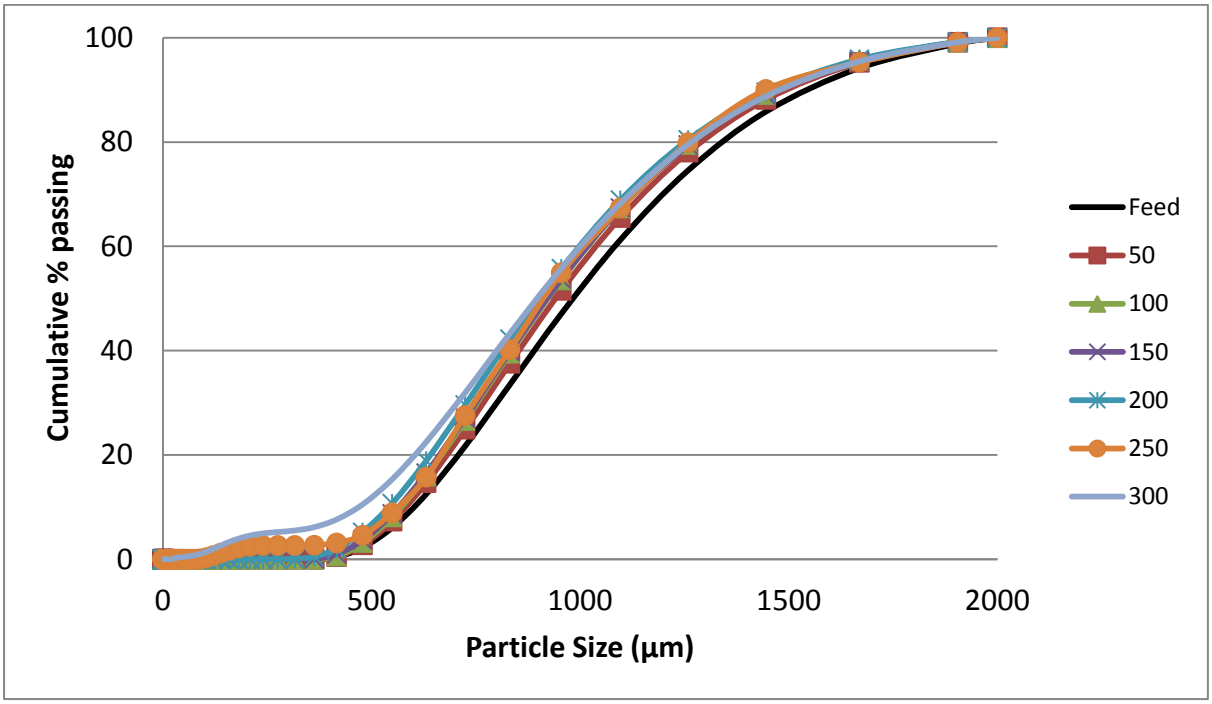

Figure 6a: Cumulative distribution plots from breakage of silica particles at variable low energy inputs for 10 mm grinding media with the mass of the silica bed particles constant at 10 g and a drop height of 1.2 m.

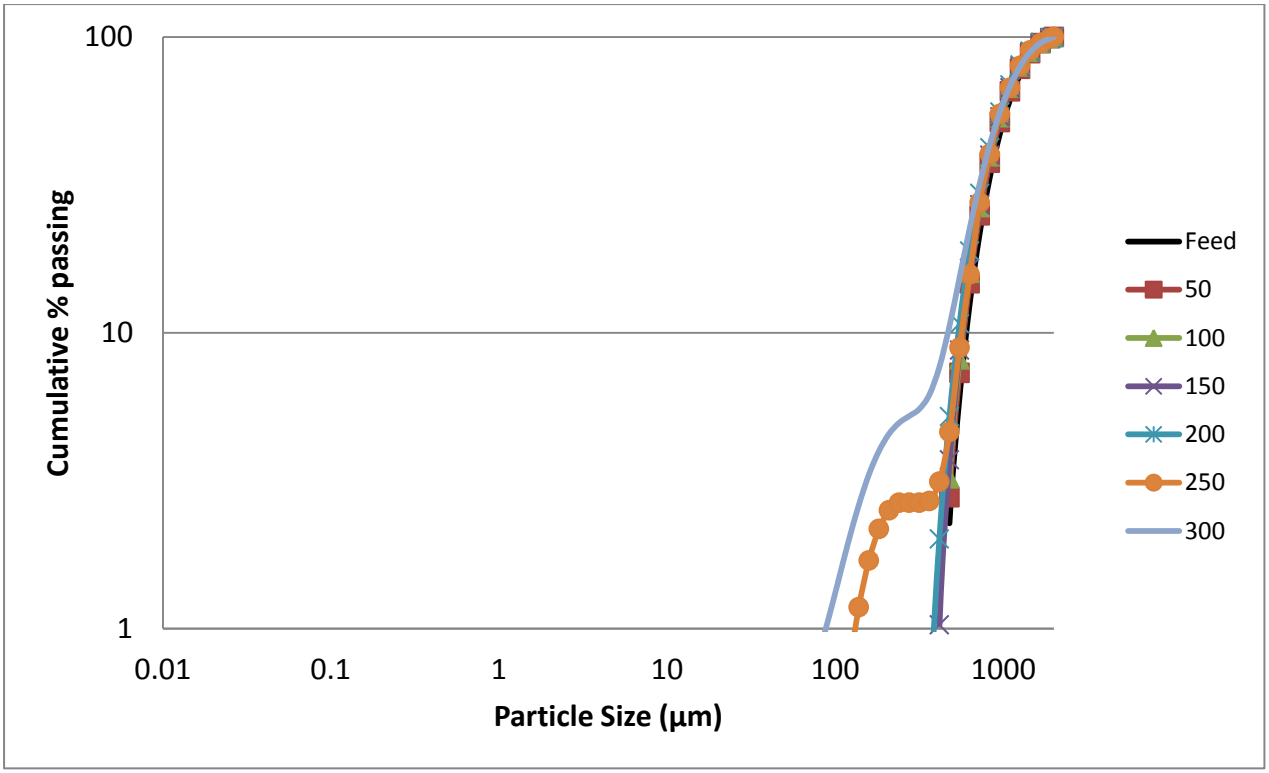

Figure 6b: Gaudin-Schumann plot from breakage of silica particles at variable low energy inputs for 10 mm grinding media with the mass of the silica bed particles constant at 10 g and a drop height of 1.2 m.

As one increases the number of impacts from 250 to 600, at high energy input, breakage starts to happen and there are fines which are generated, meaning that there's a minimum amount of impact and specific energy that was required to break the particles. To check for reproducibility, the drop tests were repeated by performing two runs on different dates (after a month to be precise) using 10 mm grinding media for 100 impacts. One sample from the feed was taken from the sample, ran through the Malvern to get the PSD. Another fresh feed sample was also taken from the same sample, ran through the Malvern to get the PSD as well. With the two PSD's the average values were obtained and a standard deviation was obtained between the runs. The same procedure was followed with 100 impact runs on the sample. It can be observed that the curves for both tests lied on top of each other with small deviations as depicted in Figure 6c below. Error bars represent standard deviations of two replicates. It was found that the results are indeed reproducible with the variability at each point not being significant as shown by small error bars.

In Figure 7 we represent the PSD results of the 10 mm media size that shows the extended number of drops from 250 to 600. It can be observed that there is additional breakage taking place as one increase the impact energy and more fines are produced.

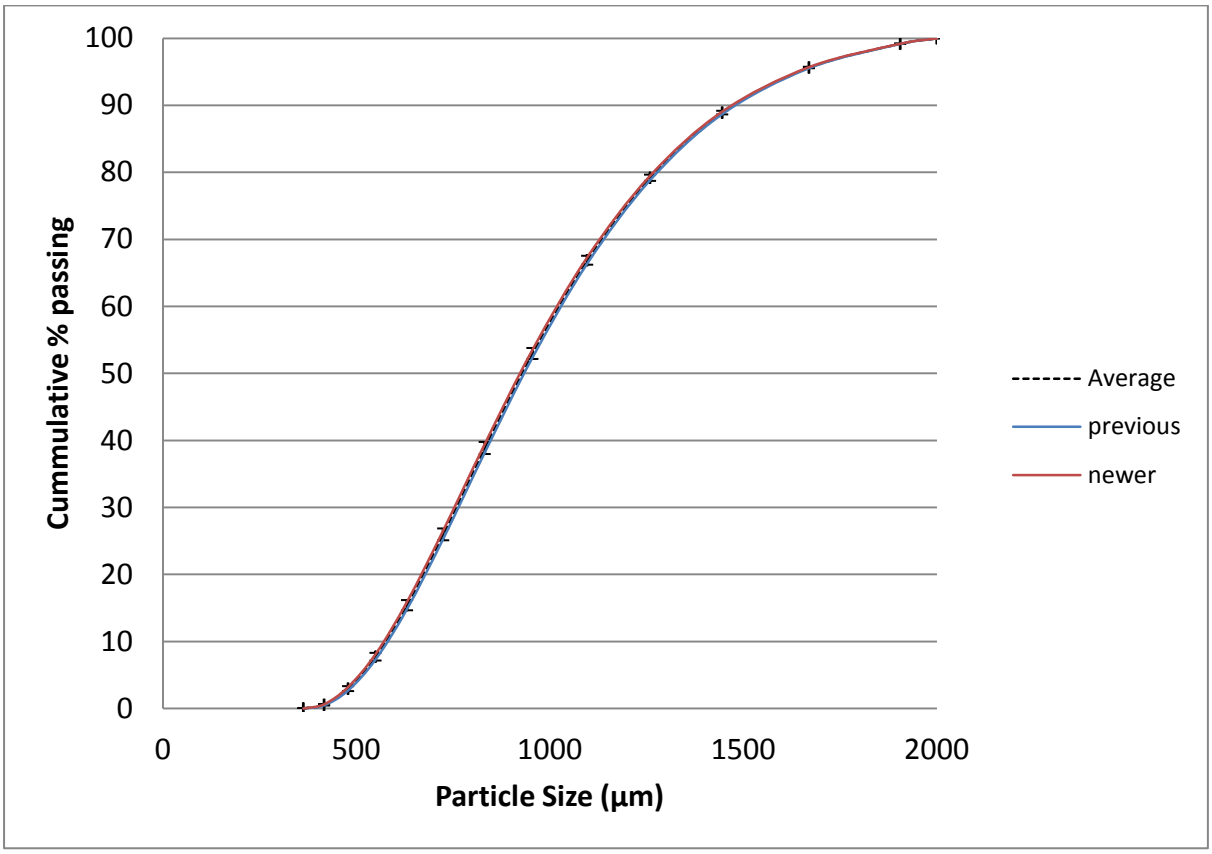

Figure 6c: Comparison of the data accuracy plots from breakage of silica particles using 10 mm grinding media for 100 impacts with the mass of the silica bed particles constant at 10 g and a drop height of 1.2 m at different days.

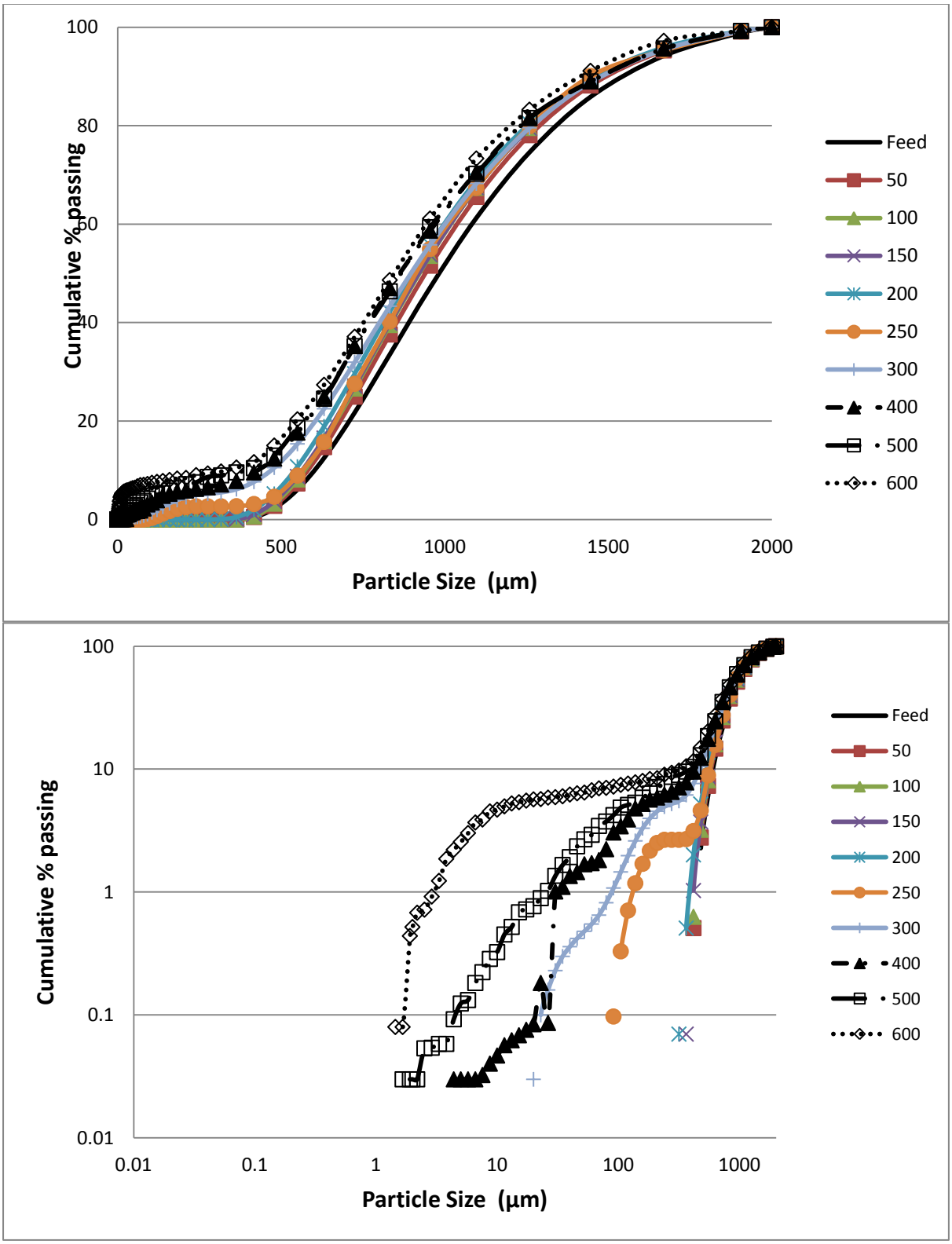

Figure 7: Cumulative distribution plots from breakage of silica particles at variable high energy inputs for 10 mm grinding media with the mass of the silica bed particles constant at 10 g and a drop height of 1.2 m.

Table 1: Energy distribution vs. number of impacts at a drop height of 1.2 m for all grinding media sizes.

Number of Impacts	**Total Impact Energy (E_T) (J)**			**Specific Energy (E_S) (J/g)**		
	Grinding Media Size (mm)			Grinding Media Size(mm)		
	10	**20**	**30**	**10**	**20**	**30**
0	0.0	0.0	0.0	0.0	0.0	0.0
50	2.3	33.8	58	0.2	3.38	5.8
100	4.6	67.6	116	0.5	6.76	11.6
150	6.9	101.4	174	0.7	10.14	17.4
200	9.3	135.2	233	0.9	13.52	23.3
250	11.6	-	-	1.2	-	-
300	13.9	202.7	349	1.4	20.27	34.9
400	18.5	-	465	1.9	-	46.5
500	23.1	-	582	2.3	-	58.2
600	27.8	-	698	2.8	-	69.8

It can be seen from Table 1 that, for the 10 mm grinding media, the minimum input energy and specific energy required for breakage is 11.6 J and 1.2 J/g respectively, as the curves for up to 200 drops are similar, and only demonstrate breakage after 250 drops. Figure 7 illustrates the effect of increasing number of impacts on the resultant PSD and thus shows that more fines are produced. Figure 8 shows the cumulative distribution representation for intermediate ball size (20 mm) of silica bed particles impacted for increasing the number of drops from 0-300 impacts. As one increases the input energy and breaking the particles for longer times more fines are formed as the product. It can be seen that the intermediate grinding media (20 mm) starts to break the particles at a minimum energy input and specific energy of 33.8 J and 3.4 J/g respectively when the ball was dropped at 50 impacts. It can be seen from the figure that the higher the energy input, the finer the product.

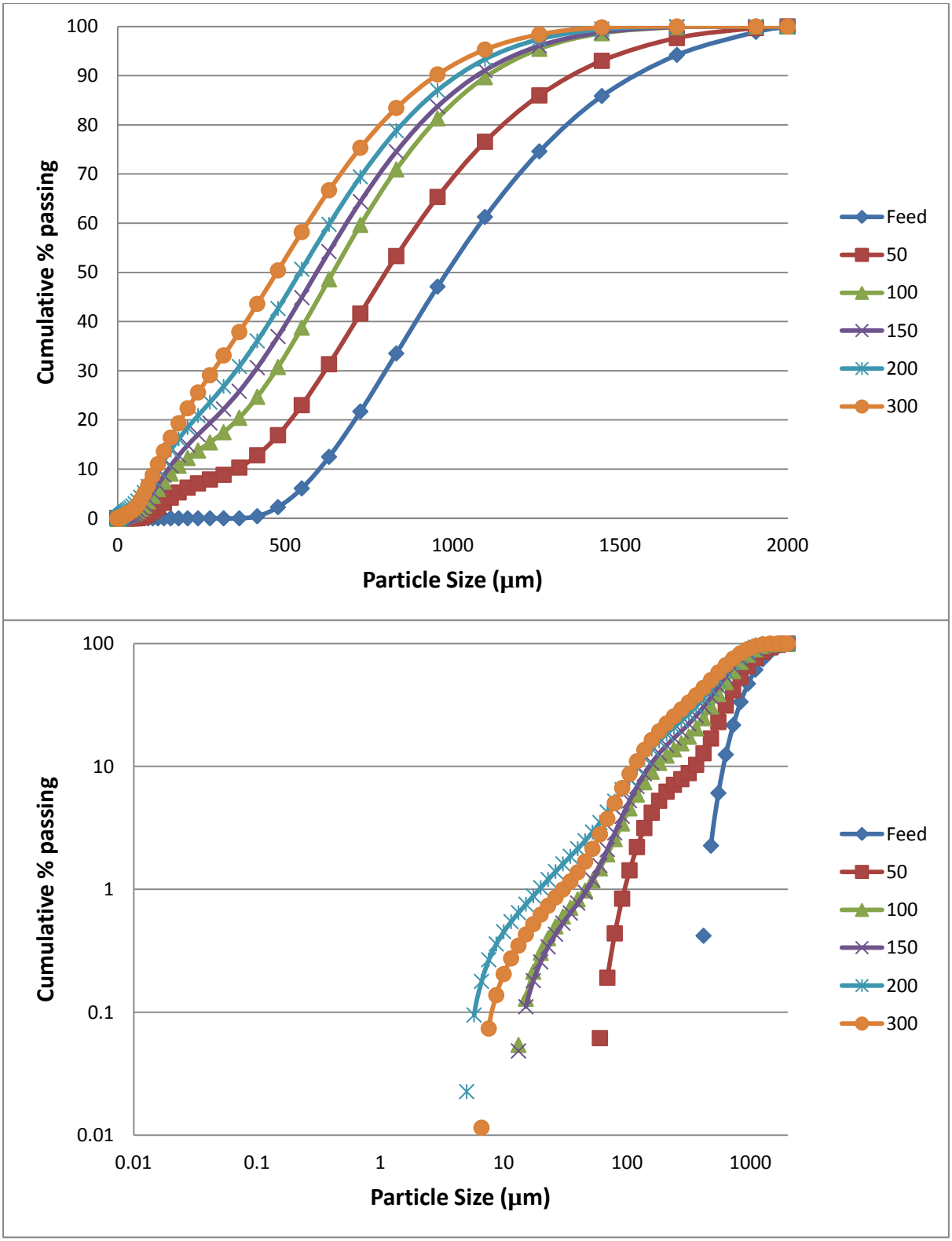

Figure 8: Particle size distribution plots for intermediate media size (20 mm) for varying specific energy input at a constant drop height of 1.2 m and a bed height of 10 g of particles.

The particle size distributions of silica sand (bed) particles impacted for increasing the number of drops from 0-600 impacts for the larger grinding media (30 mm) are illustrated in Figure 9. At varying amount of energy input, it can be seen that increasing the number of impacts shifts the particle size distribution of the impacted products towards the finer range.

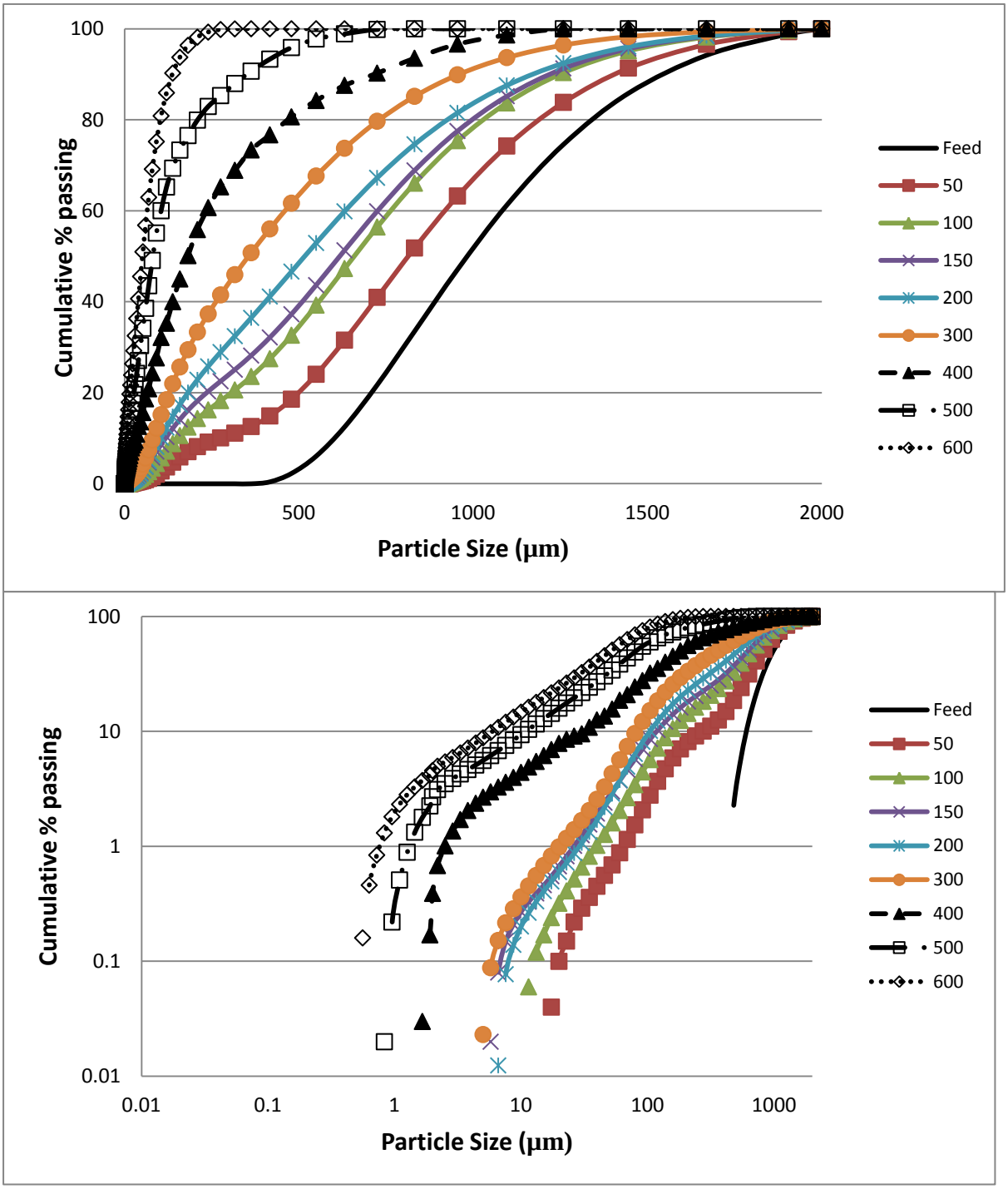

Figure 9: Cumulative distribution plots from breakage of silica particles at variable energy inputs for 30 mm grinding media with the mass of the silica bed particles constant at 10 g and a drop height of 1.2 m.

Depicted in Figure 10 below is a comparison of all three ball sizes at the same number of impacts (300). It can be observed that the amount of breakage increases as the mass of the grinding media increases. The same behaviour was observed when the same comparison was analysed at 50 and 100 impacts as depicted in Appendix B.

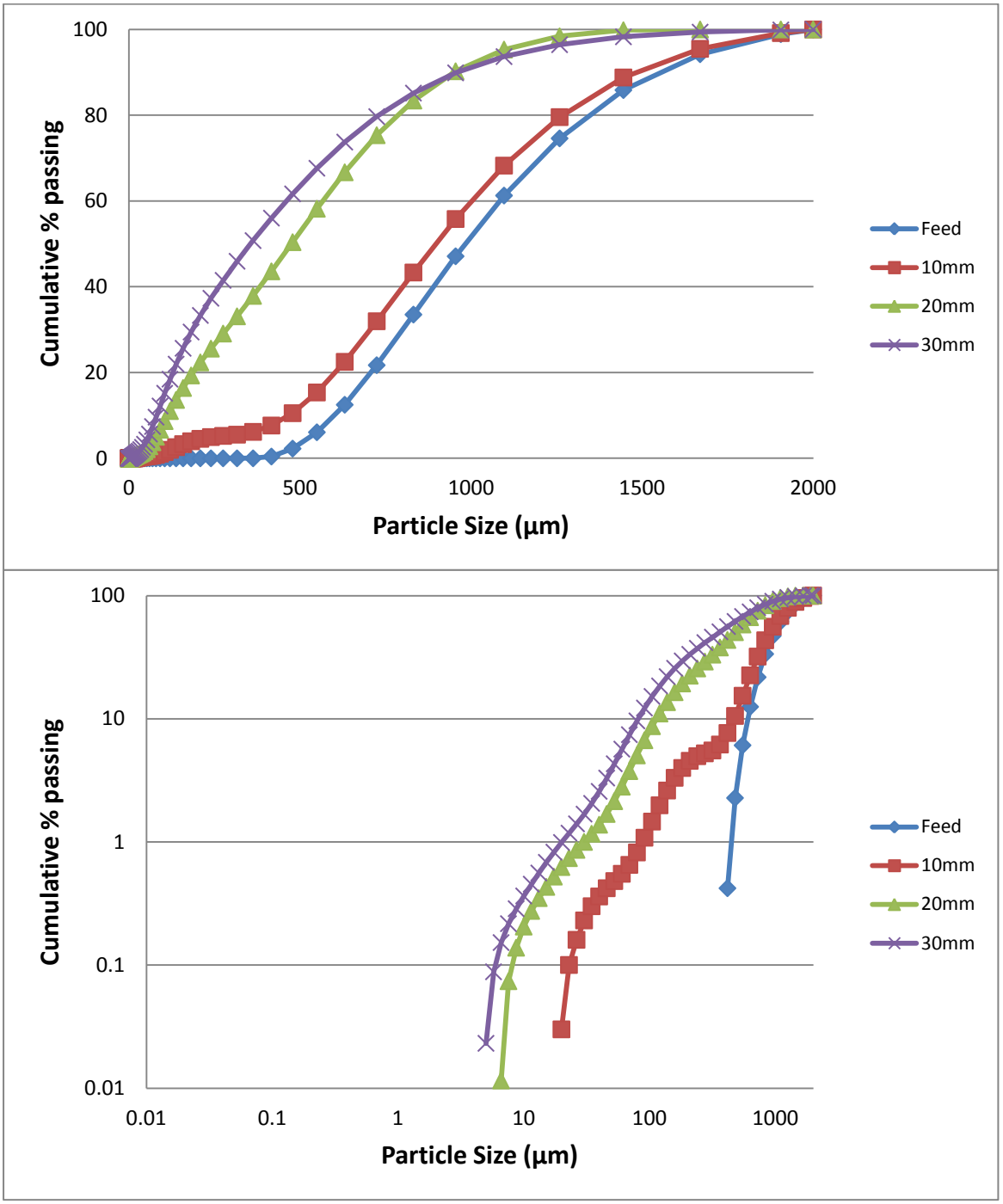

Figure 10: Particle Size distribution plots for all three grinding media sizes (10 mm, 20 mm and 30 mm) at the same number of impacts (300) with the mass of the silica bed particles constant at 10 g and a drop height of 1.2 m.

4.2 Effect of mass of sample (bed height)

4.2.1 Small media size (10mm)

The effect of mass of the particles (bed height) on the resultant particle size distribution (PSD) was investigated using three different grinding media sizes (10 mm, 20 mm and 30 mm). The number of impacts was kept constant at 50, and the drop height was also constant at 1.2 m. Figure 11 to Figure 13 below shows the cumulative distribution plots as one increases the bed height (mass of particles) from 10 g to 30 g. It can be seen from the Figures below that there are less fines produced as the mass of particles increases for the bigger grinding media sizes (20 mm and 30 mm). This can be attributed to the cushioning effect. As for the smaller media size (10 mm), there was not enough noticeable breakage taking place to compare. It can be observed that the same input energy will produce different particle size distributions and that the smaller the bed height, the more fines will be produced. Another interesting aspect of the data presented in Figure 11 to Figure 13 is that, we are not only creating more fines, but there is a reduction of the median diameter (d_{50}).

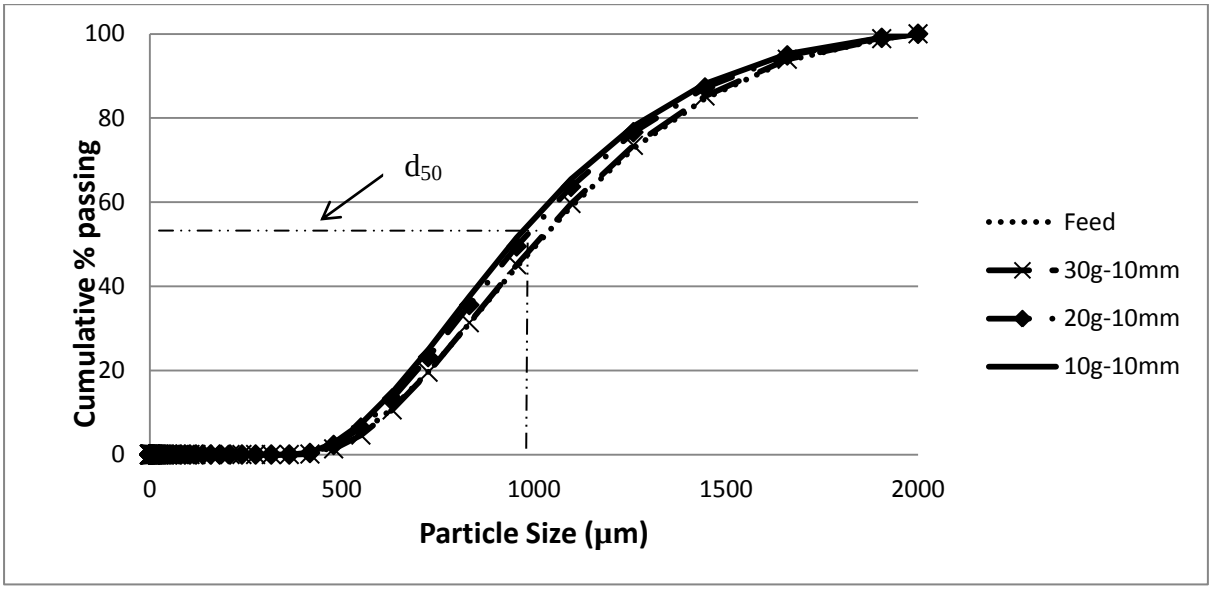

Figure 11: Effect of increasing mass of the particles (bed height) from 10 g, 20 g and 30 g using 10 mm ball size at a constant drop height of 1.2 m and constant number of impacts of 50.

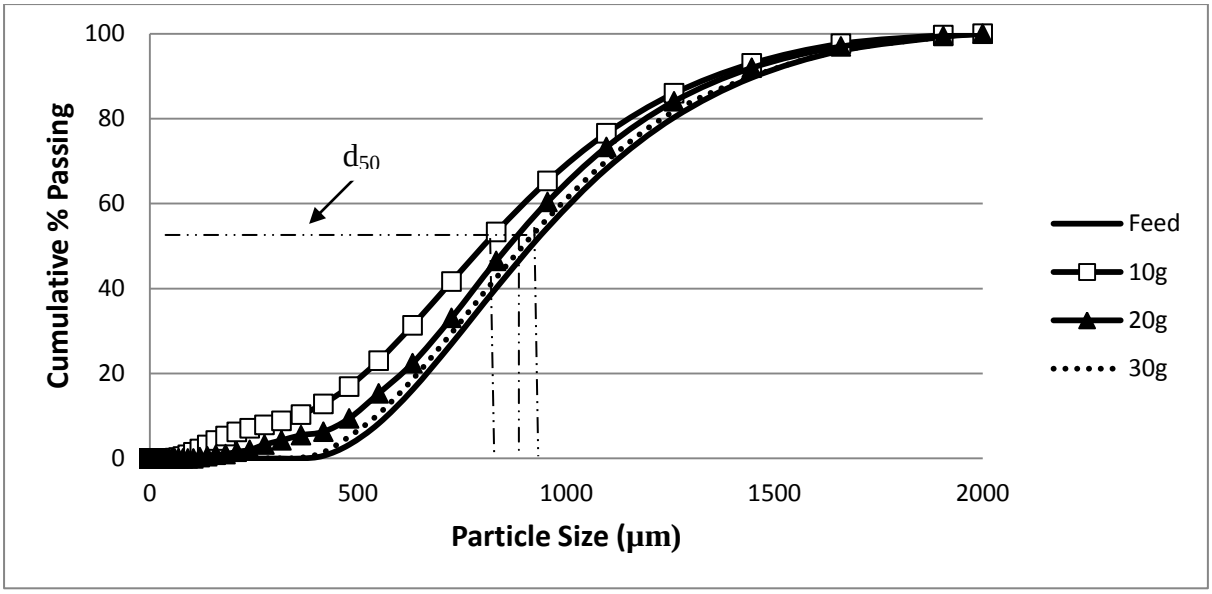

Figure 12: Effect of increasing mass of the particles (bed height) from 10 g, 20 g and 30 g using 20 mm ball size at a constant drop height of 1.2 m and constant number of impacts of 50.

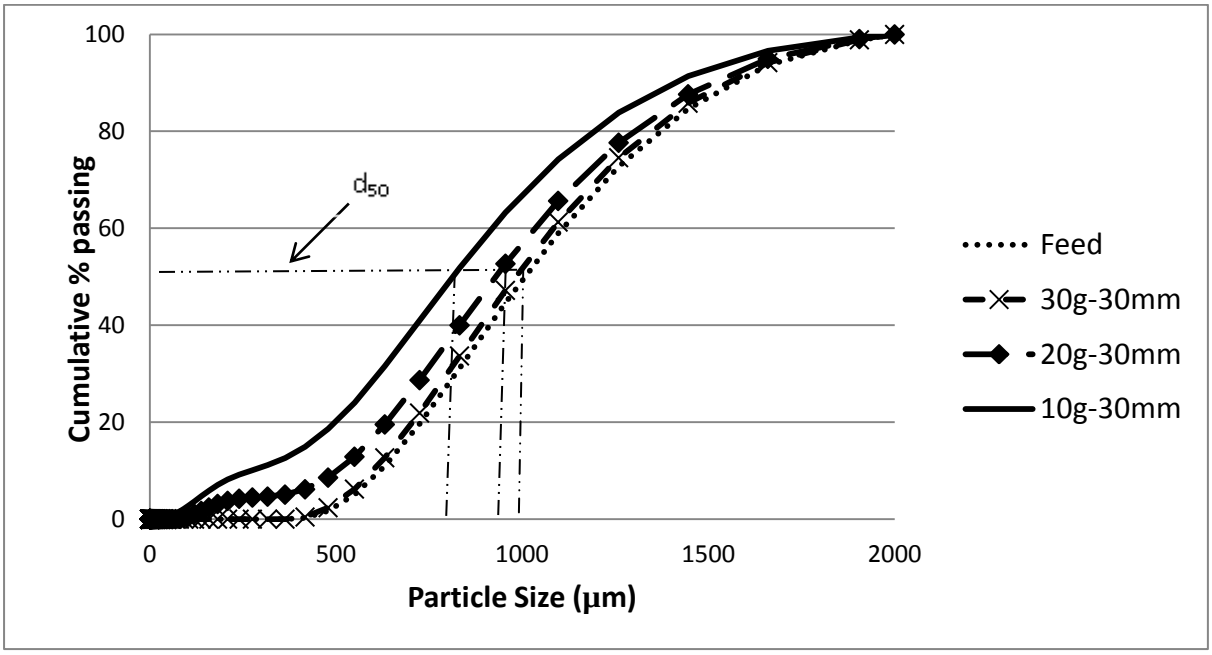

Figure 13: Effect of increasing mass of the particles (bed height) from 10 g, 20 g and 30 g using 30 mm ball size at a constant drop height of 1.2 m and constant number of impacts of 50.

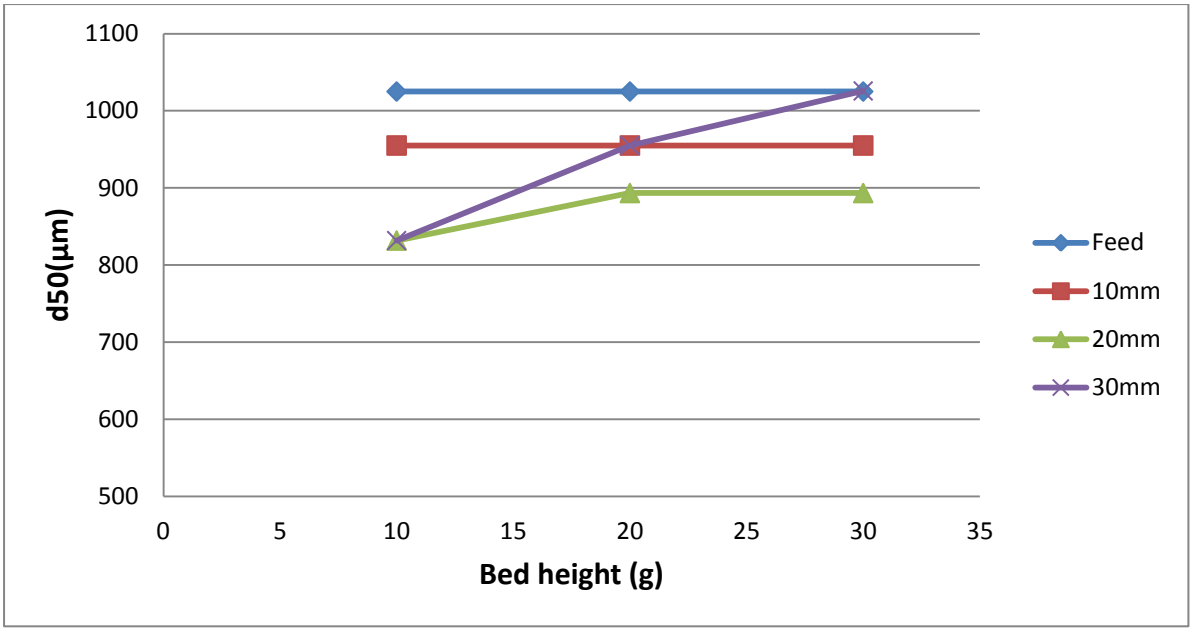

Figure 14: Effect of increasing mass of the particles (bed height) from 10 g, 20 g and 30 g for three ball sizes at a constant drop height of 1.2 m and constant number of impacts of 50.

The same experimental data that was presented in Figures 11 to 13 are now presented differently as shown in Figure 14 above. It can be observed that there is a reduction in the median size (d_{50}) as the mass of the silica bed particles increases. For the smallest grinding media, the amount of breakage is the same, regardless of the bed height. At a smallest bed height of 10 g, it can be seen that it doesn't matter if one uses 20 mm or 30 mm grinding media to perform breakage As the bed height is increased to 20 g, it is now evident that the choice of the grinding media plays a role in determining the amount of fines that are produced. It can be seen that the 20 mm ball size produces more fines compared to the 10 mm and 30 mm ball sizes. The intermediate grinding media (20 mm) continues to produce more fines at a higher bed height of 30 g. The 10 mm and 30 mm ball sizes seem to perform the same amount of breakage at the highest bed height as shown from Figure 14 above.

4.3 Effect of drop height

The effect of the drop height was investigated for three grinding media sizes at three different heights, namely 0.55 m, 1.2 m and 1.75 m. For this particular set of experiments, the number of impacts and mass of the particles (bed height) were kept constant at 50 and 10 g, respectively.

4.3.1 Small media size (10mm)

Figure 15 below shows the cumulative % passing curve as a function of the particle size. It can be observed that as the energy input is increased (increasing drop height), the curves just lie on top of each other. This suggests that for this particular grinding media at 50 impacts, there is minimal breakage taking place.

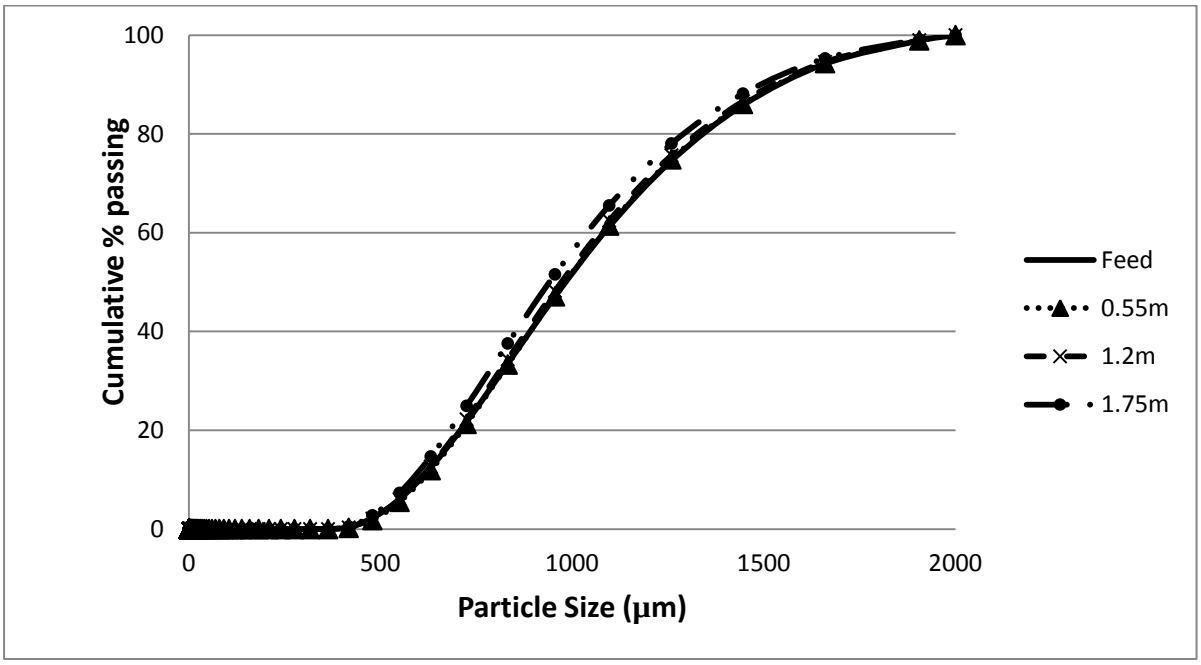

Figure 15: Cumulative distribution plots for varying drop height from 0.55 m, 1.2 m and 1.75 m using 10 mm ball size with the mass of the silica bed particles of 10 g and 50 numbers of drops.

4.3.2 Intermediate media size (20mm)

Figure 16 below shows the cumulative % passing curve as a function of the particle size. It can be observed that the intermediate grinding media performs breakage as one increase the drop-height.

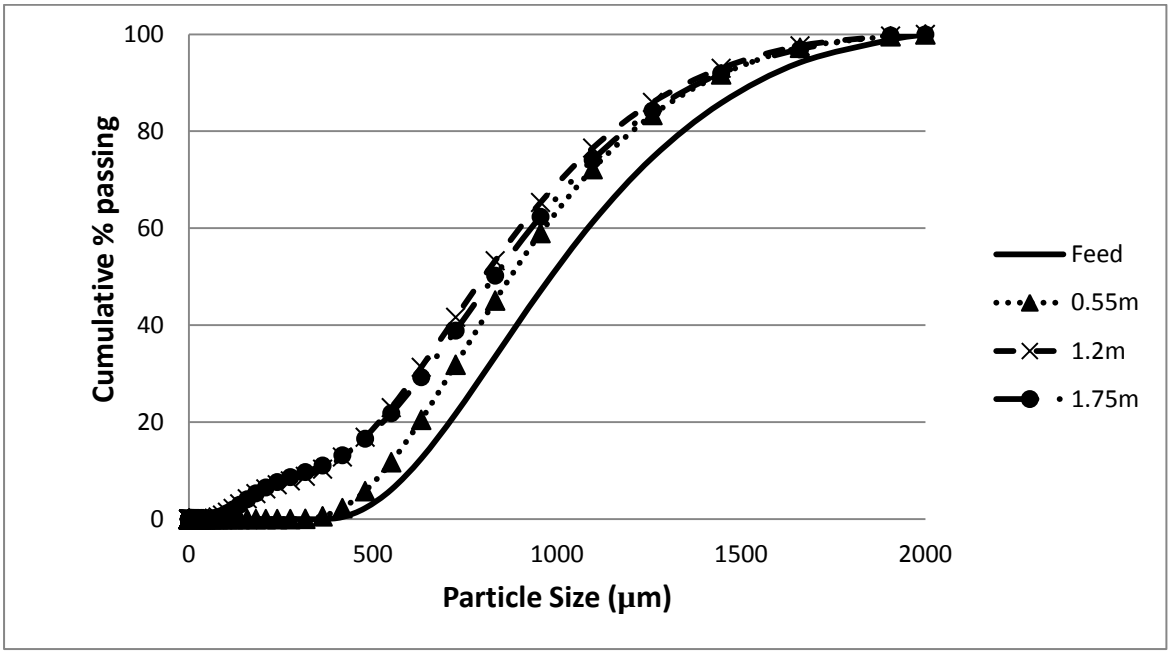

Figure 16: Cumulative distribution plots for varying drop height (0.55 m, 1.2 m and 1.75 m) using 20 mm ball size as a drop weight with the bed height of 10 g and 50 numbers of impacts.

4.3.3 Big media size (30mm)

Figure 17 depicts the energy distribution when the 30 mm ball size is used as a drop-weight to impact silica particles. It can be seen that there is breakage taking place as the drop-height increases. Figure 18 below shows a comparison between the d_{50} of the resultant particle size distributions produced by the three grinding media sizes at three different drop-heights. It can be observed that 20 mm and 30 mm ball sizes achieve more breakage as compared to the 10 mm ball size when the drop height increases.

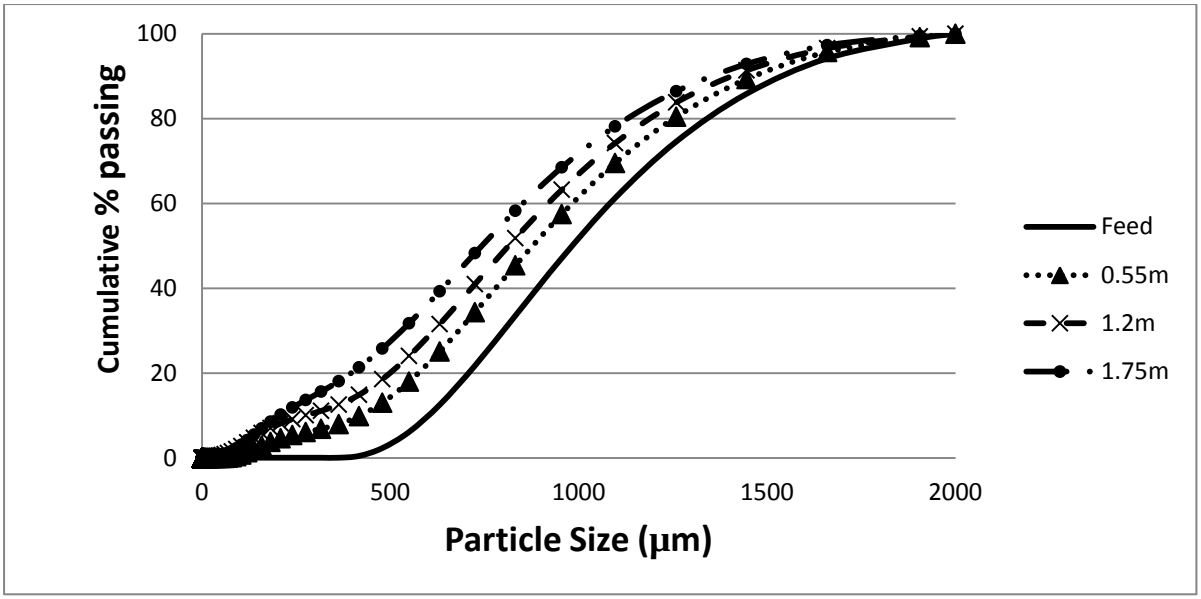

Figure 17: Cumulative distribution plots for varying drop height (0.55 m, 1.2 m and 1.75 m) using 30 mm ball size as a drop weight with the bed height of 10 g and 50 numbers of impacts.

Figure 18 shows a combined summary of different grinding balls at a particular drop height. It can also be seen that the bigger ball size (30 mm) achieves more breakage as compared to the other two grinding balls. The energy of the 30 mm ball size is distributed on a very small amount of particles at a higher drop-height.

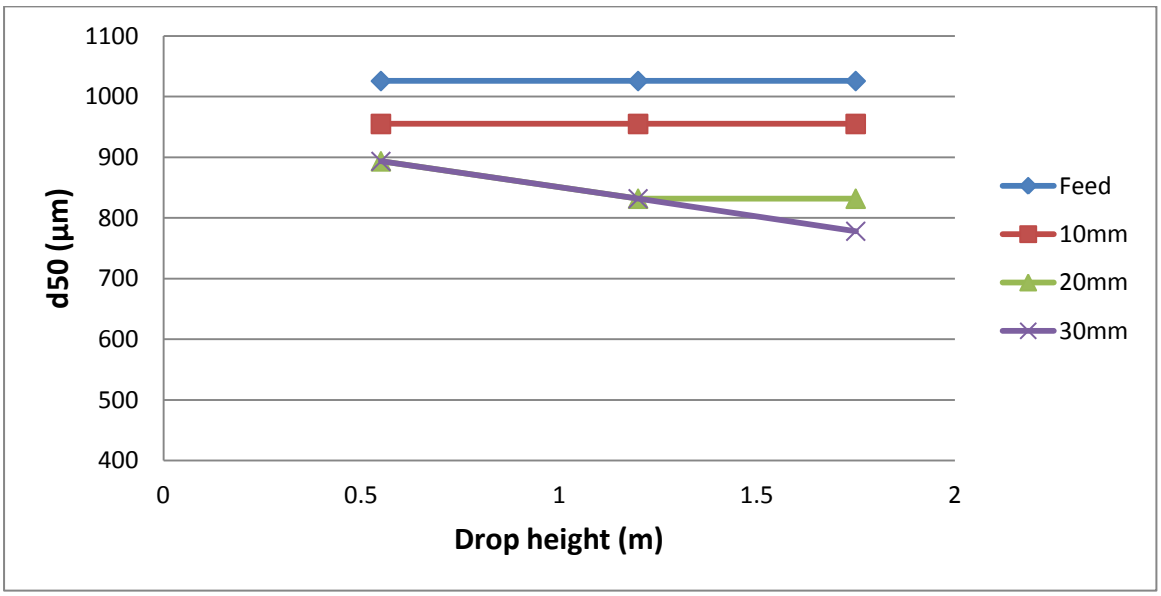

Figure 18: Effect of increasing drop height from 0.55 m, 1.2 m and 1.75 m for three ball sizes at a constant bed height of 10 g and constant number of impacts of 50.

4.4 Effect of media size

The effect of varying the grinding media size was also investigated. The overall comparison of the PSD for varying the drop height is represented in Figure 19 below. For the individual PSD plots refer to Appendix C. It can be observed that as the grinding media is increased from 10 mm to 30 mm, there is more breakage taking place.

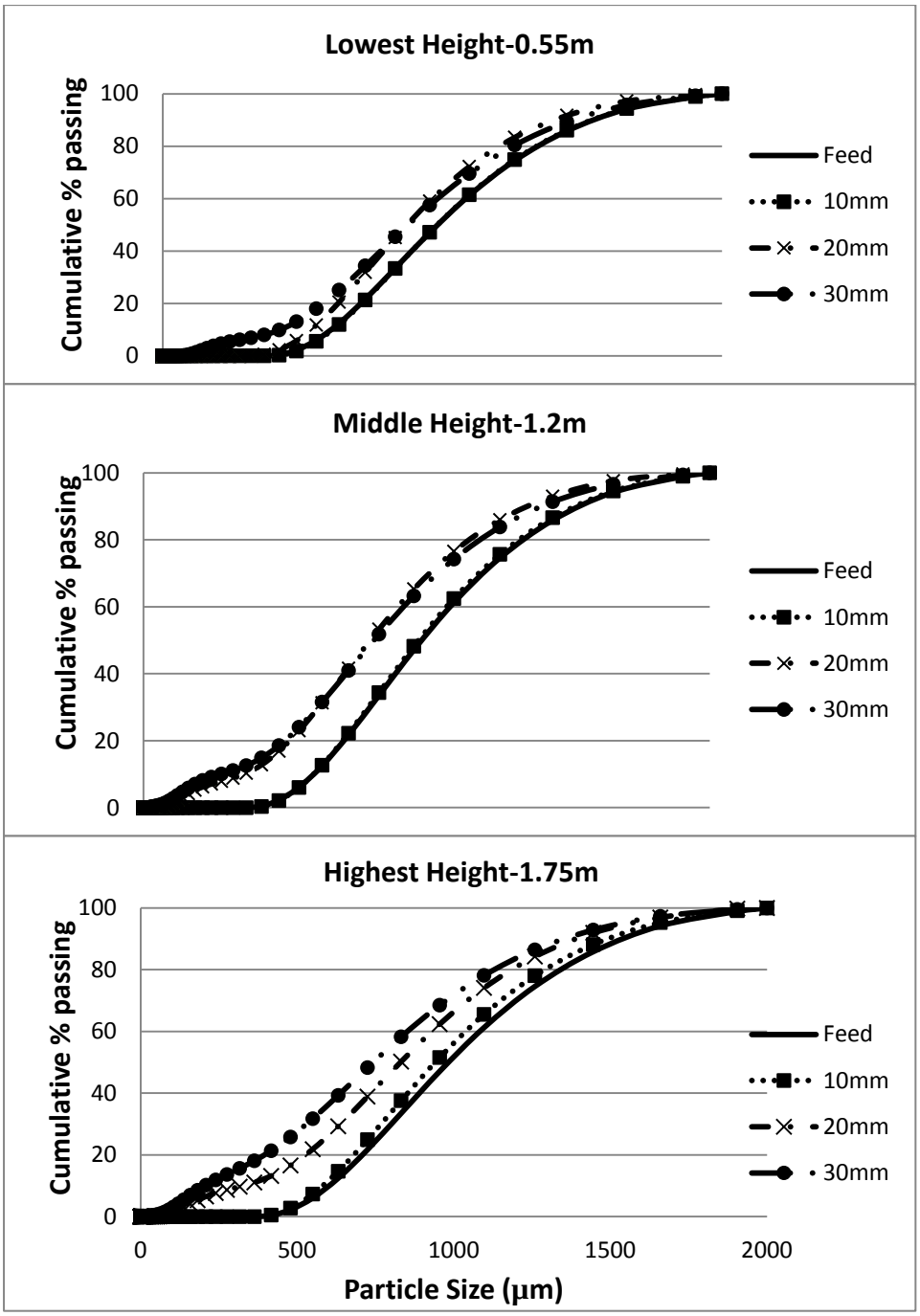

Figure 19: Comparison of the particle size distribution plots for varying drop-height (0.55 m, 1.2 m and 1.75 m) for 10 mm , 20 mm and 30 mm ball sizes with the bed height of 10 g and 50 numbers of impacts for all three grinding media.

4.5 Effect of energy intensity on the resultant PSD

The effect of energy intensity was investigated by varying the drop-height (h) and the number of impacts (N), independently. In addition, it is possible to keep the overall energy input constant, keeping the number of impacts the same at 50, by choosing the height at which one of the grinding media sizes is dropped (either 10 or 30 mm) and adjusting the drop height of the other. For this particular experiment, using 10 mm ball size at its highest drop height of 1.75 m, the height at which 30 mm ball size should be dropped at can be calculated to be 0.065 m (refer to Appendix B for the calculation). Since the same specific energy might give identical products, the products from the two grinding media experiments could lie on top of each other for the same total energy input.

4.5.1 Drop-height variation

The two plots in Figure 19 and 20 demonstrate the effect of energy intensity for different grinding media (10 mm and 30 mm). It can be seen that for the same energy intensity, different product size distributions are obtained.

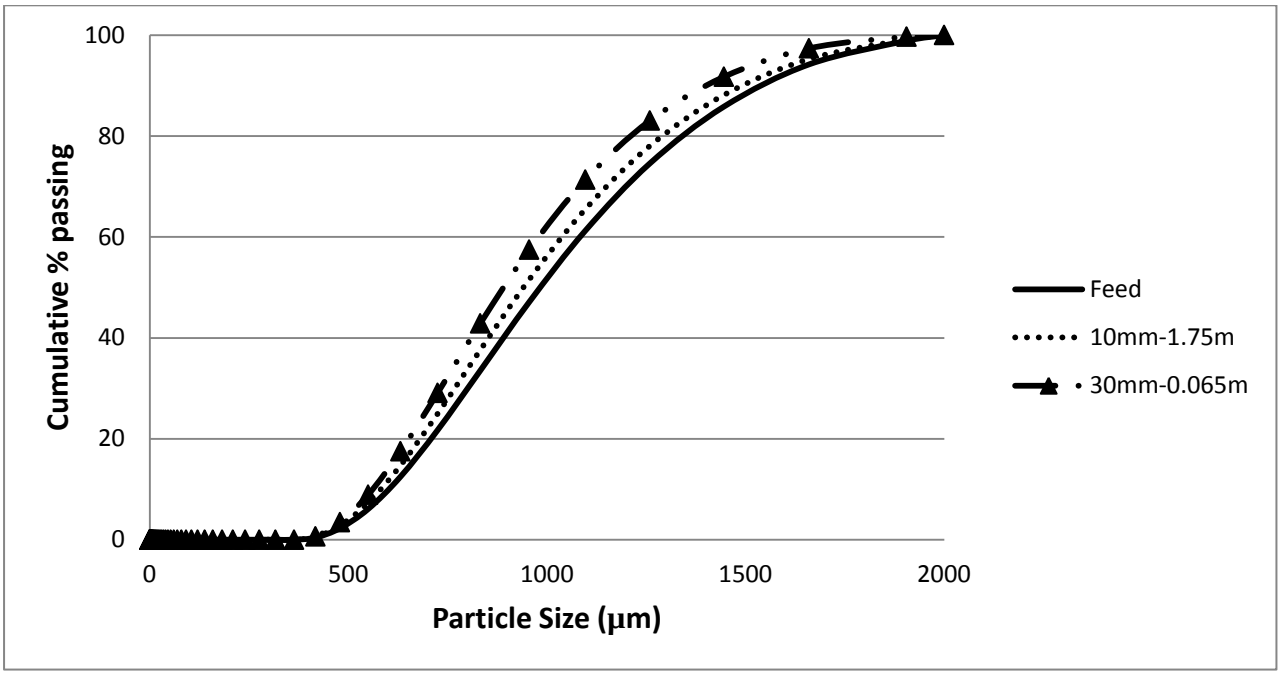

Figure 20: Particle size distribution plots for varying drop-height and media size at constant overall input energy.

4.5.2 Number of impacts variation

Assuming total impact energy to be the same, keeping the height constant at 1.2 m, the number of drops required can be determined by using the 10 mm ball size, one can determine its impact energy. Once the impact energy is determined, the total impact energy can then be calculated and assumed to be the same for the bigger ball size (see Appendix B for the calculation). For this case the number of impacts was varied and it can be seen that the resultant PSDs do not lie on top of each other as shown in Figure 21 below.

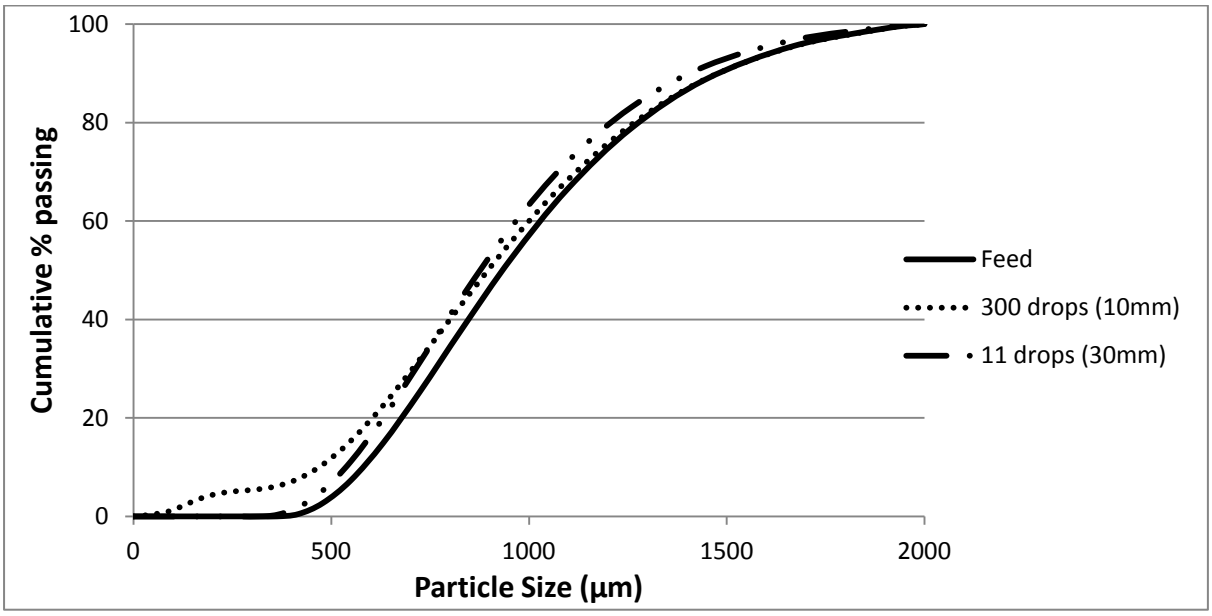

Figure 21: Cumulative distribution plots for varying number of impacts and media size at constant overall input energy.

4.6 Attainable Region Analysis

Representing the particle size distribution in mass fraction space as opposed to the cumulative distribution function representations that are often used in this field of comminution will enable the use of the Attainable Region to be used in optimizing the objective function, in this case, maximizing the amount of size class two. It should be emphasised that the choice of the particle size cut offs of each of size class one, two and three were arbitrary. The mass in each size class as a fraction of the total mass in that stream is represented as m_i with i being the number of that size class. In this work the feed is classified as size class one and the next lower size as class two with size class three being the smallest.

The objective function is to maximize production of size class two and minimize the production of size class three (fines). It should be clarified that for all the results which will be presented, the lines are used to connect the points and they do not represent any model.

Table 2: Mass fraction of Size Class Ranges

Size Class	**Particle Size Range (µm)**
Size Class One (m_1)	2000 – 600
Size Class Two (m_2)	600 – 200
Size Class Three (m_3)	< 200

4.6.1 Mass fraction vs. Number of impacts

Figure 22 - 24 below show the variation of the size classes (m_1, m_2 and m_3) versus the number of impacts for the 10 mm and 20 mm media sizes respectively. This is the same data as presented in Figures 11 – 13, but now grouped into size classes, enabling one to represent the size distribution as a set of three points. Due to the logarithmic scale in Figure 11, 12 and 13, a comparison between the mass fractions with one another would be misleading and the correct information about this issue is shown in the curves below. It can be seen that the amount of material in size class one (large particles) decreases with the number of impacts increasing, whereas size classes two (intermediate particles) and three (fines) increases.

4.6.1.1 Small grinding media size (10 mm)

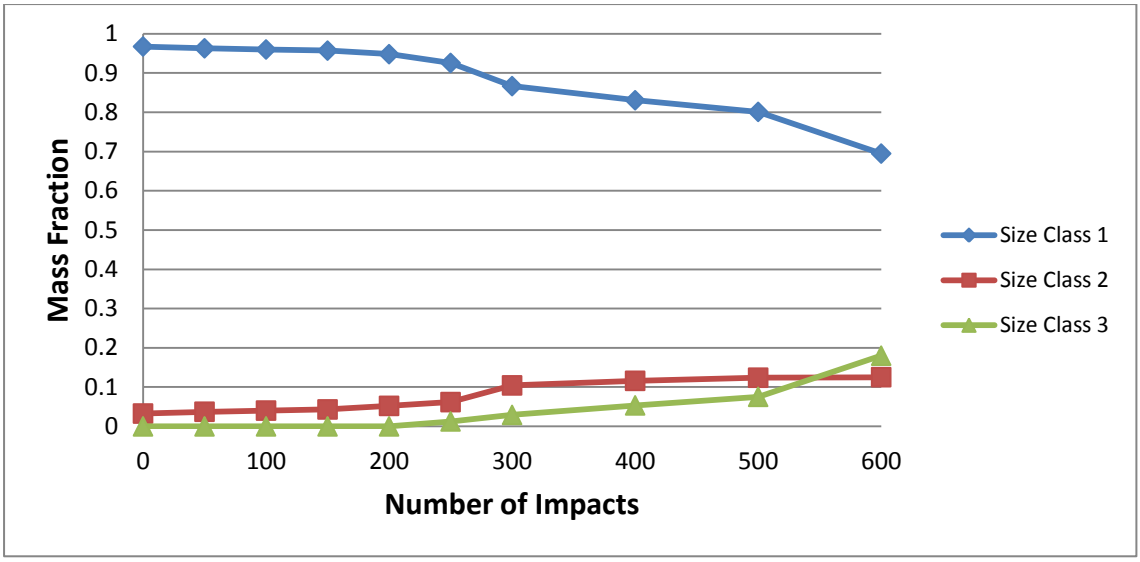

Figure 22: Mass fraction vs. number of impacts for 10 mm ball size as drop weight at a drop height of 1.2 m and 10 g as mass of silica bed particles.

4.6.1.2 Intermediate grinding media size (20 mm)

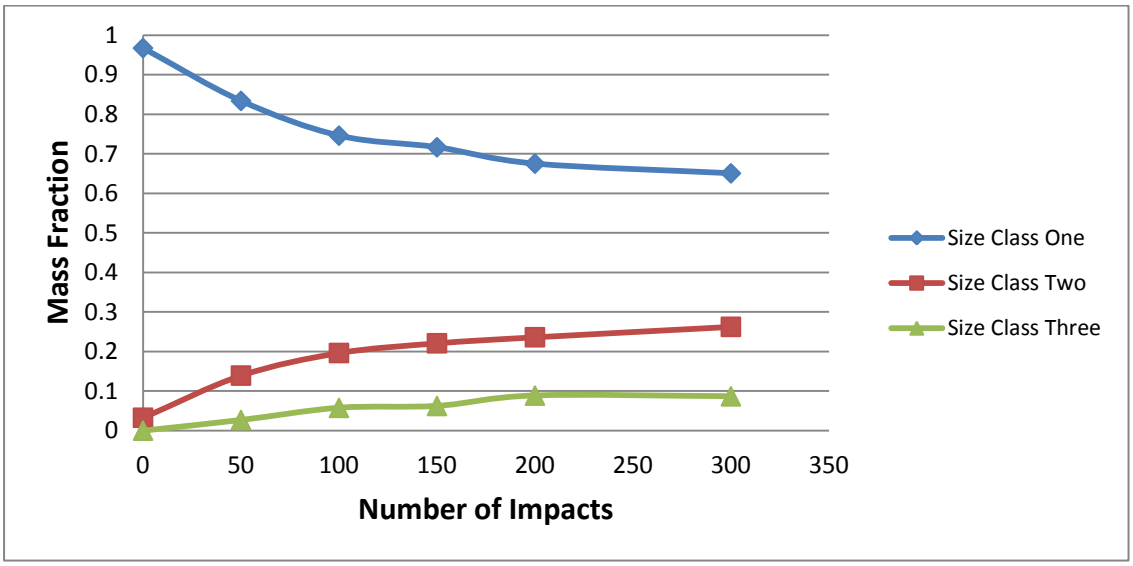

Figure 23: Mass fraction vs. number of impacts for 20 mm ball size as drop weight at a drop height of 1.2 m and 10 g as mass of silica bed particles.

4.6.1.3 Big grinding media size (30 mm)

Figure 24 below shows a plot of the mass fractions of the three size classes (m_1, m_2 and m_3) as a function of the number of impacts. As size class one deceases, size classes two increases until a maximum value of size class two is achieved. Size class three continues to increase with an increasing number of impacts. The maximum value for size class two is 0.31 after 400 impacts.

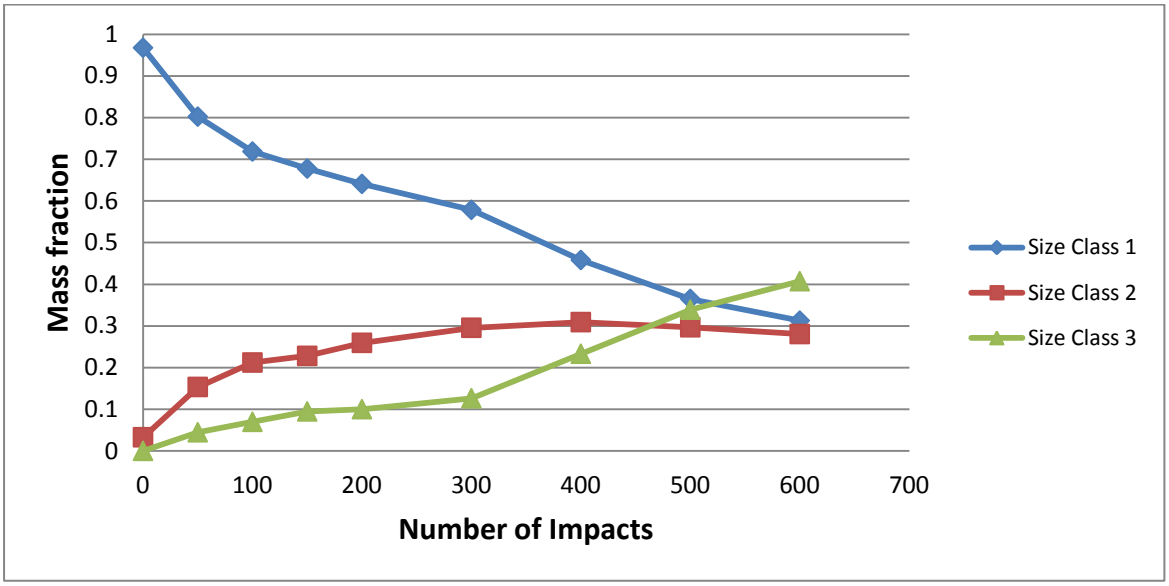

Figure 24: Mass fraction vs. number of impacts using 30 mm grinding media as drop weight at a drop height of 1.2 m and 10 g as mass of silica bed particles.

Figure 24 provides a summary of the mass fraction for different grinding media sizes as a function of number of impacts. It can be seen that for all three feed sizes, size class one (larger particles) always decreases and creates size class two (intermediate particles). The rest of the particles reports into size class three (fine particles). The number of impacts influences the formation of the intermediate size and the fines as well. It should also be stated that the number of impacts for the 20 mm ball size is not the same (Figure 25) as the other cases for the 10 mm and 30 mm ball sizes. The main reason for that is because the 20 mm ball size was used later in the experiments, as discussed in the experimental section.

It can be noticed that there is a change in breakage of size classes for different grinding media sizes. The change in breakage from the 10 mm to 20 mm balls is much larger than the change in breakage from the 20 mm to 30 mm balls, suggesting that eventually the amount of breakage will reach an asymptote, or limit.

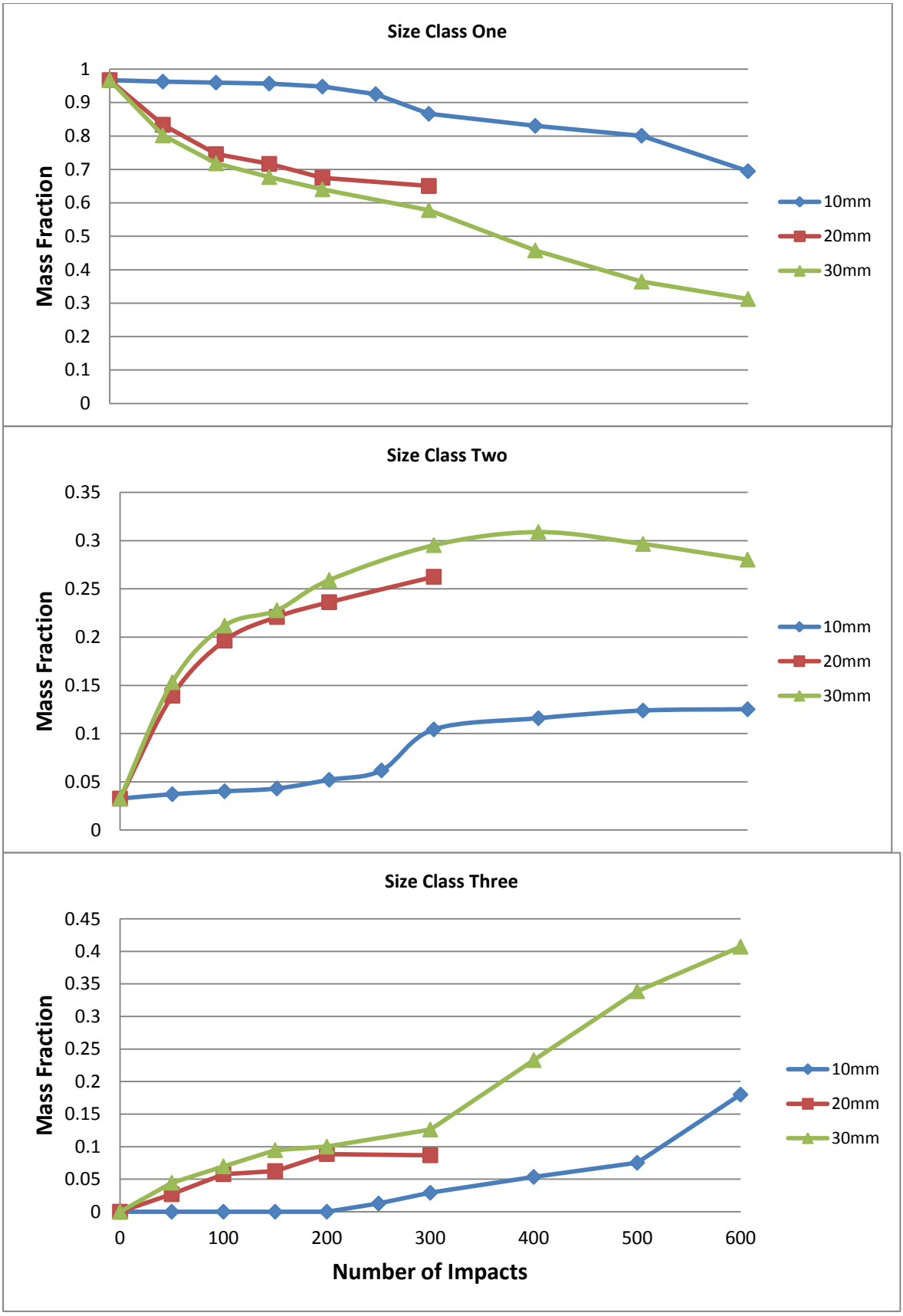

Figure 25: Comparison of the mass fraction vs. number of impacts for different grinding media sizes (10 mm, 20 mm and 30 mm) at drop height of 1.2 m.

4.6.2 Mass fraction vs. Drop Height

The effect of drop height was investigated and the results are presented below. Figure 26 to Figure 28 shows the plot of drop height against the mass fraction of size classes. The value at h = 0 m corresponds to the amount of each size class in the feed material and the total number of drops was kept constant at 50 for each point in all the three figures.

For the two large grinding media, it can be observed that as the drop-height increases the mass fraction of size class one decreases.

The trend that is shown in Figure 26 is that the mass fraction of size class one (coarse) decreases to form the intermediate and the fines as the drop height increases. On the other hand, the amount of material in size class one is relatively unchanged as the drop height is increased for the 10 mm ball size. This shows that the energy of impact of the smallest grinding media size is not large enough to exceed the inherent strength of the particles within the bed. The plots in Figure 27 and Figure 28 indicate how the mass fractions of size class two and three increases as the drop height increases for all different grinding media sizes. It can be seen that the bigger grinding media (30 mm) achieves more fines as compared to the other two ball sizes

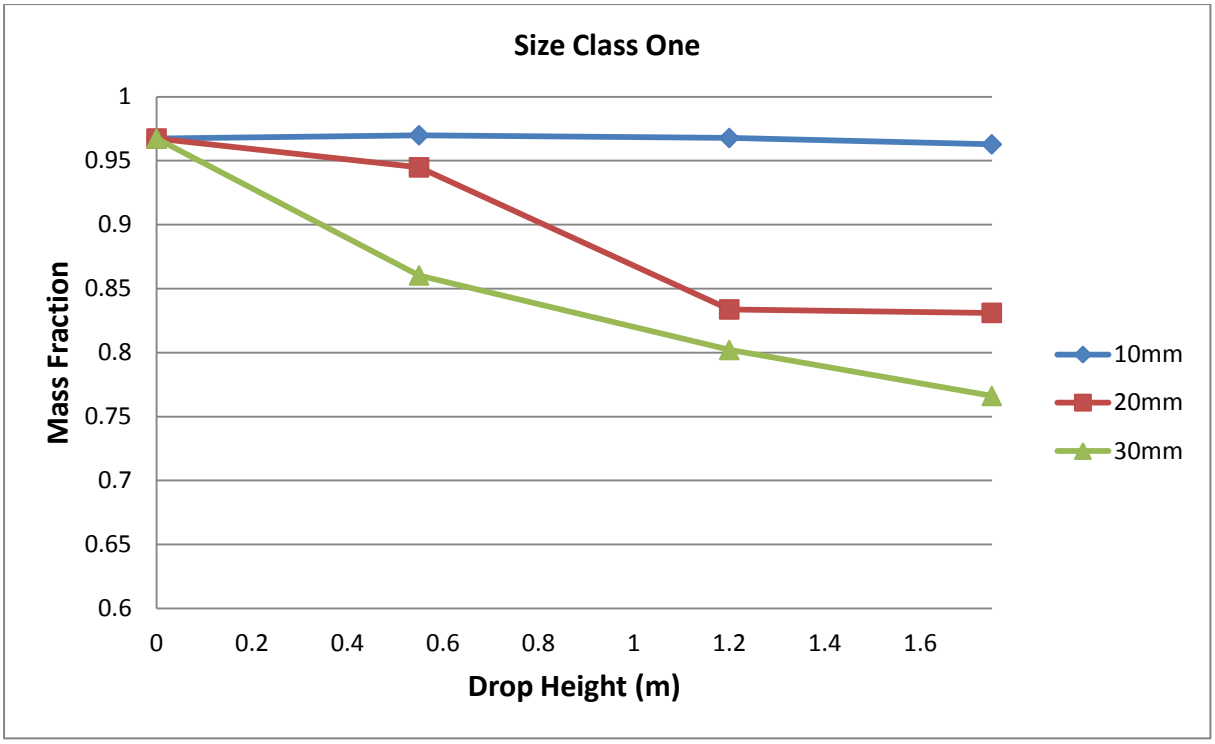

Figure 26: Mass fraction in size class one vs. drop height for different grinding media sizes (10 mm, 20 mm and 30 mm) as one kept the number of impacts at 50 drops and the mass of the silica bed particles at 10 g.

As stated before, there is no breakage for the smallest grinding media diameter, so the amounts of material in size class two and three remain unchanged with increasing drop height. It is of interest to see that the amount of breakage that occurs for the 20 mm grinding media appears to change behaviour between a drop height of 0.55 m and 1.2 m. At a drop height of 1.5 m, the amount of material in each size class changes very little, with all material broken from size class one reporting to size class two. At a drop height of 1.2 m, the amount of material in size class one decrease dramatically, along with a sharp increase in the amount of size class two and three for that grinding media size. This suggests that the inherent strength of the particles lies somewhere between the energies delivered by 50 drops at a drop height of 0.55 m (E = 15.5 J) and 50 drops from a height of 1.2 m (E = 33.8 J). This behaviour suggests that one would have to operate with a ball size larger than 10 mm in order to achieve breakage of this type of material in the range of drop heights up to 2 m.

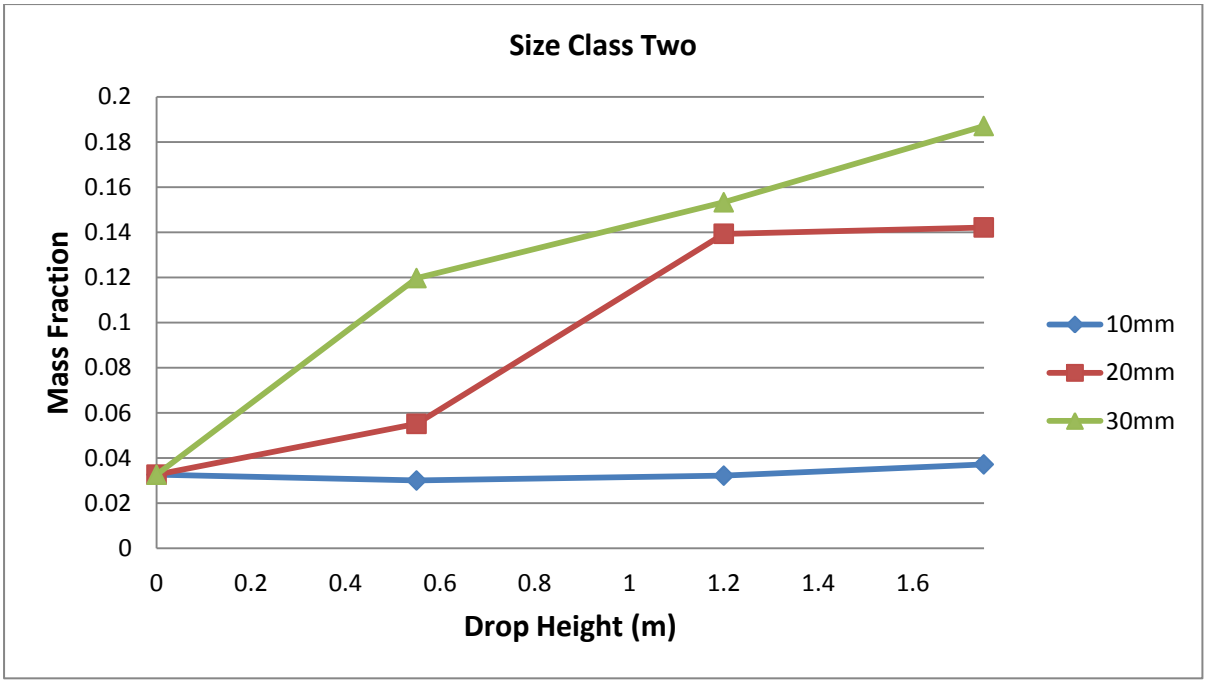

Figure 27: Mass fraction in size class two vs. drop height for different grinding media sizes (10 mm, 20 mm and 30 mm) as one kept the number of impacts at 50 drops and the mass of the silica bed particles at 10 g.

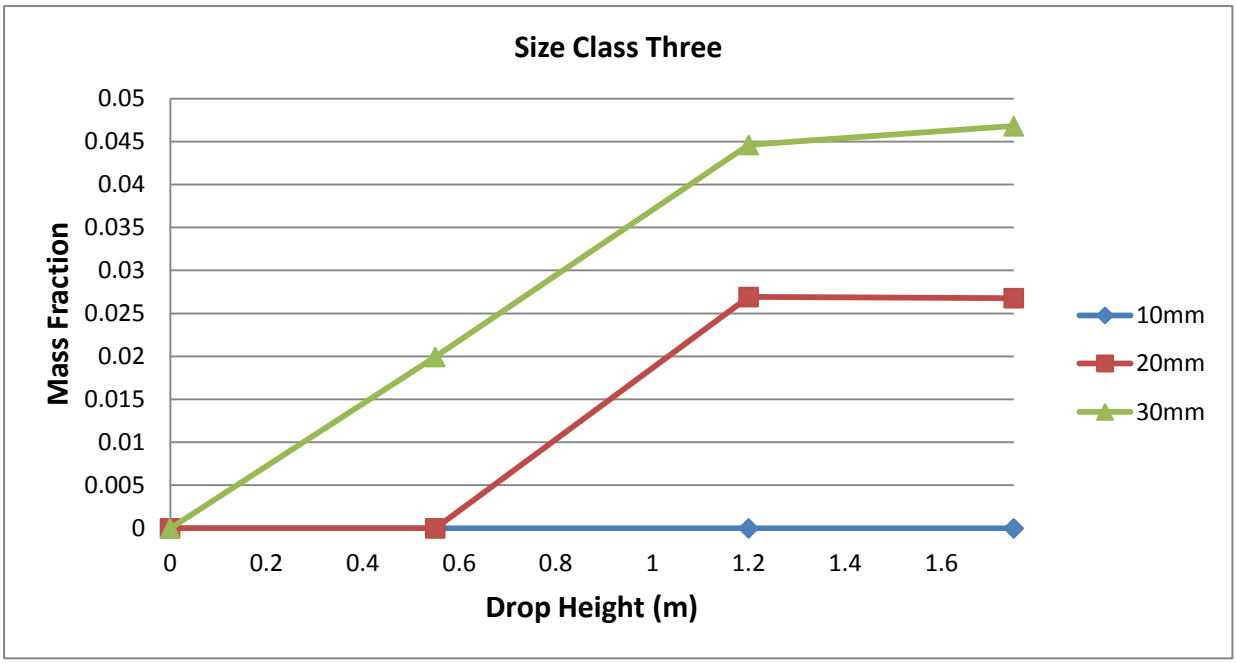

Figure 28: Mass fraction of size class three vs. drop height for different grinding media sizes (10 mm, 20 mm and 30 mm) as one kept the number of impacts at 50 drops and the mass of the silica bed particles at 10 g.

4.6.3 Size Class One (m1) vs. Size Class Two (m2)

4.6.3.1 Small grinding media size (10 mm)

Figure 29 is a representation of the mass fraction of the material in size class two as a function of size class one (the M_1 v M_2 Attainable Region). This plot shows the transformation of particles in size class one (large particles) to particles of size class two (intermediate particles). It can be observed that an increase in number of impacts produces size class two until a maximum value of 0.13 is obtained after 600 impacts. The lines do not represent any model, but they are used to aid the reader with the connections.

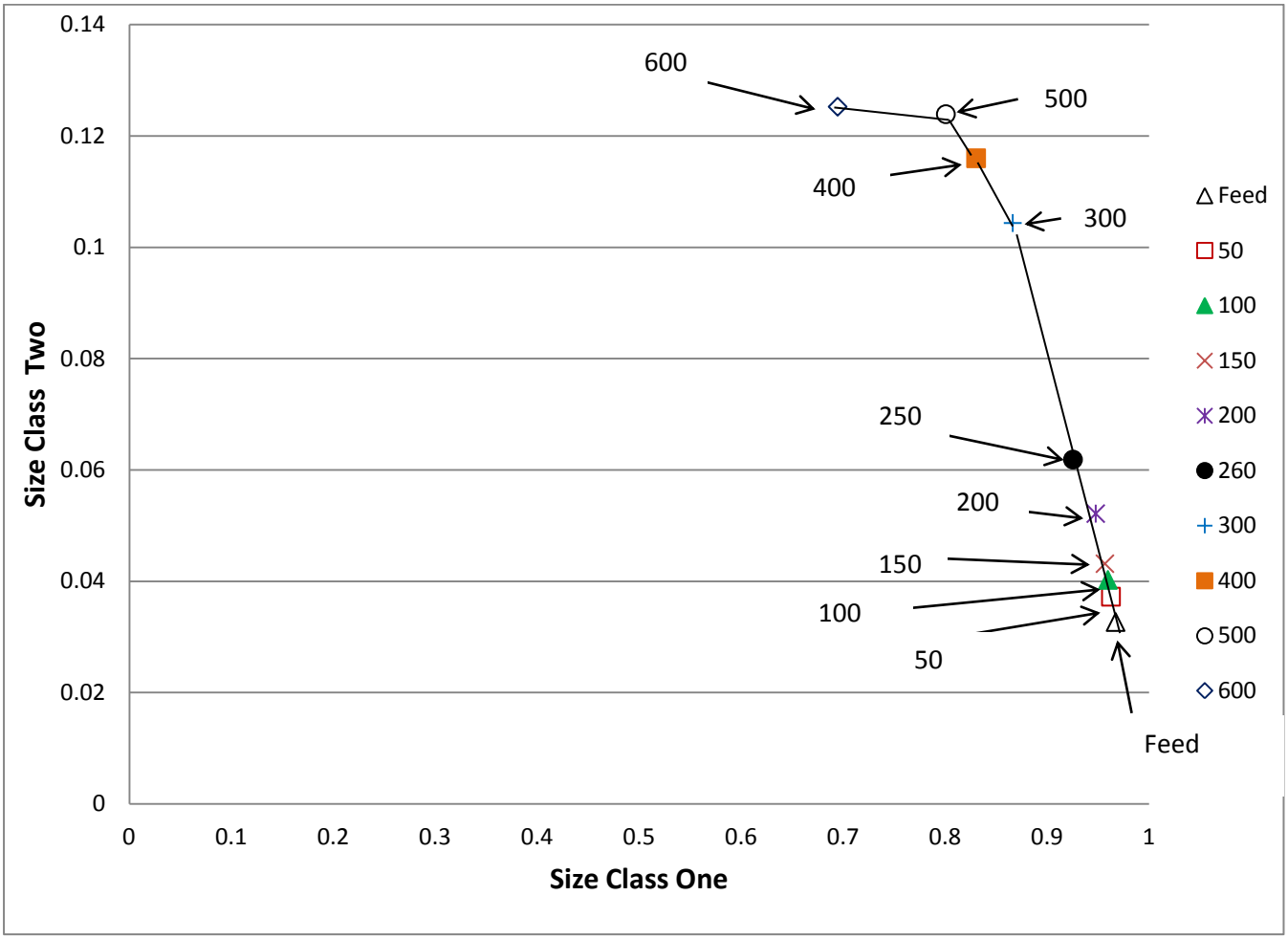

Figure 29: Mass fraction of size class two vs. size class one plots for small grinding media (10 mm) at a drop height of 1.2 m and 10 g of silica bed particles.

4.6.3.2 Intermediate grinding media size (20 mm)

Plotted in Figure 30 is the AR profile for size class one as a function of size class two for 20 mm grinding media. The figure illustrates that as one increases the number of impacts, size class one is consumed at a relatively constant rate (relatively straight line). It is can be noticed that there is no maximum value for size class two, meaning that one needs to increase the number of impacts beyond 300 in order to determine the optimum value for size class two.

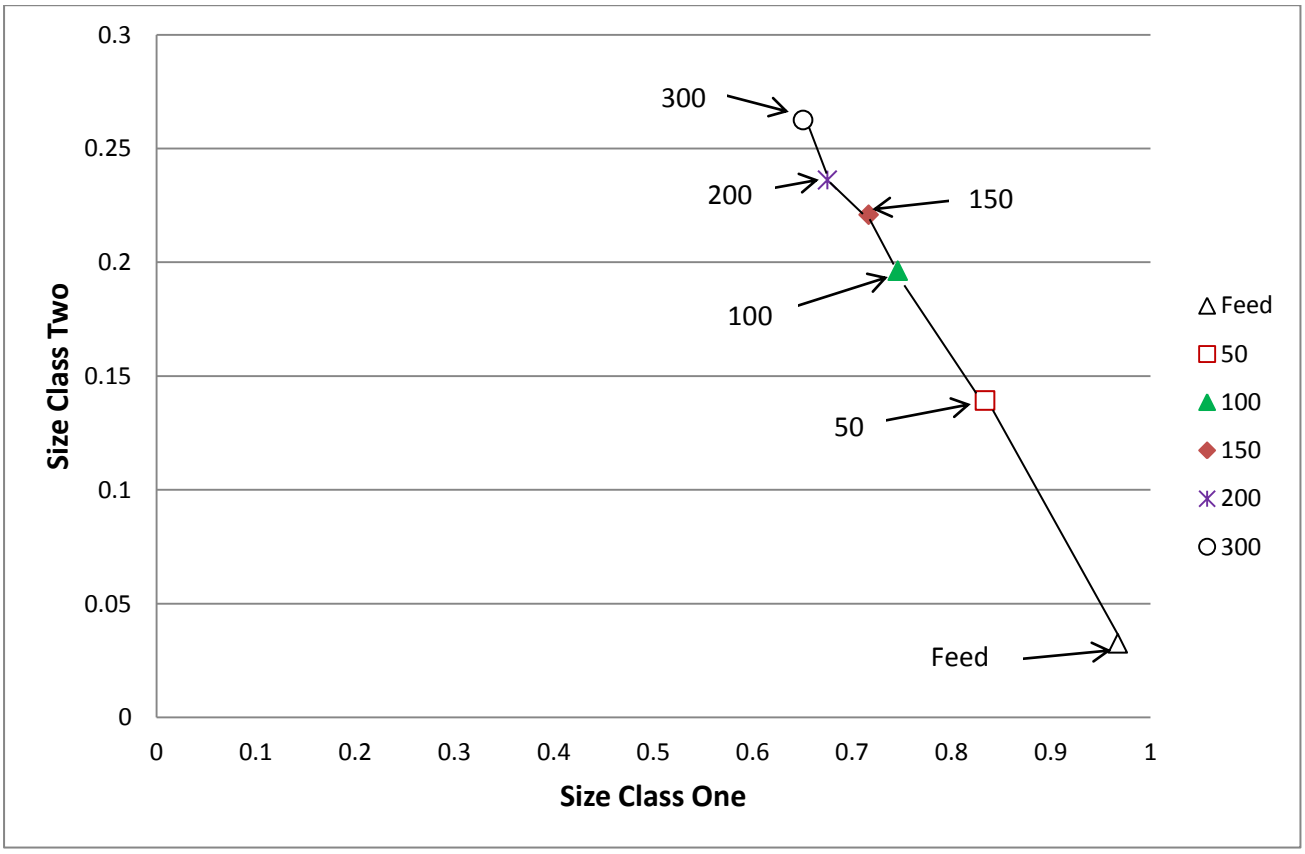

Figure 30: Mass fraction of size class two vs. size class one plots for intermediate grinding media (20 mm) at a drop height of 1.2 m and 10 g of silica bed particles.

4.6.3.3 Big grinding media size (30 mm)

Figure 31 below shows the AR trajectory for the large grinding media. It clearly shows that at these process conditions, for an objective to maximize the mass fraction in size class two, the number of impacts is about 400 drops. As noted before , as the energy input is increased, the mass fraction of particles in size class one (large particles) decreases and the products are distributed among the size class two (intermediate particles) and size class three (fines).

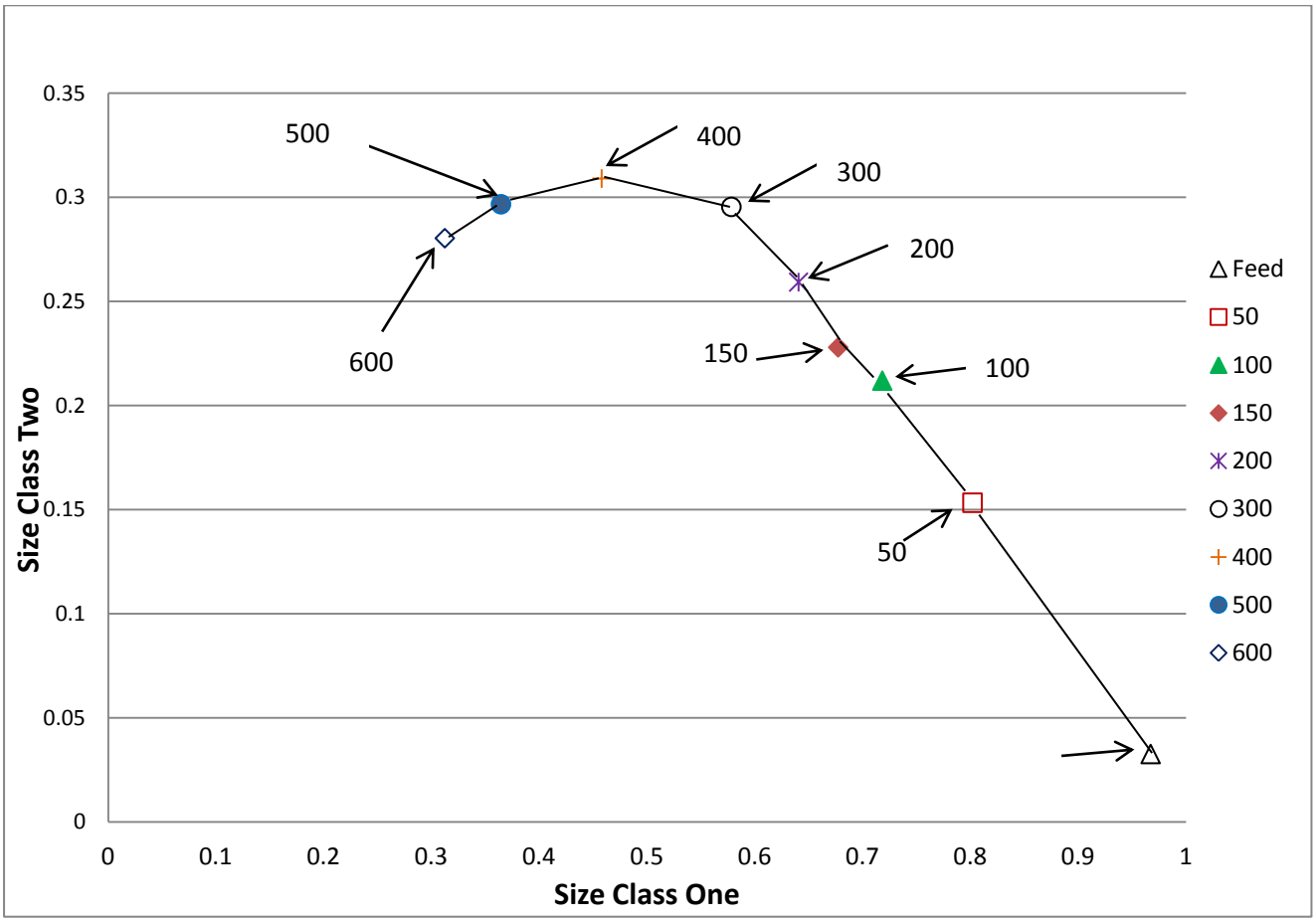

Figure 31: Mass fraction of size class two vs. size class one profile for bigger media size (30 mm) at a drop height of 1.2 m and 10 g of silica bed particles.

A comparison of the AR profiles for all three grinding media sizes are shown in Figure 32a below. It can be seen that as one increases the number of impacts, the mass fraction of size class one decreases to form mass fraction of size class two. It can also be seen that the 20 mm and 30 mm grinding media performs similar breakage with the time scale being the only difference. It should also be highlighted that since the mass fraction of the size classes were chosen arbitrary, if one changes the size class range (Table 2) to another arbitrary size class range (Table 3), the trends do not change as shown in Figure 32b below but it is only the amounts in each of the size classes that vary.

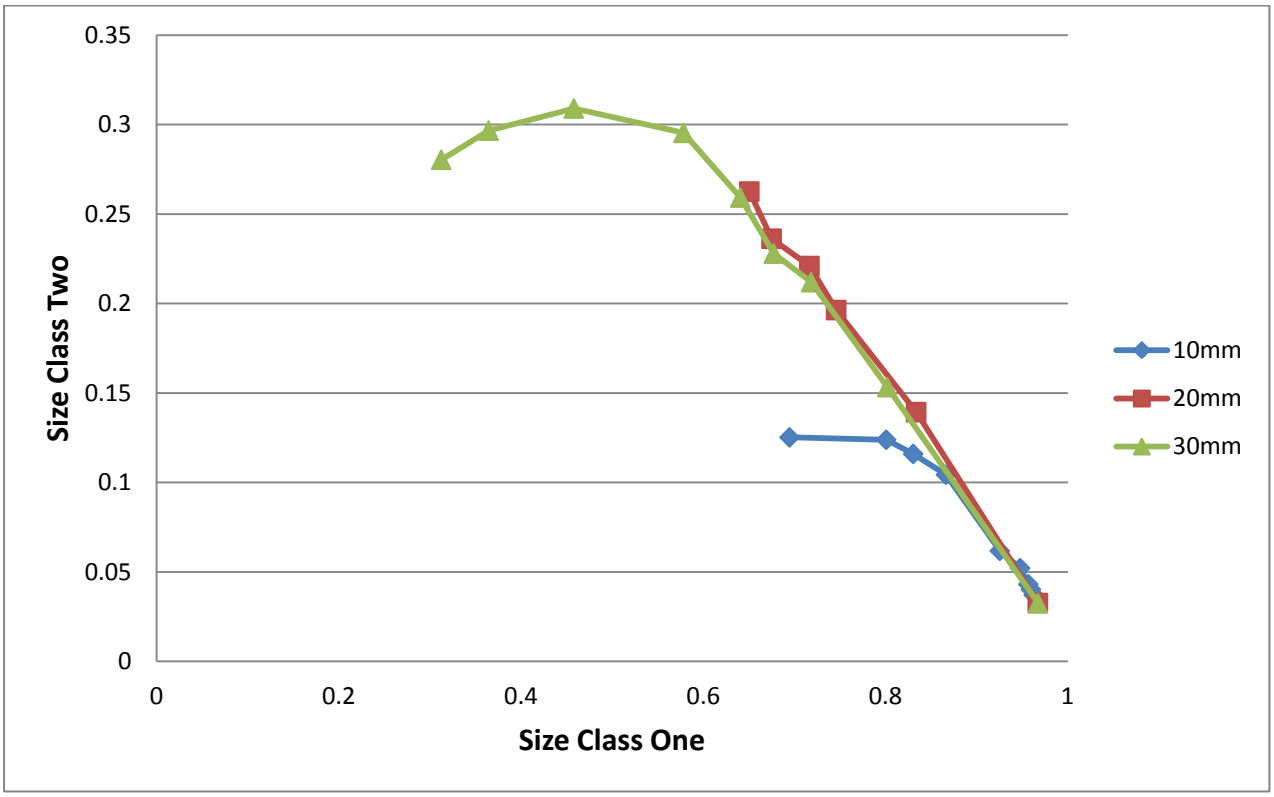

Figure 32a: Comparison of mass fraction of size class two vs. size class one plots for three different grinding media sizes (10 mm, 20 mm and 30 mm) at drop height of 1.2 m and a bed height (mass of bed particles) of 10 g.

Table 3: Mass fraction of the second arbitrary size class ranges

Size Class	**Particle Size Range (µm)**
Size Class One (m_1)	2000 – 800
Size Class Two (m_2)	800 – 300
Size Class Three (m_3)	< 300

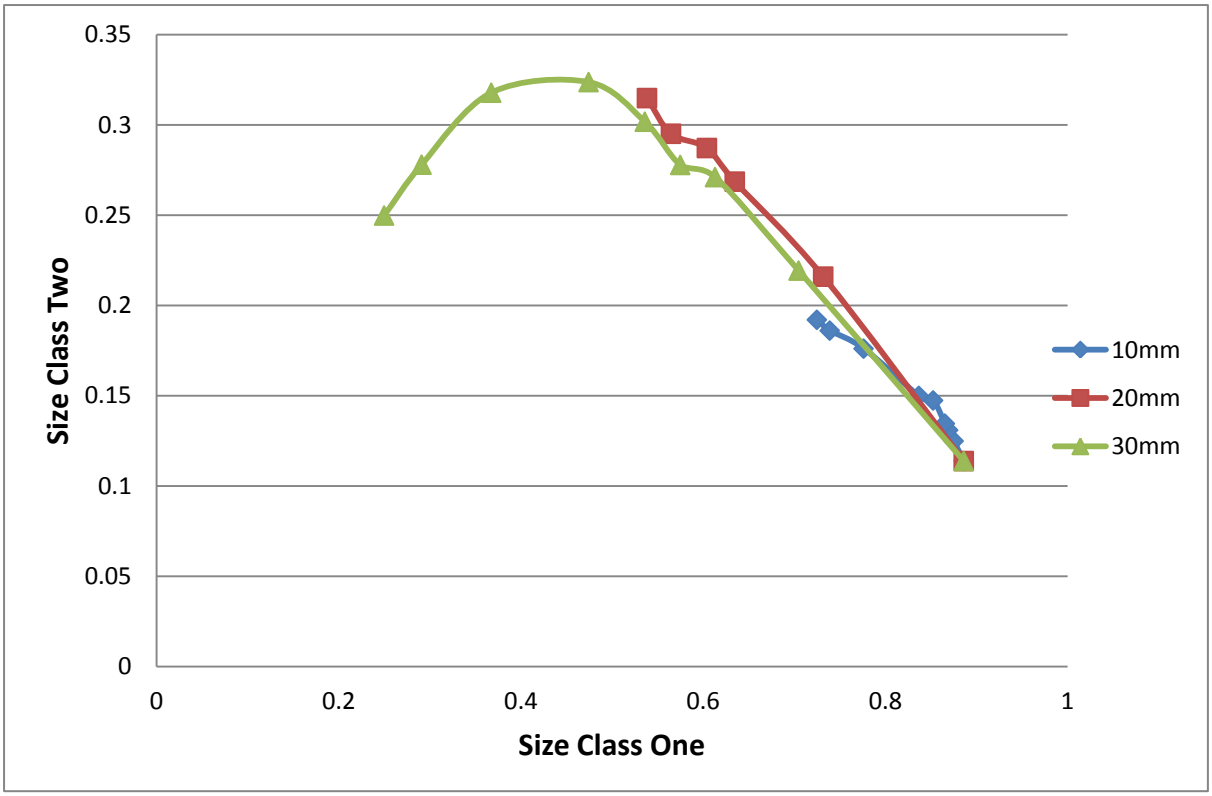

Figure 32b: Comparison of mass fraction of size class two vs. size class one plots for three different grinding media sizes (10 mm, 20 mm and 30 mm) at drop height of 1.2 m and a bed height (mass of bed particles) of 10 g.

4.6.4 Size Class One vs Size Class Three

Figure 33 shows how the mass fraction of size class three (fines) increases as the mass fraction of size class one (feed) decreases for all three different grinding media. It can be seen that the same trend is observed whereby the 10 mm grinding media produces more fines for the same reduction in the amount of size class one, compared to the 20 mm and 30 mm ball sizes.

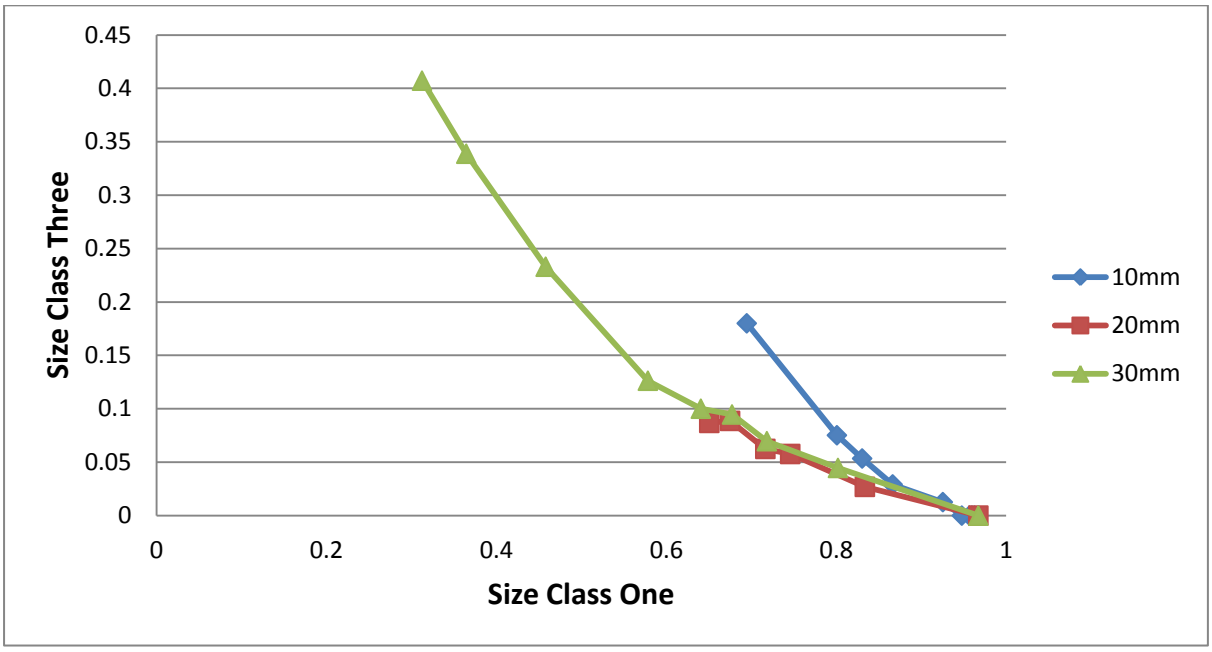

Figure 33: Comparison of mass fraction of size class three vs. size class one for three different grinding media sizes (10 mm, 20 mm and 30 mm) at drop height of 1.2 m and a bed height (mass of bed particles) of 10 g.

4.7 Effect of impact energy on the size classes

The effect of input impact energy was investigated to determine the breakage behaviour of silica bed particles at a constant drop height of 0.55 m. The mass fractions were then plotted as a function of impact energy. Figure 34 to Figure 35 below shows the same behaviours that were observed in the results section 4.5, whereby the size class one decreases to form size class two and three as the impact energy increases. The difference between what is plotted there and what is plotted here is that the x- axis is in terms of the impact energy. This will allow one to determine the optimum impact energy that can be achieved for the production of

size class two. It can also be noticed that small grinding media doesn't perform as much breakage as compared to the 20 mm and 30 mm ball sizes.

4.7.1 Small grinding media size (10 mm)

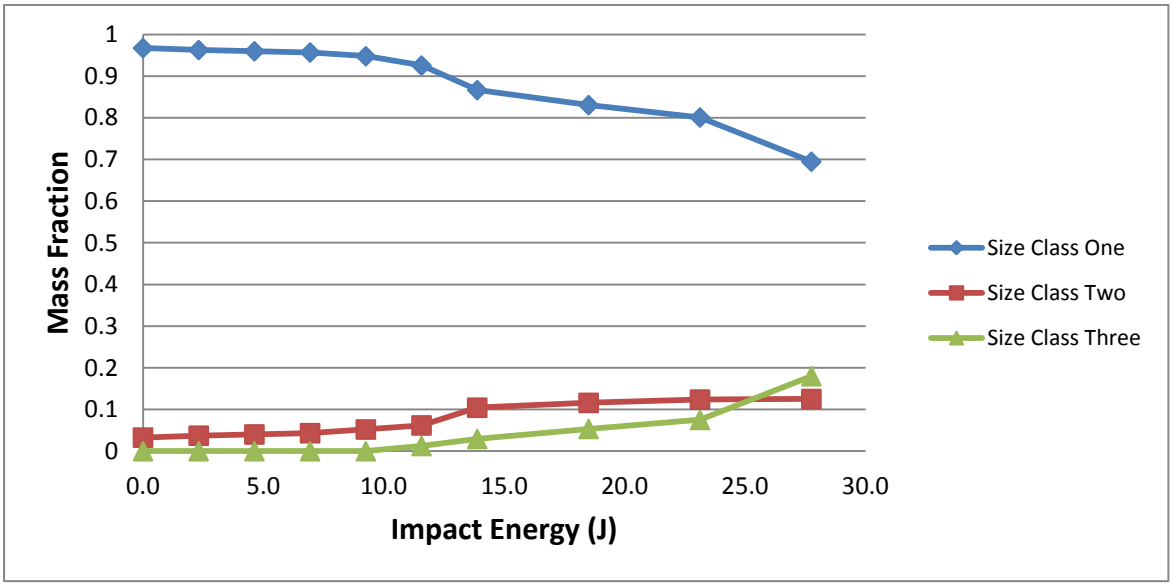

Figure 34: Mass fraction vs. Impact Energy for 10 mm ball size at constant drop height of 1.2 m and 10 g as mass of silica bed particles.

4.7.2 Intermediate grinding media size (20 mm)

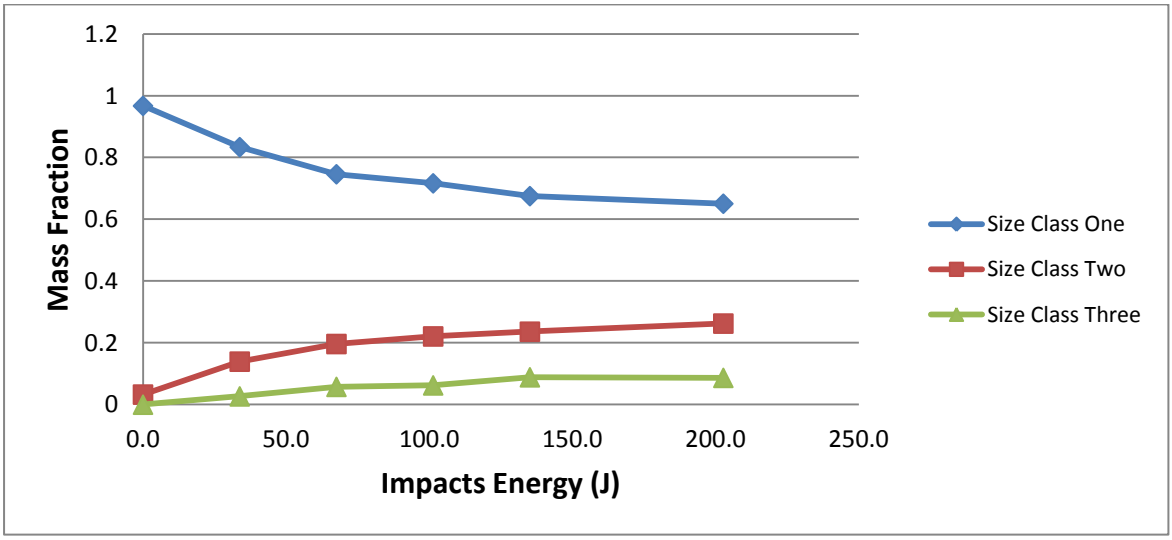

Figure 35: Mass fraction vs. Impact Energy for 20 mm ball size at constant drop height of 1.2 m and 10 g as mass of silica bed particles.

4.7.3 Big grinding media size (30 mm)

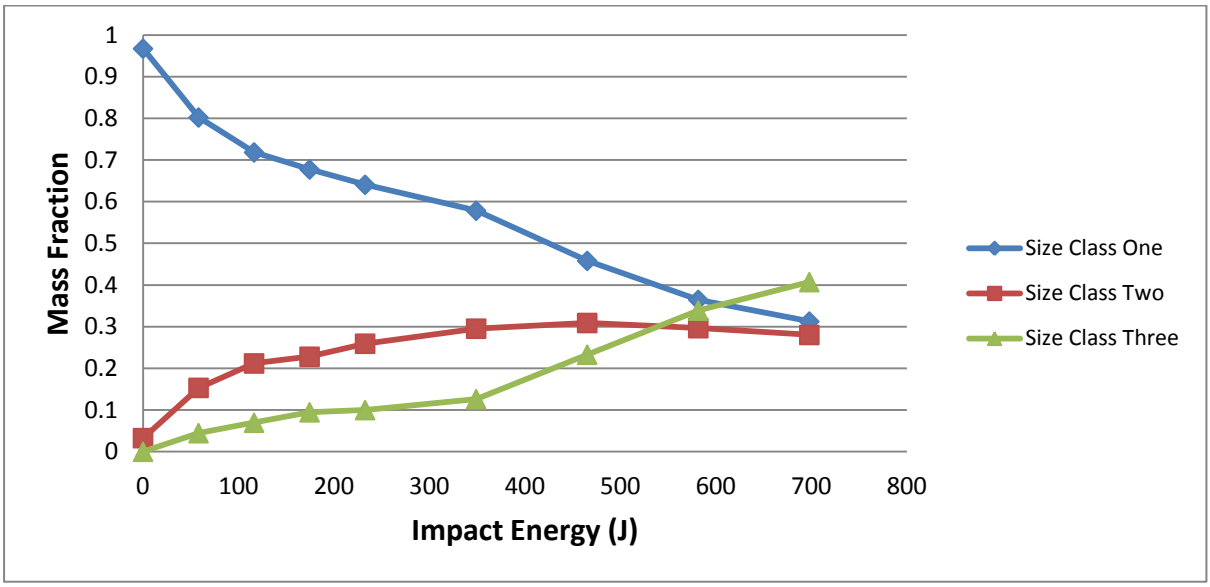

Figure 36: Mass fraction of size classes vs. Impact Energy for 30 mm ball size at constant drop height of 1.2 m and 10 g as mass of silica bed particles.

As can be seen from the above Figure 36, the same trend is observed as discussed previously as one increases the impact energy. The corresponding size class two as a function of impact energy for all three grinding media is shown in Figure 37 below. Two variables were considered for this plot, namely the number of impacts (N) and the drop height (h). It can be observed that the mass fraction of size class two increases as the impact energy increases. As one varies the number of impacts, it can be observed that there's an optimum value of mass fraction of size class two which is obtained. Initially, grinding using smaller media size appears to give the optimum value of size class two, compared to both the 20 mm and 30 mm media sizes. It can be seen that at an impact energy less than 100 J, there is more production of size class two with both the 10 mm and 20 mm grinding media sizes, compared to the 30 mm media. However, the overall energy of the smaller media is much less than that of the largest media size, so the maximums in size class two production were not achieved. When the drop height is varied, it can be seen that the curves overlap on top of each other. The same trend is also observed whereby there is an increase in the formation of size class two as the impact energy increases as well.

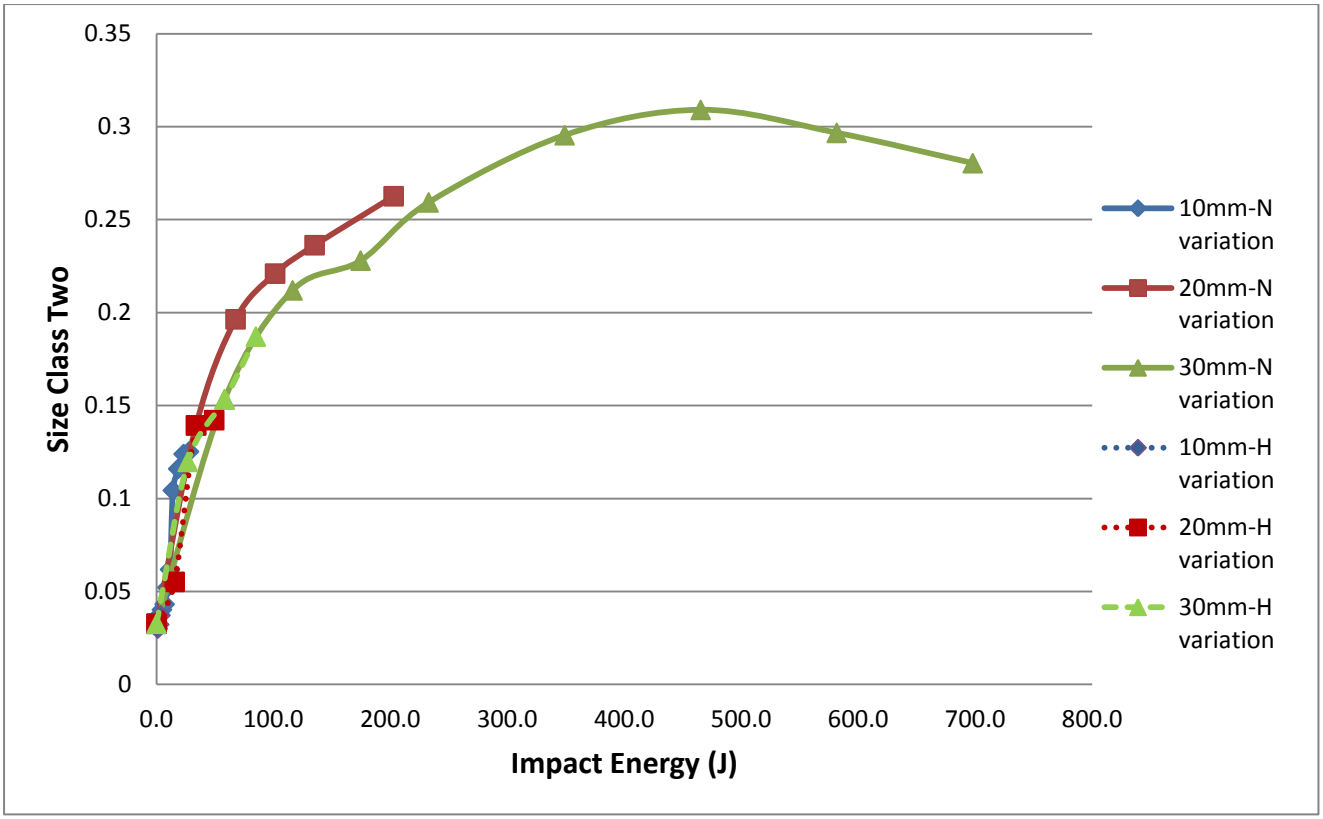

Figure 37: Mass fraction of size class two vs. Impact Energy for 10 mm, 20 mm and 30 mm grinding media sizes at a drop height of 1.2 m while varying the number of impacts.

4.8 Specific Energy as a function of mass fraction

It was shown previously (Section 4.2 and 4.3) that the amount of breakage depended on both the drop weight and the bed height and it may be useful to normalize the data to remove the effect of bed height. Therefore, we plot here the same data as a function of specific energy, which is the amount of energy delivered per mass of particles. This is presented in terms of specific energy versus the mass fraction of each size class. For the purpose of discussion the 30 mm grinding media was chosen and is shown in Figure 38 below. It can be seen from Appendix D3 that the trends are similar for the 10 mm and 20 mm grinding media sizes.

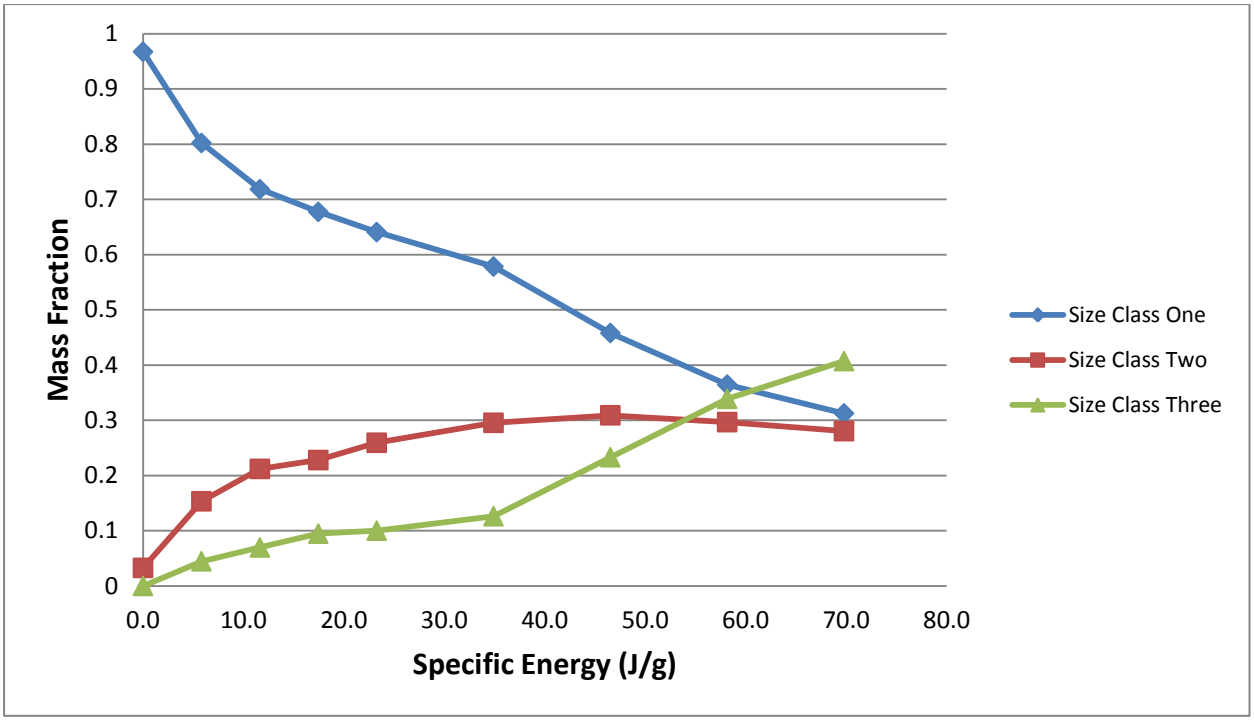

Figure 38: Specific Energy (J/g) as a function of the mass fraction of size classes for 30 mm grinding media at drop height of 1.2 m

Figure 38 represents the specific energy vs. mass fraction in size class one for the all three grinding media sizes when the drop height and the number of impacts was kept constant at 0.55 m and 50 respectively. The mass fraction in size class one plotted here is the TOTAL M_1 after 50 drops. It is not the same as the previous size class ones (**Error! Reference source not found.**), where the mass fraction in size class one is instantaneous as one increases the number of impacts from 1,2,3 etc. It can be observed from Figure 39 below that as one increase the bed height (mass of sample) and specific energy, there is less breakage taking place.

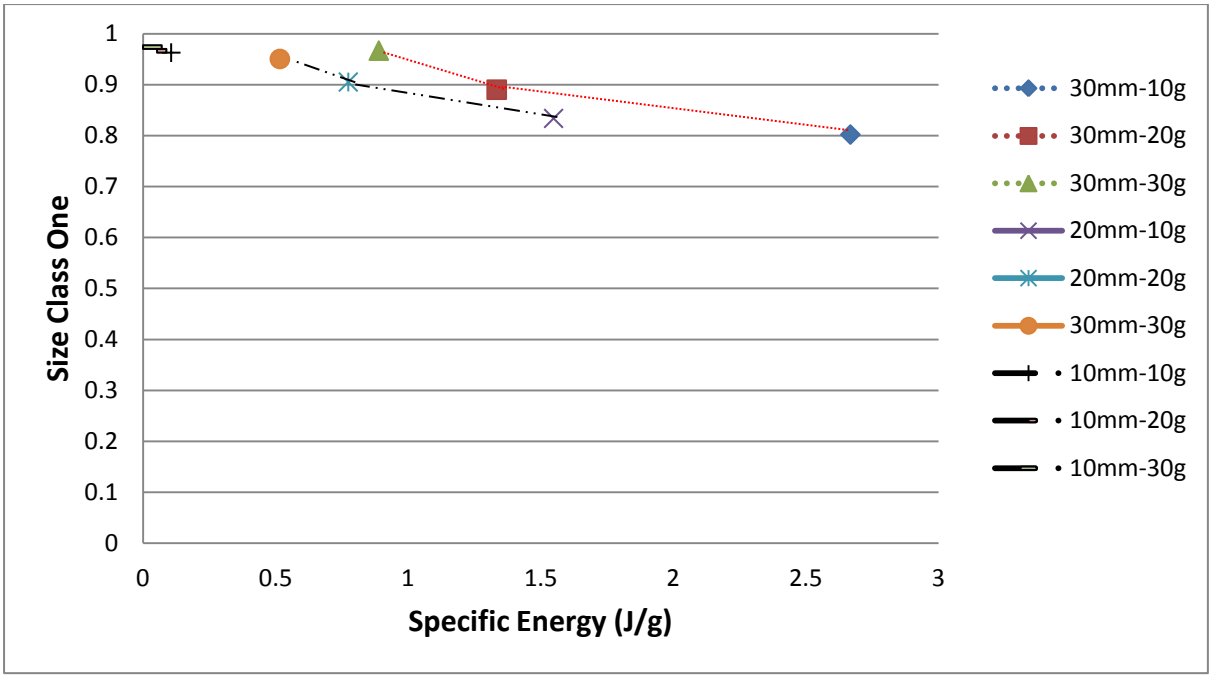

Figure 39: Mass fraction of size class one as a function of varying specific energy at different bed heights (10 g, 20g and 30g) for three different grinding media sizes (10 mm, 20 mm and 30 mm) at constant drop height of 0.55 m and 50 impacts.

The overall mass fraction of size class one after 50 impacts was plotted as a function of specific energy for all the cases tested as depicted in Figure 40 below. It can be seen that there is a trend which shows that as the specific energy increases the mass fraction of size class one decreases to produce the smaller classes. Tabulated below (Table 3) is the data used in plotting Figure 40. Generally there is a decrease in the amount of material in size class one as specific energy increases.

Table 4: Specific energy vs. mass fraction of size class one for different runs at 50 drops

Case (Run) No	h (drop height)	M_p (bed height)	d_m (Ball Size (mm))	E_s (Specific Energy)	Size Class One
1	0.55	10	10	0.106	0.970
2	0.55	20	10	0.053	0.966
3	0.55	30	10	0.035	0.974
4	0.55	10	20	1.549	0.890
5	0.55	20	20	0.774	0.905
6	0.55	30	20	0.516	0.966
7	0.55	10	30	2.668	0.860
8	0.55	20	30	1.334	0.890
9	0.55	30	30	0.889	0.967
10	1.2	10	10	0.232	0.968
11	1.2	10	20	3.379	0.834
12	1.2	10	30	5.822	0.802
13	1.75	10	10	0.338	0.963
14	1.75	10	20	4.928	0.831
15	1.75	10	30	8.490	0.766

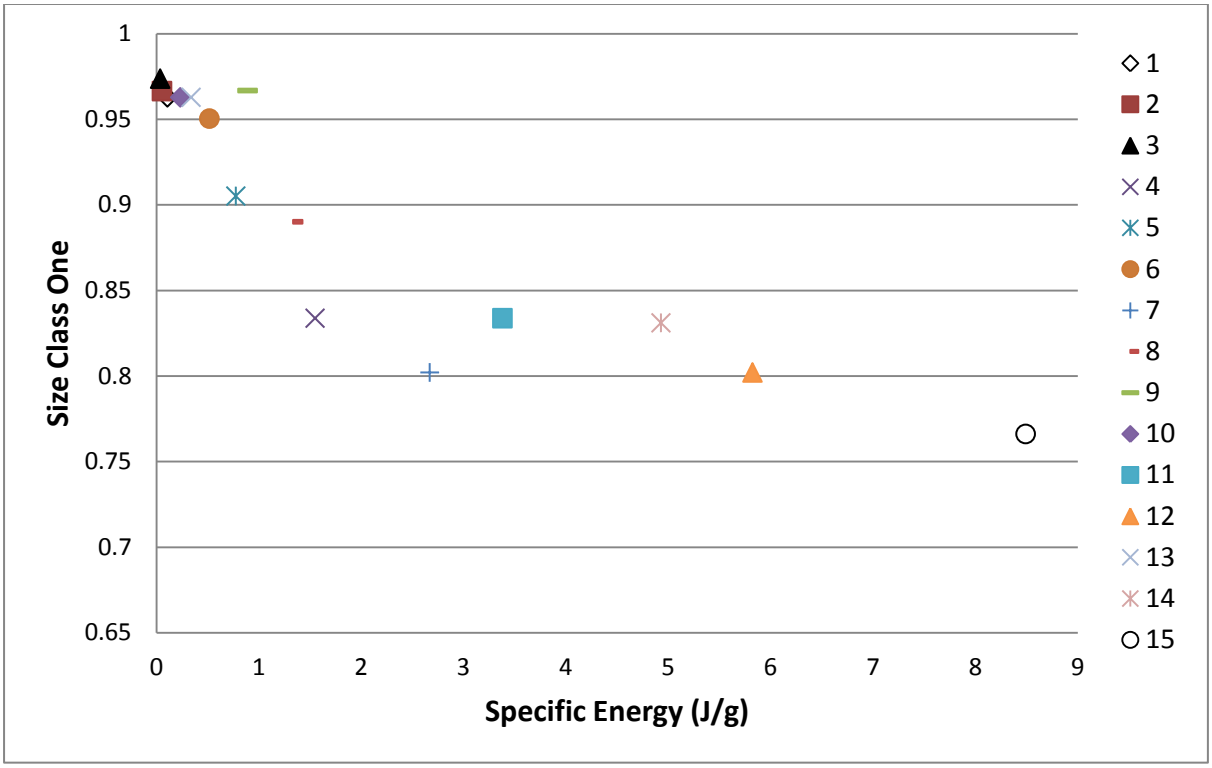

Figure 40: Mass fraction of size class one as a function of varying specific energy at different run numbers for three different grinding media sizes (10 mm, 20 mm and 30 mm) at constant drop height of 0.55 m and 50 impacts.

We can look at some of the trends between the cases in more detail to determine which conditions produce the most breakage of size class one. Figure 41 below depicts the plot of the variation of drop height as a function of mass fraction of size class one after 50 impacts when the bed height (mass of the particles) was kept constant at 10 g. It can be seen that as the drop height increases, the size class one decreases to produce intermediate size classes. It can also be noticed that as the grinding media increases from 10 mm to 30 mm, the mass fraction of size class one decreases as well.

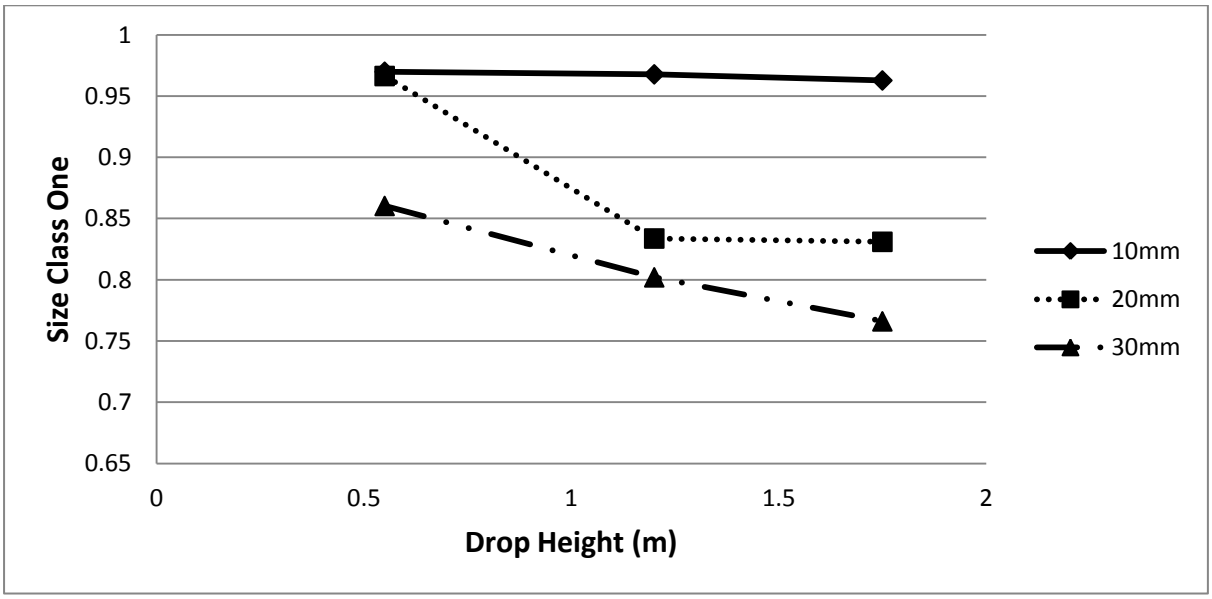

Figure 41: Mass fraction of size class one as a function of varying drop height for three different grinding media sizes (10 mm, 20 mm and 30 mm) at constant drop height of 0.55 m and 50 impacts.

The mass fraction of size class one after 50 impacts was also plotted as a function of grinding media size by keeping the bed height constant at 10 g. It can be noticed that as one increases the ball size, the mass fraction of size class one decreases. It is also evident that the mass fraction of size class one decrease as well when the drop height is increased from 0.55 m to 1.75 m.

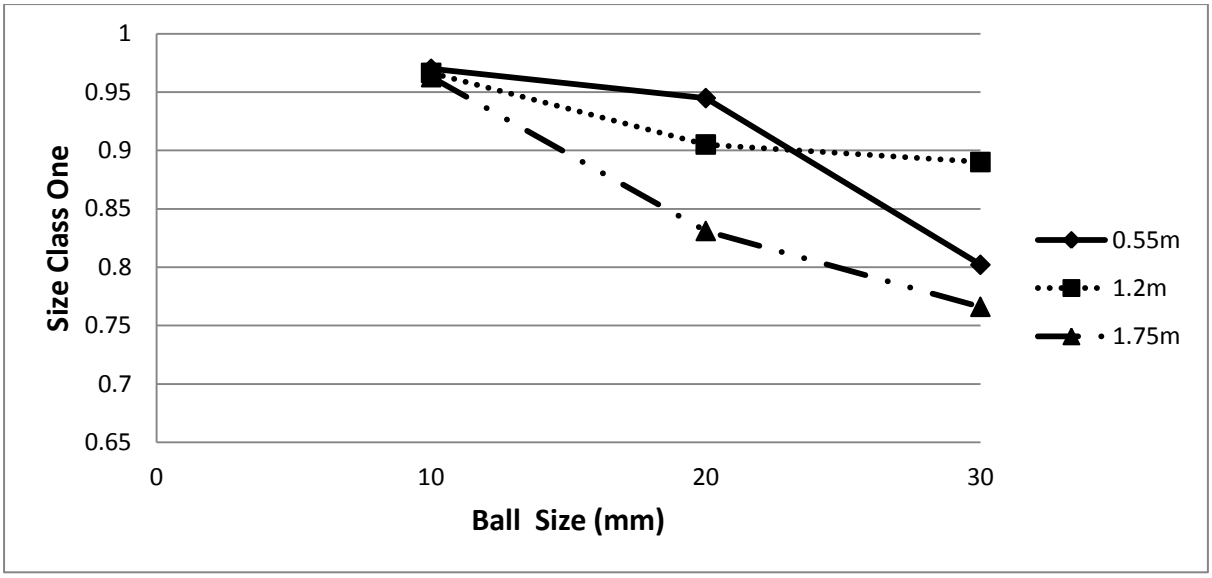

Figure 42: Mass fraction of size class one vs. grinding media size for varying drop height while keeping bed height and number of impacts constant at 10g and 50 respectively.

The same analysis of determining how the overall mass fraction is affected by variation of bed height and grinding media was also investigated by keeping the drop height constant at 0.55m. It can be observed that the mass fraction of size class one increases as the bed height (mass of the particles) increases for the 10 mm and 30mm ball sizes. It can also be noticed that at a constant bed height, as the grinding media size increases from 10 mm to 30 mm, the mass fraction of size class one decrease.

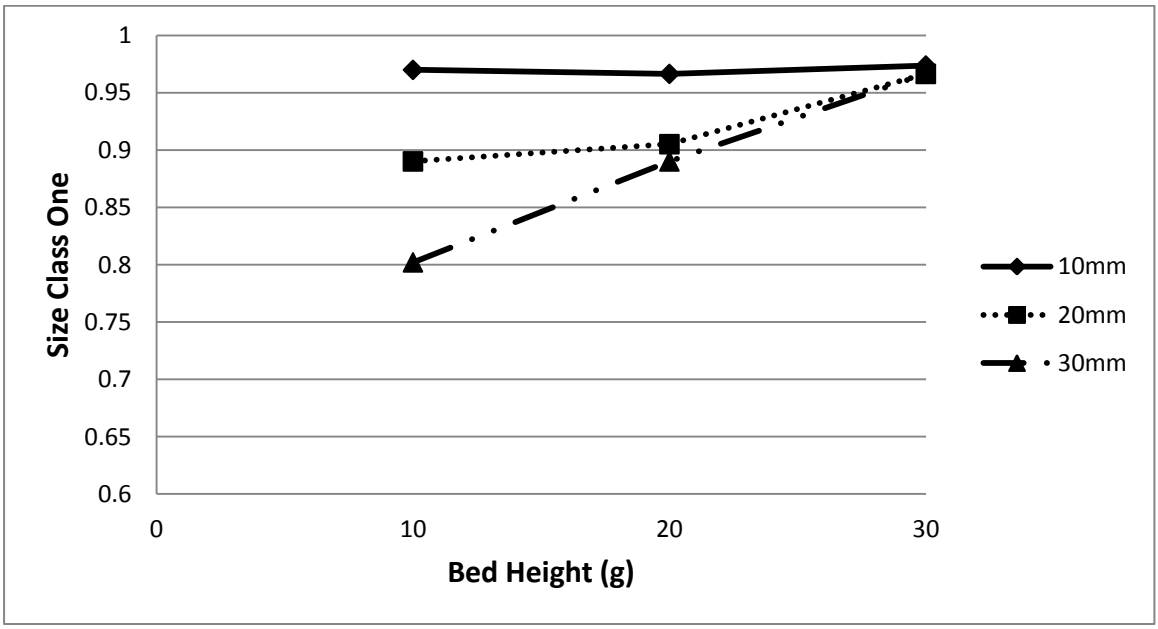

Figure 43: Mass fraction of size class one as a function of bed height for three different grinding media sizes (10 mm, 20 mm and 30 mm) at constant drop height of 0.55 m and 50 impacts.

CHAPTER 5

5 DISCUSIONS

From the results section, it was observed from Figure 6 that the 10 mm ball size curves lie on top of each other at low energy input (0 – 200 impacts) and only after 250 impacts there's breakage taking place. This suggests that there's a possible strength threshold of particles at 200 drops. It can be seen from Table 1 that, for the 10 mm grinding media, the minimum input energy and specific energy required for breakage is 11.6 J and 1.2 J/g respectively. This can be attributed to the chipping mechanism and the fact that a greater proportion of the input energy is consumed in causing the primary fracture of the parent particles and little energy is left for subsequent breakage of the fragments. As the fineness of the breakage products increases with an increase in the applied energy, the difference can be large. This type of breakage is only able to chip off small edges of the particles, which is representative of abrasion-type breakage. It was shown that increasing the impact energy from 11.6 J to 27.8 J increases the production of fine particles (Figure 7). It can be seen from figure 6 and 7 that both the impact energy and the number of impacts have an effect on the breakage behaviour. It was also observed that some minimum amount of impact energy had to be exceeded before any breakage could take place.

For Figure 8 it seems like the amount or grinding begins to decreases as the number of drops increases, suggesting breakage may be approaching a plateau. Also, the largest size remaining in Figure 8 is about 1500 µm, where it looks to be a little LARGER for the larger grinding media (30 mm). This would suggest that there is another type of breakage occurring between the 20 mm and 30 mm media sizes. On the other hand, there are more fines made in the 30 mm case, which might suggest that there is a higher influence of the cushioning effect for the 30 mm where there are more fines.

The resultant PSD for the 30 mm grinding media (Figure 9) shows that there is sufficient amount of energy input to break the particles. The results indicate that breakage is influenced both by the mass of the drop weight and the impact energy. This observation agrees with what Whittles et al (2006) also found.

The two plots (Figure 8 and Figure 9) are different from the first plots (Figure 7). Unlike the 10 mm case, there is a significant difference between the curves, even for only 50 drops. This suggests that these media sizes are now large enough to cause breakage by another mechanism that is not abrasion. The results as shown in the above figures are consistent with the findings of Sahoo et al (2004), Awachie (1983), Narayanan (1985), Sahoo (2004) and Weedon et al (2000).

Krogh (1980) stipulated that when there is regularity in the physical properties of the particles used, for which in this project the silica ore did, no particles will be broken below a certain energy level. The experiment performed agrees with Krogh's theory especially looking at Figure 7. For the lowest ball size, there was little noticeable breakage up until the total energy delivered to the particle bed exceeded ~1 J/g (<200 impacts). The 10 mm ball could only deliver specific energies between 0.23 -0.93 (J/g) and there was no size reduction observed until the specific energy was increased to 1.2 (J/g) whereby there were fines formed. However when the same material was subjected to high energies delivered by the 20 mm and 30 mm ball sizes there was a clear and significant size reduction. Therefore, from the results above it can be deduced that specific energy, 0.93 J/g, is below the minimum required energy to break this particular bed of silica sand. The tests verified the assumption that the fineness increases with the energy input.

The number of impacts effect on the resultant PSD showed that there is a small grinding difference between 20mm and 30 mm ball sizes (Figure 10). A larger grinding difference is observed between 10 mm and 30 mm grinding media sizes. It can also be noticed that when scaled up (additional mass) the 20 mm and 30 mm seems to do the same amount of grinding while their curves always cross each other as shown in Appendix C. This suggests that the energy delivered to the particle bed by the 20 mm media is sufficient for breakage and the additional energy delivered by the larger media is wasted to the cushioning of the particles within the bed. The same trend holds at different number of impacts.

It was shown from the results (section 4.2) that at a constant drop height of 1.2 m, the smaller the bed height, the more fines produced. When using the 10 mm ball size, not enough noticeable breakage took place compared to 20 mm and 30 mm ball sizes (Figure 11). It was also observed that deeper bed dissipates more energy as expected. The effect of increasing the bed height also showed that there is a reduction in the median size (d_{50}) for each media size. The trend observed from Figure 11 to 13 showed that the bed height have an effect on

the resultant PSD. The results suggest that, in any type of a mill, the mass of the particles have an influence on the size reduction. From the results presented, with the objective of producing fines, one will need to charge the mill with less material compared to more material.

The effect of the drop height was investigated as explained in the results (section 4.3) and it was shown that 20 mm and 30 mm ball sizes achieve more breakage as compared to the 10 mm ball size when the drop height increases. This is expected since the mass of the particles was kept constant as the drop-height was increased thus increasing the breakage area of the particles. There is some breakage of the feed for the 10 mm case. However, breakage does not increase as one increase the drop height as expected, so it shows that there are some particles that break even at low energies. The results mean that in any type of a mill, the height at which the grinding media is raised to has an effect on the product size distribution. The effect of grinding media size on the relation between product fineness and specific energy is based on the fact that the stress intensity and the number of stress events also change with changing media size. With increasing grinding media size, the mass of an individual grinding medium increases and, thus, the stress intensity also increases. It was also shown that increasing the drop height only makes a difference until it reaches a point where breakage occurs similarly regardless of the energy input. Another interesting behaviour that is observed when the median size (d_{50}) is plotted as a function of the bed height (Figure 14) is that the 30 mm line shows that 30 mm grinding media at the largest bed height is virtually unchanged from the feed, yet the smaller media produce breakage. This implies that the breakage does not only depend on the specific energy but also on the grinding media size.

The drop height effect on the mass fraction showed that as the drop-height increases the mass fraction of size class one decreases (Figure 27 to Figure 29). This is what was expected because, for the same amount of bed height (10 g) and the same grinding media size, as you increase the drop height, you increase the amount of energy delivered to the particles in the bed and the greater the amount of breakage from size class one should be. Also, as you increase the ball size for a constant drop height (h), the amount of breakage out of size class one increases, as expected. This is because bigger grinding media (20 mm and 30 mm) have more energy compared to the small media (10 mm). The input energy should increase as the drop height increases since they are directly proportional as shown from Equation 1. By increasing the ball size and drop height, the energy is expected to increase.

The mass of grinding media showed to have an effect on the resultant PSD (Figure 19). It was observed that 10 mm size produced more fines while 30 mm media size achieve more breakage. This was expected because there is a change in surface area as the media size increases, which corresponds to more particles taking part in the initial impact, thus producing more fines. The energy delivered to the particles increases with increase in media size and more energy is delivered to the bed. Therefore, the energy of impact is divided among more particles.

When analysis the AR profiles that were presented in the results section, it was observed that the mass fraction of size class two initially increases, passes through a maximum and then decreases as the particles of size class two are re-broken. The extent of grinding can now easily be interpreted from this simple geometric plot of Figure 34. It can be observed that an increase in size class one produces size class two until a maximum value of 0.31 is obtained. The same trend is observed as the one Khumalo (2007) obtained. The results confirm that an optimum impact energy exists for the breakage of silica particles. If the impact energy is insufficient, breakage does not occur, and this leads to inefficient use of energy. When the impact energy is too high, excessive quantities of fines were produced resulting in overgrinding.

These results indicate that proper control of the energy applied to the particles is necessary if overgrinding is to be avoided or if the specific energy required to achieve breakage is to be minimized. The figure illustrates the usefulness of the Attainable Region (AR) analysis to inform experimental design. One can see from Figure 34 that the AR profiles for the 20 mm and 30 mm grinding media are almost identical up to about $m_1 = 0.6$. This phenomenon should be investigated in further research. It should be explained again that the 20 mm grinding media was used later in the experiments after the breakage results of the 10 mm and 30 mm were found and therefore it is then suggested that further experiments (increasing the number of impacts to 600) be carried out using the 20 mm ball size to determine the breakage behaviour and be compared with the 10 mm and 30 mm ball size.

The mass fraction of size class three as a function of size class one for all three grinding media sizes were compared (Figure 34). It was observed that mass fraction of size class three (fines) increases as the mass fraction of size class one (feed) decreases for all three different grinding media sizes. The collection of material in size class three could follow one of two general patterns.

First, as the strength of particles increases with decreasing size, at some point the impact energy between the grinding media and the particles will not be sufficient for breakage. Therefore, the amount of material in size class three will increase and then plateau at a value of $m_3 < 1$. Secondly, the amount of energy delivered by each impact may be larger than the inherent strength of the cut-off size of size class three (209 µm) and therefore the amount of material in size class three will continue to increase until $m_3 = 1$. In this work, we have not explored the breakage at high enough impact energies (or overall numbers of drops) to determine which behaviour our material follows. There is a balance between the impact energy delivered to the particles and the surface area possible for contact which increases with larger media diameter. As the grinding media increases, the impact energy increases and more energy is delivered to the bed particles thus involving more particles in the collision because of the larger media size. Therefore, the energy of impact is being divided among more particles. The rate of production of size class three begins relatively slow, and then increases as the amount of size class one continues to decrease. The AR analyses can take advantage of this concavity as demonstrated by Metzger et al (2009). Again, more work is needed to determine the breakage behaviour for the 20 mm media at larger overall impact energies.

The effect of input impact energy was investigated to determine the breakage behaviour of silica bed particles at a constant drop height of 0.55 m (Figure 34-37). There is a maximum value of size class two (0.31) which is obtained after using 465 J of energy. It can clearly be observed that for a particular energy value the optimum values of mass fraction of size class two is obtained by grinding using smaller media size. It can be seen that at an impact energy less than 100 J, there is more size class two with both the 10 mm and 20 mm grinding media sizes. There is a need to perform more experimentation to determine the maximum amount of size class two achievable with the smaller media sizes, but that was beyond the scope of this work. We can use this approach to determine the optimal usage of energy to produce size class two, the desired size class.

When the effect of specific energy was investigated on the mass fraction and the resultant PSDs (Figure 38) and compared with the impact energy effects (Figure 37), it can be observed that there is no difference in data except that the x-axis is compacted for the specific energy analysis. It can be seen that specific energy has an effect on the size class. It is seen that when the specific energy increases size the same behaviour is observed as in the section 4.6. This is in line with Bwalya's (2005) finding that the higher the energy input the finer the

product. The graph (Figure 39) allows one to use specific energy as a fundamental parameter and hopefully develop a model that will give an indication of the likelihood of breakage when events occur where a bed of particles in impacted with some specified amount of energy. The results for all grinding media sizes are presented in Appendix D3.

The overall mass fraction of size class one after 50 impacts was investigated as explained from the results section (section 4.7). It was observed that as one increases the bed height (mass of sample M_p) and specific energy, there is less breakage taking place. This is due to the cushioning effect which takes place when the small grinding media is used at the smallest drop height. When the data of the 10 mm grinding media is plotted on the same graph with the 20 mm and 30 mm ball size, the points are too small to notice the trend, but the trend is clearly observed in Appendix F (Figure F.1).

After performing the experiments, one can ask how to relate the information obtained from the drop weight test to the ball mill. Based on the data obtained from this work, the drop weight tests experiments on the silica bed particles can be useful in designing or improving the industrial process for operating a mill. The results suggest that in a ball mill, one needs to use large grinding media in order to obtain more breakage. With an objective function of producing the greatest amount of size class two by breaking size class one and minimizing the fines (size class three), one can operate the mill using small grinding media.

The next question that one can pose regarding the feed material is that do we fill the mill as much possible, or keep it as empty as possible? To answer this question, the results of the bed height as discussed showed that to obtain more breakage, one needs to empty the mill as much as possible (low powder filling) to avoid cushioning effects. This obviously has disadvantages for continuous operation, because a less filled milled has a reduced throughput. Therefore a balance must be struck between the amount of product desired and the amount of energy lost to inefficiencies (overgrinding and/or the cushioning effect).

In a ball mill, the height at which the grinding media is raised to before impacting the particles plays a crucial role in the resultant PSDs. Based on the drop height results presented, it can be seen that to obtain more breakage, the ball mill should be designed in a way which favors higher drop heights (larger mill diameters). The residence time the particles spends in the mill also has an effect on the ball mill and from the work carried out, it was shown that as one increases the number of impacts, which is equivalent to residence time in a ball mill, more breakage takes place.

CHAPTER 6

6 CONCLUSIONS

The effect of grinding media on the breakage of silica bed was investigated to determine which grinding media produces more breakage on the silica bed particles. Three different ball sizes, 10 mm, 20 mm and 30 mm were used as grinding media as one varied the number of impacts (N), drop height (h) and the bed height (M_p). Breakage was characterized by measuring the particle size distributions (PSDs) after breakage and separating the continuously measured range into three size classes, size class one (the feed material), size class three (the fine material) and size class two (that material in between). It was shown that different grinding media produces different product size distribution, with the bigger grinding media being the one which shifted the PSD more to the left, thus breaking the silica bed particles faster compared to the smaller grinding media. It can be concluded that the grinding media plays a major role in determining the resultant PSD.

Another aspect that was investigated was the effect of the number of impacts on the breakage characteristics of silica bed particles. For each and every grinding media used, it was evident that as the number of impacts increases, more fines are produced. This is what is expected, as in any type of a mill, the more the residence time, the more fines are produced. It was also evident that for the smallest grinding media, fines were formed at less number of impacts as compared to the bigger grinding media sizes. It also suggests that there is possibly a different breakage mechanism of breakage for the larger and smaller media - abrasion for the smaller, massive fracture and/or cleavage for the larger. It can therefore be concluded that the number of impacts has an effect on the PSD.

The effect of the input impact energy was also investigated by varying the drop height from 0.55 m, 1.2 m and 1.75 m, for different grinding media sizes. It was shown that the impact energy has an effect on the PSD. There is a minimum amount of impact energy that needs to be reached in order for breakage to occur. An optimum impact energy can be determined for the breakage of a bed of silica particles of a given size in order to avoid over grinding and minimize energy usage. Over grinding can occur during the impact breakage of bed of silica particles when excessively high values of impact energy are applied.

For the experiments which were carried using 30 mm grinding media, at drop height of 1.2 m and a bed height of 10 g, an optimum impact energy was found to be 465 J. It can be concluded that impact energy greatly affects the PSDs as well.

For the case of varying drop height (h) and different grinding media sizes (d_m), we found that the smallest grinding media size tested does cause significant breakage with respect to the 20 mm and 30 mm as shown in section 4.6.2 regardless of the drop height. However it is also of interest to notice that it takes some 10 J of energy to cause grinding of consequence with the smallest grinding media size as it was shown in section 4.7.1. For the other grinding media sizes (20 mm and 30 mm) the mass fraction of size class one decreases, while the mass fractions of size class two and three increases, with an increase in drop height. For the intermediate grinding media size (20 mm), there appears to be a switch in behaviour from minimal breakage at the lowest height (0.55 m) to much more breakage at the intermediate drop height of 1.25 m, suggesting that the inherent energy of the particles is eclipsed somewhere between the energy delivered at these two drop heights. For the largest grinding media size (30 mm), there is a large, almost constant change in the amount of breakage of size class one and the production rates of size classes two and three as the drop height increases.

We also investigated the effect of the bed height (mass of the particles - M_p); three bed heights (10, 20 and 30 g) were subjected to impacts for different grinding media at the same drop height (h) and number of impacts (N). It was evident that drops on the small bed height produce more fines as compared to larger bed heights. It can be concluded that the resulting particle size distributions are highly dependent on the bed height.

The effect of specific energy (J/g) on the PSD was also investigated. The variables tested were the variation of the number of impacts, drop height and the bed height (mass of particles). It was shown that the use of specific energy as a control variable could prove to be an extremely valuable tool in analysing the breakage process.

Experiments aimed at determining the effect of energy intensity were carried for the two extreme grinding media sizes, namely, the 10 mm and 30 mm. Assuming the total energy to be the same for both grinding media sizes, two cases were considered. In the first case, the drop height was varied while the number of impacts was kept constant at 50. For the second

case, the drop height was kept constant while the number of impacts was varied. For both cases, it was shown that the product size distribution were not the same.

We can conclude that particle size distribution for different ball size differs, irrespective of the energy intensity being the same. Therefore, breakage is not only a function of the total amount of energy applied, but also how that energy is applied – either through numerous low energy impacts or a few, high energy impacts.

One of the main objectives was to determine the policy to determine the optimum mass fraction of size class two (m_2). It was shown that the traditional way of representing the particle size distribution as cumulative plots doesn't allow one to easily identify maximums in m_2 as a function of the reduction of size class one. The Attainable Region (AR) analysis was employed to express the required size class two as a function of size class one (m_1). The AR enabled one to represent the PSDs as points in a space and to easily connect the points into a single trajectory from which the optimum amount of the mass fraction in size class two can be obtained. From this, one can easily see what specific energy and number of impacts one should use to achieve the optimum. For our case, more experiments are required to determine the optimum m_2 though our preliminary results suggest that impacts with the smaller media will produce more of the intermediate size class. It can be concluded that the AR tool gives advantages over the traditional PSD presentation.

CHAPTER 7

7 RECOMMENDATIONS

- Future work should focus on setting up an automated drop weight test machine because the manual experiments are time-consuming and one can make a mistake after performing a lot of drops (500 or so), which will lead to more delays.
- Longer test runs should be carried out using the intermediate grinding media (20 mm) size to further determine the breakage of silica particles at higher impacts.
- Use other analytical techniques like image analysis which involves digitally capturing images of samples using high speed camera during breakage to relate impact to breakage.
- Discrete Element Modeling (DEM) Simulations to predict the breakage and give greater insight into the relationship between input energy and resultant breakage.
- Grinding experiments to be performed in a ball mill and compare the results with the actual drop test results.

CHAPTER 8

8 REFERENCES

Austin, L.G., Klimple, R.R. & Luckie P.T.,1984. *Process Engineering of size Reduction: Ball milling*, Society of mining enigineers, New York.

Austin, L.G., Bagga, P., 1979. *An Analysis of fine dry grinding in ball mills*. Powder technology, 28, 83-90.

Bozkurt, V., Ozgur, I., 2007. *Dry grinding kinetics of colemanite*. Powder Technology 176, 88-92.

Bunge, F., 1992. Mechanischer Zellaufschluß in Ru¨hrwerkskugelm¨uhlen. Dissertation, TU Braunschweig, VDI—Verlag Du¨sseldorf.

Bunge, F., Schwedes, J., 1990. Mechanical disintegration of Micro-Organisms. European Symposium on Comminution: Part II. Ljubljana. pp. 55–77, Preprints 7.

Davis, E.W., 1919. *Fine crushing in ball mills, AIME Transactions,* **61:** 250-296.

Deniz, V., Omur, T., 2002. *Investigation of the breakage kinetics of pumice samples as dependent on powder filling in a ball mill.* Int. J. Miner.Process. 67, 71-78.

Herbst, J.A., and Fuerstenau, D.W., 1980, *Scale-up Procedures for Continuous Grinding Mill Design Using Population Balance Models*, International Journal of Mineral Processing, Vol. 7, pp. 1-31.
http://web.wits.ac.za/Academic/Centres/COMPS/Research/AR/ARTheory/Introduction.htm. Acessed: 14/09/08 at 11:00 am.

Khumalo, N., Glasser, D., Hildebrandt, D., Hausberger, B., Kauchali, S., 2006. *The application of the attainable region analysis to comminution*. Chemical Engineering Science 61, 5969–5980

Khumalo, N., Glasser, D., Hildebrandt, D., Hausberger, B., 2007. *An experimental validation of a specific energy-based approach for comminution*. Chemical Engineering Science 62, 2765–2776

Krogh, S. R., 1980. *Crushing Characteristics*. Powder Technology, 27 (1980) 171-181

King, R. P. and Bourgeios, F., 1993, *A new conceptual model for ball milling*. XVIII International Mineral Processing Congress. Sydney, Australia. **1**, pp. 81-86.

Malvern instruments Ltd, LabPlus international, 2000. Laser diffraction for particle size analysis – why use mie theory. Malvern Worcs WR14 1XZ UK.

Mastersizer 2000 integrated systems for particle sizing Document.

Metzger, M.J., Glasser, D., Hausberger, B., Hildebrandt, D., Glasser., B.J.2007. *Use of the attainable region analysis to optimize particle breakage in a ball mill.* Chemical engineering Science 64, 3766 - 3777.

N. Khumalo, et al., *Improving comminution efficiency using classification: An attainable region approach*, Powder Technol. (2008), doi:10.1016/j.powtec.2008.03.001

Napier-Munn T.J., Morrell S., Morrison R.D., and Kojovic T., *Mineral Comminution circuits their operation and optmisation*, The University of Queensland, JKMRC, 1996.

Pauw, 1988. O.G. Pauw, The minimization of overbreakage during repetitive breakage of single ore particles. *Powder Technol.* **56** (1988), pp. 251–257.

Remes, A., 18/04/2007. *Modelling and analysis of Mineral Grinding Processes*.

Shi, F., 2004. *Comparison of grinding media – Cylpebs Verus Balls.* Minerals Engineering 17, 1259-1268.

Shoji, K., Austin, L.G., Smalia, F., Brame, K., Luckie, P.T., 1982. *Further studies of ball and powder filling effects in ball milling*. Powder Technology 31, 121-126.

Stadler, N., Polke, R., Schwedes, J., Vock, F., 1990. Naßmahlung in Ru¨hrwerksm¨uhlen. Chem.-Ing.-Tech. 62, 907–915.

Stehr, N.,1982. Zerkleinerung und Materialtransport in Ru¨hrwerkskugelm¨uhlen. Dissertation, TU Braunschweig.

Stehr, N., Schwedes, J., 1982. Technological investigations on the comminution at a continuously operated ball mill. Preprints International Symposium on Recent Advances in Particulate Sciences and Technology, Madras, India, Part 1. pp. B103–B119.

Stehr, N., 1988. Naßfeinstmahlung mit Ru¨hrwerksm¨uhlen in der Keramik, Grundlagen und Technische Ausfu¨hrungen. Symposium Moderne Mahlverfahren in der Keramik, Bayreuth. 19.

Tavarez, L.M., 1998, Energy absorbed in breakage of single particle in drop weight testing,

0892-6875(98)00118-6

Tavares, L.M., 2007. *Breakage of single particles: quasi-static*. In: Salman, A.D., Ghadiri, M., Hounslow, M.J. (Eds.), Handbook of Powder Technology, vol. 12, Particle Breakage.

Thiel, J.P., Schwedes, J., 1990. Comminution of coal in an agitated ball mill. European Symposium on Comminution, Ljubljana. pp. 667–680, Preprints 7.

Wills, B.A., 1992. *Mineral Processing Technology*, 5th ed, Pergamon Press, New York.

Weit, H., 1987. Betriebsverhalten und Maßstabsvergro¨ßerung von Ru¨hrwerkskugelm¨uhlen. Dissertation, TU Braunschweig.

Weit, H., Schwedes, J., Stehr, N., 1986. Comminution and transport behavior of agitated ball mills. World Congress Particle Technology: Part II. Nu¨rnberg. pp. 709–724, Preprints 1.

Yan, D., Partyka, T., 2007. *Fine grinding in a horizontal ball mill.* Mineral Engineering 20, 320-326.

Yashim, S., Kanda, Y., Sano, S., 1986. *Relationships between particle size and fracture energy or impact velocity Required to fracture as Estimated from Single Particle Crushing.* Powder technology, 51, 277-282.

CHAPTER 9

9 APPENDICES

9.1 APPENDIX A 1: Experimental data plotting particle size distributions varying the number of impacts

9.1.1 Reproducibility data for 10 mm ball size

Table A 1.1: Raw Experimental Data for reproducibility plots

Size (µm)	Vol % Previous	Size (µm)	Vol % Recent
0.01	0	0.01	0
0.011	0	0.011	0
0.013	0	0.013	0
0.015	0	0.015	0
0.017	0	0.017	0
0.02	0	0.02	0
0.023	0	0.023	0
0.026	0	0.026	0
0.03	0	0.03	0
0.035	0	0.035	0
0.04	0	0.04	0
0.046	0	0.046	0
0.052	0	0.052	0
0.06	0	0.06	0
0.069	0	0.069	0
0.079	0	0.079	0
0.091	0	0.091	0
0.105	0	0.105	0
0.12	0	0.12	0
0.138	0	0.138	0
0.158	0	0.158	0
0.162	0	0.162	0
0.209	0	0.209	0
0.24	0	0.24	0
0.275	0	0.275	0
0.316	0	0.316	0
0.363	0	0.363	0
0.417	0	0.417	0
0.479	0	0.479	0
0.56	0	0.56	0
0.631	0	0.631	0
0.724	0	0.724	0

0.832	0	0.832	0
0.955	0	0.955	0
1.096	0	1.096	0
1.259	0	1.259	0
1.445	0	1.445	0
1.66	0	1.66	0
1.905	0	1.905	0
2	0	2	0
2.188	0	2.188	0
2.512	0	2.512	0
2.884	0	2.884	0
3.311	0	3.311	0
3.802	0	3.802	0
4.385	0	4.385	0
5.012	0	5.012	0
5.754	0	5.754	0
6.607	0	6.607	0
7.566	0	7.566	0
8.71	0	8.71	0
10	0	10	0
11.482	0	11.482	0
13.183	0	13.183	0
15.136	0	15.136	0
17.378	0	17.378	0
19.953	0	19.953	0
22.908	0	22.908	0
26.303	0	26.303	0
30.2	0	30.2	0
34.674	0	34.674	0
39.811	0	39.811	0
45.709	0	45.709	0
52.481	0	52.481	0
60.256	0	60.256	0
69.183	0	69.183	0
79.433	0	79.433	0
91.201	0	91.201	0
104.713	0	104.713	0
120.226	0	120.226	0
138.038	0	138.038	0
158.499	0	158.499	0
181.97	0	181.97	0
208.93	0	208.93	0
239.883	0	239.883	0
275.423	0	275.423	0
316.228	0	316.228	0

363.078	0	363.078	0
416.669	0.47	416.669	0.63
478.63	2.7	478.63	3.22
549.541	7.32	549.541	8.13
630.957	14.87	630.957	15.95
724.436	25.35	724.436	26.6
831.764	38.23	831.764	39.5
954.993	52.39	954.993	53.55
1096.478	66.41	1096.478	67.35
1258.925	78.86	1258.925	79.52
1445.44	88.72	1445.44	89.1
1669.587	95.56	1669.587	95.72
1905.461	99.18	1905.461	99.21
2000	100	2000	100

8.1.2 Particle Size Distribution data for small grinding media (10 mm)

Table A1.2: PSD data for 10 mm grinding media

	Feed	**50**	**100**	**150**	**200**	**250**	**300**	**400**	**500**	**600**
Size (µm)	Vol Under (%)									
0.01	0	0	0	0	0	0	0	0	0	0
0.011	0	0	0	0	0	0	0	0	0	0
0.013	0	0	0	0	0	0	0	0	0	0
0.015	0	0	0	0	0	0	0	0	0	0
0.017	0	0	0	0	0	0	0	0	0	0
0.02	0	0	0	0	0	0	0	0	0	0
0.023	0	0	0	0	0	0	0	0	0	0
0.026	0	0	0	0	0	0	0	0	0	0
0.03	0	0	0	0	0	0	0	0	0	0
0.035	0	0	0	0	0	0	0	0	0	0
0.04	0	0	0	0	0	0	0	0	0	0
0.046	0	0	0	0	0	0	0	0	0	0
0.052	0	0	0	0	0	0	0	0	0	0
0.06	0	0	0	0	0	0	0	0	0	0
0.069	0	0	0	0	0	0	0	0	0	0
0.079	0	0	0	0	0	0	0	0	0	0
0.091	0	0	0	0	0	0	0	0	0	0
0.105	0	0	0	0	0	0	0	0	0	0
0.12	0	0	0	0	0	0	0	0	0	0
0.138	0	0	0	0	0	0	0	0	0	0
0.158	0	0	0	0	0	0	0	0	0	0
0.162	0	0	0	0	0	0	0	0	0	0
0.209	0	0	0	0	0	0	0	0	0	0
0.24	0	0	0	0	0	0	0	0	0	0

0.275	0	0	0	0	0	0	0	0	0	0
0.316	0	0	0	0	0	0	0	0	0	0
0.363	0	0	0	0	0	0	0	0	0	0
0.417	0	0	0	0	0	0	0	0	0	0
0.479	0	0	0	0	0	0	0	0	0	0
0.56	0	0	0	0	0	0	0	0	0	0
0.631	0	0	0	0	0	0	0	0	0	0
0.724	0	0	0	0	0	0	0	0	0	0
0.832	0	0	0	0	0	0	0	0	0	0
0.955	0	0	0	0	0	0	0	0	0	0
1.096	0	0	0	0	0	0	0	0	0	0
1.259	0	0	0	0	0	0	0	0	0	0
1.445	0	0	0	0	0	0	0	0	0	0.08
1.66	0	0	0	0	0	0	0	0	0.03	0.08
1.905	0	0	0	0	0	0	0	0	0.03	0.44
2	0	0	0	0	0	0	0	0	0.03	0.52
2.188	0	0	0	0	0	0	0	0	0.03	0.68
2.512	0	0	0	0	0	0	0	0	0.0536	0.72
2.884	0	0	0	0	0	0	0	0	0.05421	0.92
3.311	0	0	0	0	0	0	0	0	0.05821	1.2352
3.802	0	0	0	0	0	0	0	0	0.05821	1.8653
4.385	0	0	0	0	0	0	0.03	0.03	0.09243	2.213
5.012	0	0	0	0	0	0	0.03	0.03	0.12413	2.5638
5.754	0	0	0	0	0	0	0.03	0.03	0.13241	3.0253
6.607	0	0	0	0	0	0	0.03	0.03	0.18231	3.6854
7.566	0	0	0	0	0	0	0.0325	0.0325	0.22312	3.896
8.71	0	0	0	0	0	0	0.040235	0.040235	0.28623	4.53624
10	0	0	0	0	0	0	0.04685	0.04685	0.32513	4.68753
11.482	0	0	0	0	0	0	0.05685	0.05685	0.45232	4.9853
13.183	0	0	0	0	0	0	0.062358	0.062358	0.52113	5.26534
15.136	0	0	0	0	0	0	0.068512	0.068512	0.685231	5.38742
17.378	0	0	0	0	0	0	0.07586	0.07586	0.72351	5.55232
19.953	0	0	0	0	0	0	0.0842	0.0842	0.76821	5.68235
22.908	0	0	0	0	0	0	0.1823	0.1823	0.89321	5.71243
26.303	0	0	0	0	0	0	0.0862	0.0862	1.02362	5.87423
30.2	0	0	0	0	0	0	1.01242	1.01242	1.35682	5.92412
34.674	0	0	0	0	0	0	1.1032	1.1032	1.6621	6.02142
39.811	0	0	0	0	0	0	1.3524	1.3524	1.92543	6.22142
45.709	0	0	0	0	0	0	1.4526	1.4526	2.3568	6.36587
52.481	0	0	0	0	0	0	1.6852	1.6852	2.6874	6.45632
60.256	0	0	0	0	0	0	1.72122	1.72122	2.92653	6.74123
69.183	0	0	0	0	0	0	1.82142	1.82142	3.4563	6.985412
79.433	0	0	0	0	0	0	2.23521	2.23521	3.75412	7.052362
91.201	0	0	0	0	0	0.097298	3.0536	3.0536	4.23214	7.21423
104.713	0	0	0	0	0	0.330067	3.43	3.43	4.874523	7.45623

120.226	0	0	0	0	0	0.708124	3.9	3.9	5.1245	7.64125
138.038	0	0	0	0	0	1.18119	4.8	4.8	5.34124	7.8241
158.499	0	0	0	0	0	1.699299	5.22	5.22	5.874	8.03253
181.97	0	0	0	0	0	2.172621	5.66	5.66	6.35421	8.3235
208.93	0	0	0	0	0	2.511659	5.88	5.88	7.16	8.4453
239.883	0	0	0	0	0	2.664366	6.22	6.22	7.5634	9.02142
275.423	0	0	0	0	0	2.665119	6.53	6.53	8.6523	9.35421
316.228	0	0	0	0	0.07	2.665119	7.11	7.11	8.9653	9.7563
363.078	0	0	0	0.07	0.51	2.700091	7.81	7.81	9.5632	10.5632
416.669	0.42	0.51	0.63	1.03	2.01	3.138987	9.56	9.56	10.4235	11.6542
478.63	2.27	2.78	3.22	3.72	5.21	4.622345	12.36	12.36	12.9856	15.0213
549.541	6.08	7.32	8.13	8.74	10.73	8.910682	17.65	17.65	18.6243	20.3524
630.957	12.49	14.7	15.95	16.55	18.9	15.75055	24.87	24.87	24.5324	27.3625
724.436	21.72	24.95	26.6	27.11	29.61	27.56314	35.22	35.22	35.2134	37.1232
831.764	33.52	37.58	39.5	39.86	42.24	40.22439	46.98	46.98	46.352	48.635
954.993	47.11	51.56	53.55	53.74	55.76	54.94277	58.66	58.66	59.362	61.1266
1096.478	61.27	65.52	67.35	67.38	68.9	67.36459	70.55	70.55	70.234	73.326
1258.925	74.6	78.07	79.52	79.46	80.45	79.8912	81.55	81.55	81.55	83.2453
1445.44	85.86	88.16	89.1	89.02	89.57	90.08674	88.99	88.99	88.99	91.1323
1669.587	94.22	95.28	95.72	95.66	95.9	95.3	95.66	95.66	95.66	97.2361
1905.461	98.9	99.12	99.21	99.2	99.25	99.13079	99.24	99.24	99.24	99.24
2000	100	100	100	100	100	100	100	100	100	100

8.1.2 Particle Size Distribution data for the intermediate grinding media (20 mm)

Table A1.3: PSD data for 20 mm grinding media

	Feed	**50**	**100**	**150**	**200**	**300**
Size (µm)	Vol Under (%)					
0.01	0	0	0	0	0	0
0.011	0	0	0	0	0	0
0.013	0	0	0	0	0	0
0.015	0	0	0	0	0	0
0.017	0	0	0	0	0	0
0.02	0	0	0	0	0	0
0.023	0	0	0	0	0	0
0.026	0	0	0	0	0	0
0.03	0	0	0	0	0	0
0.035	0	0	0	0	0	0
0.04	0	0	0	0	0	0
0.046	0	0	0	0	0	0
0.052	0	0	0	0	0	0
0.06	0	0	0	0	0	0

0.069	0	0	0	0	0	0
0.079	0	0	0	0	0	0
0.091	0	0	0	0	0	0
0.105	0	0	0	0	0	0
0.12	0	0	0	0	0	0
0.138	0	0	0	0	0	0
0.158	0	0	0	0	0	0
0.162	0	0	0	0	0	0
0.209	0	0	0	0	0	0
0.24	0	0	0	0	0	0
0.275	0	0	0	0	0	0
0.316	0	0	0	0	0	0
0.363	0	0	0	0	0	0
0.417	0	0	0	0	0	0
0.479	0	0	0	0	0	0
0.56	0	0	0	0	0	0
0.631	0	0	0	0	0	0
0.724	0	0	0	0	0	0
0.832	0	0	0	0	0	0
0.955	0	0	0	0	0	0
1.096	0	0	0	0	0	0
1.259	0	0	0	0	0	0
1.445	0	0	0	0	0	0
1.66	0	0	0	0	0	0
1.905	0	0	0	0	0	0
2	0	0	0	0	0	0
2.188	0	0	0	0	0	0
2.512	0	0	0	0	0	0
2.884	0	0	0	0	0	0
3.311	0	0	0	0	0	0
3.802	0	0	0	0	0	0
4.385	0	0	0	0	0	0
5.012	0	0	0	0	0.022688	0
5.754	0	0	0	0	0.09525	0
6.607	0	0	0	0	0.17865	0.01153
7.566	0	0	0	0	0.267901	0.073843
8.71	0	0	0	0	0.360026	0.13805
10	0	0	0	0	0.452327	0.204945
11.482	0	0	0	0	0.54646	0.274839
13.183	0	0	0.05433	0.048531	0.646434	0.349177
15.136	0	0	0.129162	0.111106	0.757781	0.430657
17.378	0	0	0.214245	0.181114	0.885565	0.52189
19.953	0	0	0.305012	0.257041	1.033733	0.624148
22.908	0	0	0.401413	0.341275	1.203932	0.737103
26.303	0	0	0.500758	0.432616	1.396971	0.860737

30.2	0	0	0.602987	0.531868	1.613962	0.998535
34.674	0	0	0.710389	0.642461	1.859639	1.162517
39.811	0	0	0.830498	0.774291	2.145046	1.37741
45.709	0	0	0.979327	0.947646	2.490837	1.683877
52.481	0	0	1.184289	1.195836	2.928655	2.137783
60.256	0	0.061751	1.48478	1.564743	3.499972	2.804733
69.183	0	0.191369	1.929847	2.10951	4.252831	3.752215
79.433	0	0.439002	2.568574	2.883473	5.231727	5.033295
91.201	0	0.841068	3.442067	3.930606	6.472153	6.680483
104.713	0	1.429688	4.564413	5.266457	7.984409	8.687938
120.226	0	2.212026	5.919766	6.878562	9.755991	11.02218
138.038	0	3.158495	7.450044	8.714855	11.742	13.61744
158.499	0	4.205552	9.07163	10.70411	13.88514	16.4054
181.97	0	5.261294	10.69299	12.76919	16.12726	19.32722
208.93	0	6.236522	12.25632	14.86755	18.4474	22.37001
239.883	0	7.092384	13.78685	17.02709	20.88988	25.58218
275.423	0	7.889901	15.43727	19.3858	23.59978	29.09725
316.228	0	8.838327	17.50688	22.19707	26.81769	33.11344
363.078	0	10.31445	20.43555	25.822	30.8689	37.87769
416.669	0.42	12.81682	24.70535	30.63697	36.06867	43.59975
478.63	2.27	16.90151	30.75211	36.95983	42.65478	50.40038
549.541	6.08	23.0058	38.768	44.88688	50.64125	58.20129
630.957	12.49	31.3237	48.60014	54.21914	59.76211	66.69531
724.436	21.72	41.64203	59.65057	64.39467	69.42936	75.33624
831.764	33.52	53.31416	70.94268	74.55839	78.81644	83.42245
954.993	47.11	65.33411	81.30787	83.72872	87.02943	90.25251
1096.478	61.27	76.55651	89.6924	91.05338	93.3451	95.30568
1258.925	74.6	85.97865	95.45985	96.04937	97.41884	98.40075
1445.44	85.86	93.01404	98.63413	98.79136	99.4367	99.82093
1669.587	94.22	97.65131	99.85328	99.85388	99.98408	99.99149
1905.461	98.9	99.66947	99.99656	99.99226	100	100
2000	100	100	100	100	100	100

8.1.3 Particle Size Distribution data for big grinding media (30 mm)

Table A1.4: PSD data for 30 mm grinding media

	Feed	**50**	**100**	**150**	**200**	**300**	**400**	**500**	**600**
Size (µm)	Vol Under (%)								
0.01	0	0	0	0	0	0	0	0	0
0.011	0	0	0	0	0	0	0	0	0
0.013	0	0	0	0	0	0	0	0	0
0.015	0	0	0	0	0	0	0	0	0
0.017	0	0	0	0	0	0	0	0	0
0.02	0	0	0	0	0	0	0	0	0
0.023	0	0	0	0	0	0	0	0	0
0.026	0	0	0	0	0	0	0	0	0
0.03	0	0	0	0	0	0	0	0	0
0.035	0	0	0	0	0	0	0	0	0
0.04	0	0	0	0	0	0	0	0	0
0.046	0	0	0	0	0	0	0	0	0
0.052	0	0	0	0	0	0	0	0	0
0.06	0	0	0	0	0	0	0	0	0
0.069	0	0	0	0	0	0	0	0	0
0.079	0	0	0	0	0	0	0	0	0
0.091	0	0	0	0	0	0	0	0	0
0.105	0	0	0	0	0	0	0	0	0
0.12	0	0	0	0	0	0	0	0	0
0.138	0	0	0	0	0	0	0	0	0
0.158	0	0	0	0	0	0	0	0	0
0.162	0	0	0	0	0	0	0	0	0
0.209	0	0	0	0	0	0	0	0	0
0.24	0	0	0	0	0	0	0	0	0
0.275	0	0	0	0	0	0	0	0	0
0.316	0	0	0	0	0	0	0	0	0
0.363	0	0	0	0	0	0	0	0	0
0.417	0	0	0	0	0	0	0	0	0
0.479	0	0	0	0	0	0	0	0	0
0.56	0	0	0	0	0	0	0	0	0.16
0.631	0	0	0	0	0	0	0	0	0.46
0.724	0	0	0	0	0	0	0	0	0.84
0.832	0	0	0	0	0	0	0	0.02	1.31
0.955	0	0	0	0	0	0	0	0.22	1.81
1.096	0	0	0	0	0	0	0	0.51	2.32
1.259	0	0	0	0	0	0	0	0.89	2.82
1.445	0	0	0	0	0	0	0	1.33	3.29
1.66	0	0	0	0	0	0	0.03	1.79	3.74

1.905	0	0	0	0	0	0	0.17	2.25	4.16
2	0	0	0	0	0	0	0.39	2.7	4.56
2.188	0	0	0	0	0	0	0.68	3.12	4.98
2.512	0	0	0	0	0	0	1.01	3.51	5.43
2.884	0	0	0	0	0	0	1.36	3.89	5.93
3.311	0	0	0	0	0	0	1.71	4.27	6.5
3.802	0	0	0	0	0	0	2.05	4.66	7.17
4.385	0	0	0	0	0	0	2.37	5.1	7.93
5.012	0	0	0	0	0	0.023092	2.68	5.59	8.79
5.754	0	0	0	0.02	0	0.088022	2.98	6.16	9.77
6.607	0	0	0	0.08	0.012439	0.152015	3.28	6.81	10.84
7.566	0	0	0	0.15	0.077285	0.216441	3.61	7.56	12.03
8.71	0	0	0	0.21	0.139121	0.286395	3.98	8.41	13.32
10	0	0	0	0.27	0.200908	0.363752	4.4	9.37	14.72
11.482	0	0	0.06	0.33	0.264568	0.45319	4.9	10.43	16.24
13.183	0	0	0.12	0.39	0.332495	0.558334	5.48	11.61	17.89
15.136	0	0	0.17	0.46	0.408088	0.681969	6.16	12.92	19.69
17.378	0	0.04	0.24	0.55	0.49519	0.825055	6.95	14.35	21.67
19.953	0	0.1	0.32	0.67	0.597925	0.98888	7.86	15.93	23.88
22.908	0	0.15	0.41	0.82	0.721457	1.176985	8.5423	17.66	26.37
26.303	0	0.22	0.52	1.01	0.87455	1.400094	9.1023	19.6	29.23
30.2	0	0.29	0.66	1.25	1.071318	1.679541	9.5236	21.77	32.52
34.674	0	0.36	0.82	1.55	1.334312	2.051917	10.856	24.24	36.31
39.811	0	0.45	1.02	1.93	1.694584	2.568829	12.583	27.08	40.65
45.709	0	0.56	1.27	2.4	2.191552	3.295532	13.5874	30.36	45.55
52.481	0	0.69	1.6	3	2.869178	4.303484	15.6325	34.17	50.97
60.256	0	0.88	2.05	3.74	3.770145	5.659412	18.652	38.55	56.81
69.183	0	1.15	2.65	4.65	4.93108	7.416037	20.853	43.52	62.94
79.433	0	1.54	3.44	5.75	6.372983	9.596197	24.352	49.07	69.14
91.201	0	2.08	4.44	7.06	8.102325	12.19499	27.652	55.1	75.19
104.713	0	2.79	5.68	8.58	10.10194	15.16909	32.142	60.012	80.85
120.226	0	3.68	7.15	10.28	12.34192	18.45644	35.263	65.2142	85.92
138.038	0	4.73	8.8	12.14	14.77561	21.97635	40	69.3521	90.25
158.499	0	5.88	10.59	14.11	17.35861	25.65791	45	73.325	93.73
181.97	0	7.04	12.44	16.13	20.05289	29.44666	50.123	76.523	96.35
208.93	0	8.15	14.32	18.18	22.85029	33.32685	55.85	79.924	98.15
239.883	0	9.14	16.23	20.28	25.7808	37.32218	60.685	82.923	99.26
275.423	0	10.07	18.26	22.51	28.93048	41.50059	65.241	85.312	99.83
316.228	0	11.11	20.61	25.05	32.4292	45.9511	68.8832	87.963	99.97
363.078	0	12.57	23.57	28.16	36.44605	50.76815	73.3652	90.6853	100
416.669	0.42	14.89	27.47	32.14	41.13805	56.00678	76.6823	93.321	100
478.63	2.27	18.57	32.64	37.25	46.62298	61.66283	80.635	95.874	100
549.541	6.08	24.05	39.25	43.65	52.9088	67.63613	84.235	97.756	100
630.957	12.49	31.55	47.29	51.3	59.8723	73.73199	87.5632	98.889	100
724.436	21.72	40.97	56.42	59.89	67.23621	79.67508	90.254	99.853	100

831.764	33.52	51.81	66.05	68.87	74.60284	85.15399	93.524	100	100
954.993	47.11	63.24	75.4	77.53	81.51856	89.88326	96.635	100	100
1096.478	61.27	74.23	83.7	85.18	87.56805	93.66872	98.635	100	100
1258.925	74.6	83.83	90.37	91.29	92.45458	96.44272	100	100	100
1445.44	85.86	91.37	95.17	95.65	96.0678	98.28633	100	100	100
1669.587	94.22	96.59	98.19	98.38	98.46912	99.37731	100	100	100
1905.461	98.9	99.37	99.68	99.71	99.71824	99.89122	100	100	100
2000	100	100	100	100	100	100	100	100	100

9.2 APPENDIX A 2: Experimental data plotting particle size distributions varying the mass of the particles (bed height)

8.2.1 Particle Size distribution data for all grinding media sizes

Table A 1.5: Cumulative PSD data for all three grinding media sizes

Particle Size (µm)		Vol Under %								
	Feed	**10g**			**20g**			**30g**		
		10 mm	20 mm	30 mm	10 mm	20 mm	30 mm	10mm	20 mm	30 mm
0.01	0	0	0	0	0	0	0	0	0	0
0.011482	0	0	0	0	0	0	0	0	0	0
0.013183	0	0	0	0	0	0	0	0	0	0
0.015136	0	0	0	0	0	0	0	0	0	0
0.017378	0	0	0	0	0	0	0	0	0	0
0.019953	0	0	0	0	0	0	0	0	0	0
0.022909	0	0	0	0	0	0	0	0	0	0
0.026303	0	0	0	0	0	0	0	0	0	0
0.0302	0	0	0	0	0	0	0	0	0	0
0.034674	0	0	0	0	0	0	0	0	0	0
0.039811	0	0	0	0	0	0	0	0	0	0
0.045709	0	0	0	0	0	0	0	0	0	0
0.052481	0	0	0	0	0	0	0	0	0	0
0.060256	0	0	0	0	0	0	0	0	0	0
0.069183	0	0	0	0	0	0	0	0	0	0
0.079433	0	0	0	0	0	0	0	0	0	0
0.091201	0	0	0	0	0	0	0	0	0	0
0.104713	0	0	0	0	0	0	0	0	0	0
0.120226	0	0	0	0	0	0	0	0	0	0
0.138038	0	0	0	0	0	0	0	0	0	0
0.158489	0	0	0	0	0	0	0	0	0	0
0.18197	0	0	0	0	0	0	0	0	0	0
0.20893	0	0	0	0	0	0	0	0	0	0
0.239883	0	0	0	0	0	0	0	0	0	0
0.275423	0	0	0	0	0	0	0	0	0	0
0.316228	0	0	0	0	0	0	0	0	0	0

0.363078	0	0	0	0	0	0	0	0	0	0
0.416869	0	0	0	0	0	0	0	0	0	0
0.47863	0	0	0	0	0	0	0	0	0	0
0.549541	0	0	0	0	0	0	0	0	0	0
0.630957	0	0	0	0	0	0	0	0	0	0
0.724436	0	0	0	0	0	0	0	0	0	0
0.831764	0	0	0	0	0	0	0	0	0	0
0.954993	0	0	0	0	0	0	0	0	0	0
1.096478	0	0	0	0	0	0	0	0	0	0
1.258925	0	0	0	0	0	0	0	0	0	0
1.44544	0	0	0	0	0	0	0	0	0	0
1.659587	0	0	0	0	0	0	0	0	0	0
1.905461	0	0	0	0	0	0	0	0	0	0
2	0	0	0	0	0	0	0	0	0	0
2.187762	0	0	0	0	0	0	0	0	0	0
2.511886	0	0	0	0	0	0	0	0	0	0
2.884031	0	0	0	0	0	0	0	0	0	0
3.311311	0	0	0	0	0	0	0	0	0	0
3.801894	0	0	0	0	0	0	0	0	0	0
4.365158	0	0	0	0	0	0	0	0	0	0
5.011872	0	0	0	0	0	0	0	0	0	0
5.754399	0	0	0	0	0	0	0	0	0	0
6.606934	0	0	0	0	0	0	0	0	0	0
7.585776	0	0	0	0	0	0	0	0	0	0
8.709636	0	0	0	0	0	0	0	0	0	0
10	0	0	0	0	0	0	0	0	0	0
11.481536	0	0	0	0	0	0	0	0	0	0
13.182567	0	0	0	0	0	0	0	0	0	0
15.135612	0	0	0	0	0	0	0	0	0	0
17.378008	0	0	0	0.04	0	0	0	0	0	0
19.952623	0	0	0	0.1	0	0	0	0	0	0
22.908677	0	0	0	0.15	0	0	0	0	0	0
26.30268	0	0	0	0.22	0	0	0	0	0	0
30.199517	0	0	0	0.29	0	0	0	0	0	0
34.673685	0	0	0	0.36	0	0	0	0	0	0
39.810717	0	0	0	0.45	0	0	0	0	0	0
45.708819	0	0	0	0.56	0	0	0	0	0	0
52.480746	0	0	0	0.69	0	0	0	0	0	0
60.255959	0	0	0.061751	0.88	0	0	0	0	0	0
69.183097	0	0	0.191369	1.15	0	0	0	0	0	0
79.432823	0	0	0.439002	1.54	0	0	0.074425	0	0	0

91.201084	0	0	0.841068	2.08	0	0	0.249438	0	0	0
104.712855	0	0	1.429688	2.79	0	0	0.574712	0	0	0
120.226443	0	0	2.212026	3.68	0	0.3	1.05307	0	0	0
138.038426	0	0	3.158495	4.73	0	0.5123	1.679599	0	0	0
158.489319	0	0	4.205552	5.88	0	0.85412	2.402381	0	0	0
181.970086	0	0	5.261294	7.04	0	1.0123	3.133059	0	0	0
208.929613	0	0	6.236522	8.15	0	1.56323	3.764471	0	0	0
239.883292	0	0	7.092384	9.14	0	2.0123	4.213318	0	0	0
275.42287	0	0	7.889901	10.07	0	3.25635	4.466916	0	0	0
316.227766	0	0	8.838327	11.11	0	4.254123	4.649288	0	0	0
363.078055	0	0	10.31445	12.57	0	5.477231	5.057771	0	0.150283	0
416.869383	0.42	0.51	12.81682	14.89	0.364261	6.285267	6.162352	0.113962	1.42509	0.113962
478.630092	2.27	2.78	16.90151	18.57	2.265937	9.418266	8.568175	1.338387	5.117902	1.338387
549.540874	6.08	7.32	23.0058	24.05	6.39208	15.31485	12.87302	4.630057	10.43826	4.630057
630.957344	12.49	14.7	31.3237	31.55	13.31826	22.42419	19.53728	10.59428	18.5975	10.59428
724.43596	21.72	24.95	41.64203	40.97	23.16785	33.09439	28.68274	19.5599	29.50706	19.5599
831.763771	33.52	37.58	53.31416	51.81	35.53924	46.5097	39.99312	31.32611	42.52525	31.32611
954.992586	47.11	51.56	65.33411	63.24	49.47718	60.40303	52.68967	45.11525	56.50504	45.11525
1096.478196	61.27	65.52	76.55651	74.23	63.64195	73.34075	65.65254	59.66397	70.0362	59.66397
1258.925412	74.6	78.07	85.97865	83.83	76.61207	84.09234	77.65642	73.48848	81.79415	73.48848
1445.439771	85.86	88.16	93.01404	91.37	87.22933	91.9846	87.6456	85.22136	89.89492	85.22136
1659.586907	94.22	95.28	97.65131	96.59	94.86631	97.00927	94.97524	93.95582	96.06829	93.95582
1905.460718	98.9	99.12	99.66947	99.37	99.03655	99.47122	99.04828	98.85127	99.28028	98.85127
2000	100	100	100	100	100	100	100	100	100	100

9.3 APPENDIX A 3: Experimental data plotting particle size distributions varying the drop height

8.3.1 Particle Size Distribution data for three grinding media sizes at different drop heights

Table A 1.6: PSD Data for three grinding media sizes at different drop heights.

10mm ball size					20mm ball size					30mm ball size				
Size	Feed	0.55m	1.2m	1.75m	Size	Feed	0.55m	1.2m	1.75m	Size	Feed	0.55m	1.2m	1.75m
0.01	0	0	0	0	0.01	0	0	0	0	0.01	0	0	0	0
0.011482	0	0	0	0	0.011482	0	0	0	0	0.011482	0	0	0	0
0.013183	0	0	0	0	0.013183	0	0	0	0	0.013183	0	0	0	0
0.015136	0	0	0	0	0.015136	0	0	0	0	0.015136	0	0	0	0
0.017378	0	0	0	0	0.017378	0	0	0	0	0.017378	0	0	0	0
0.019953	0	0	0	0	0.019953	0	0	0	0	0.019953	0	0	0	0
0.022909	0	0	0	0	0.022909	0	0	0	0	0.022909	0	0	0	0
0.026303	0	0	0	0	0.026303	0	0	0	0	0.026303	0	0	0	0
0.0302	0	0	0	0	0.0302	0	0	0	0	0.0302	0	0	0	0
0.034674	0	0	0	0	0.034674	0	0	0	0	0.034674	0	0	0	0
0.039811	0	0	0	0	0.039811	0	0	0	0	0.039811	0	0	0	0
0.045709	0	0	0	0	0.045709	0	0	0	0	0.045709	0	0	0	0
0.052481	0	0	0	0	0.052481	0	0	0	0	0.052481	0	0	0	0
0.060256	0	0	0	0	0.060256	0	0	0	0	0.060256	0	0	0	0
0.069183	0	0	0	0	0.069183	0	0	0	0	0.069183	0	0	0	0
0.079433	0	0	0	0	0.079433	0	0	0	0	0.079433	0	0	0	0
0.091201	0	0	0	0	0.091201	0	0	0	0	0.091201	0	0	0	0
0.104713	0	0	0	0	0.104713	0	0	0	0	0.104713	0	0	0	0
0.120226	0	0	0	0	0.120226	0	0	0	0	0.120226	0	0	0	0
0.138038	0	0	0	0	0.138038	0	0	0	0	0.138038	0	0	0	0
0.158489	0	0	0	0	0.158489	0	0	0	0	0.158489	0	0	0	0
0.18197	0	0	0	0	0.18197	0	0	0	0	0.18197	0	0	0	0
0.20893	0	0	0	0	0.20893	0	0	0	0	0.20893	0	0	0	0
0.239883	0	0	0	0	0.239883	0	0	0	0	0.239883	0	0	0	0
0.275423	0	0	0	0	0.275423	0	0	0	0	0.275423	0	0	0	0
0.316228	0	0	0	0	0.316228	0	0	0	0	0.316228	0	0	0	0
0.363078	0	0	0	0	0.363078	0	0	0	0	0.363078	0	0	0	0
0.416869	0	0	0	0	0.416869	0	0	0	0	0.416869	0	0	0	0
0.47863	0	0	0	0	0.47863	0	0	0	0	0.47863	0	0	0	0
0.549541	0	0	0	0	0.549541	0	0	0	0	0.549541	0	0	0	0
0.630957	0	0	0	0	0.630957	0	0	0	0	0.630957	0	0	0	0

0.724436	0	0	0	0	0.724436	0	0	0	0	0.724436	0	0	0	0
0.831764	0	0	0	0	0.831764	0	0	0	0	0.831764	0	0	0	0
0.954993	0	0	0	0	0.954993	0	0	0	0	0.954993	0	0	0	0
1.096478	0	0	0	0	1.096478	0	0	0	0	1.096478	0	0	0	0
1.258925	0	0	0	0	1.258925	0	0	0	0	1.258925	0	0	0	0
1.44544	0	0	0	0	1.44544	0	0	0	0	1.44544	0	0	0	0
1.659587	0	0	0	0	1.659587	0	0	0	0	1.659587	0	0	0	0
1.905461	0	0	0	0	1.905461	0	0	0	0	1.905461	0	0	0	0
2	0	0	0	0	2	0	0	0	0	2	0	0	0	0
2.187762	0	0	0	0	2.187762	0	0	0	0	2.187762	0	0	0	0
2.511886	0	0	0	0	2.511886	0	0	0	0	2.511886	0	0	0	0
2.884031	0	0	0	0	2.884031	0	0	0	0	2.884031	0	0	0	0
3.311311	0	0	0	0	3.311311	0	0	0	0	3.311311	0	0	0	0
3.801894	0	0	0	0	3.801894	0	0	0	0	3.801894	0	0	0	0
4.365158	0	0	0	0	4.365158	0	0	0	0	4.365158	0	0	0	0
5.011872	0	0	0	0	5.011872	0	0	0	0	5.011872	0	0	0	0
5.754399	0	0	0	0	5.754399	0	0	0	0	5.754399	0	0	0	0
6.606934	0	0	0	0	6.606934	0	0	0	0	6.606934	0	0	0	0
7.585776	0	0	0	0	7.585776	0	0	0	0	7.585776	0	0	0	0
8.709636	0	0	0	0	8.709636	0	0	0	0	8.709636	0	0	0	0
10	0	0	0	0	10	0	0	0	0	10	0	0	0	0
11.481536	0	0	0	0	11.48154	0	0	0	0	11.48154	0	0	0	0
13.182567	0	0	0	0	13.18257	0	0	0	0	13.18257	0	0	0	0
15.135612	0	0	0	0	15.13561	0	0	0	0	15.13561	0	0	0	0
17.378008	0	0	0	0	17.37801	0	0	0	0	17.37801	0	0	0.04	0
19.952623	0	0	0	0	19.95262	0	0	0	0	19.95262	0	0	0.1	0.03213
22.908677	0	0	0	0	22.90868	0	0	0	0	22.90868	0	0	0.15	0.098734
26.30268	0	0	0	0	26.30268	0	0	0	0	26.30268	0	0	0.22	0.16839
30.199517	0	0	0	0	30.19952	0	0	0	0	30.19952	0	0	0.29	0.241444
34.673685	0	0	0	0	34.67369	0	0	0	0	34.67369	0	0	0.36	0.321816
39.810717	0	0	0	0	39.81072	0	0	0	0	39.81072	0	0	0.45	0.41178
45.708819	0	0	0	0	45.70882	0	0	0	0	45.70882	0	0	0.56	0.52135
52.480746	0	0	0	0	52.48075	0	0	0	0.001275	52.48075	0	0	0.69	0.667994
60.255959	0	0	0	0	60.25596	0	0	0.061751	0.060082	60.25596	0	0	0.88	0.878231

69.183097	0	0	0	0	69.1831	0	0	0.191369	0.170497	69.1831	0	0.053962	1.15	1.187775
79.432823	0	0	0	0	79.43282	0	0	0.439002	0.367145	79.43282	0	0.175047	1.54	1.637373
91.201084	0	0	0	0	91.20108	0	0	0.841068	0.712021	91.20108	0	0.413202	2.08	2.269611
104.712855	0	0	0	0	104.7129	0	0	1.429688	1.244846	104.7129	0	0.794665	2.79	3.11573
120.226443	0	0	0	0	120.2264	0	0	2.212026	1.995855	120.2264	0	1.346099	3.68	4.192527
138.038426	0	0	0	0	138.0384	0	0	3.158495	2.962173	138.0384	0	2.057939	4.73	5.486253
158.489319	0	0	0	0	158.4893	0	0	4.205552	4.097399	158.4893	0	2.892078	5.88	6.960597
181.970086	0	0	0	0	181.9701	0	0	5.261294	5.320478	181.9701	0	3.777284	7.04	8.554764
208.929613	0	0	0	0	208.9296	0	0	6.236522	6.530772	208.9296	0	4.633037	8.15	10.21126
239.883292	0	0	0	0	239.8833	0	0	7.092384	7.648107	239.8833	0	5.403813	9.14	11.90128
275.42287	0	0	0	0	275.4229	0	0	7.889901	8.667714	275.4229	0	6.103501	10.07	13.66608
316.227766	0	0	0	0	316.2278	0	0.066635	8.838327	9.710894	316.2278	0	6.865259	11.11	15.64498
363.078055	0	0	0	0	363.0781	0	0.580328	10.31445	11.06198	363.0781	0	7.973438	12.57	18.09479
416.869383	0.42	0.245653	0.340887	0.51	416.8694	0.42	2.264355	12.81682	13.17381	416.8694	0.42	9.850788	14.89	21.35403
478.630092	2.27	1.815787	2.123987	2.78	478.6301	2.27	5.773639	16.90151	16.58663	478.6301	2.27	13.02363	18.57	25.80275
549.540874	6.08	5.515865	6.031843	7.32	549.5409	6.08	11.74139	23.0058	21.84185	549.5409	6.08	17.9864	24.05	31.73767
630.957344	12.49	11.93496	12.67147	14.7	630.9573	12.49	20.48787	31.3237	29.27526	630.9573	12.49	25.08768	31.55	39.28632
724.43596	21.72	21.29782	22.22546	24.95	724.436	21.72	31.84629	41.64203	38.89291	724.436	21.72	34.35411	40.97	48.28845
831.763771	33.52	33.3105	34.36772	37.58	831.7638	33.52	45.09334	53.31416	50.22835	831.7638	33.52	45.41312	51.81	58.27482
954.992586	47.11	47.12117	48.21183	51.56	954.9926	47.11	59.02475	65.33411	62.37167	954.9926	47.11	57.48828	63.24	68.51471
1096.478196	61.27	61.4473	62.45443	65.52	1096.478	61.27	72.21691	76.55651	74.1162	1096.478	61.27	69.52837	74.23	78.16303
1258.925412	74.6	74.85205	75.66155	78.07	1258.925	74.6	83.38645	85.97865	84.26772	1258.925	74.6	80.43387	83.83	86.45051
1445.439771	85.86	86.07506	86.61047	88.16	1445.44	85.86	91.75014	93.01404	91.95972	1445.44	85.86	89.31713	91.37	92.87401
1659.586907	94.22	94.3341	94.58336	95.28	1659.587	94.22	97.25038	97.65131	96.90924	1659.587	94.22	95.70124	96.59	97.3016
1905.460718	98.9	98.92692	98.97867	99.12	1905.461	98.9	99.61963	99.66947	99.78212	1905.461	98.9	99.19218	99.37	99.53222
2000	100	100	100	100	2000	100	100	100	100	2000	100	100	100	100

9.4 APPENDIX A 4: Experimental data plotting particle size distributions varying the energy intensity

8.4.1 Particles Size distribution data for varying the drop height

Table A1.7 (a): Energy intensity data for drop-height variation

Size	Feed	10mm-1.75m	30mm-0.065m
0.01	0	0	0
0.011482	0	0	0
0.013183	0	0	0
0.015136	0	0	0
0.017378	0	0	0
0.019953	0	0	0
0.022909	0	0	0
0.026303	0	0	0
0.0302	0	0	0
0.034674	0	0	0
0.039811	0	0	0
0.045709	0	0	0
0.052481	0	0	0
0.060256	0	0	0
0.069183	0	0	0
0.079433	0	0	0
0.091201	0	0	0
0.104713	0	0	0
0.120226	0	0	0
0.138038	0	0	0
0.158489	0	0	0
0.18197	0	0	0
0.20893	0	0	0
0.239883	0	0	0
0.275423	0	0	0
0.316228	0	0	0
0.363078	0	0	0
0.416869	0	0	0
0.47863	0	0	0
0.549541	0	0	0
0.630957	0	0	0
0.724436	0	0	0
0.831764	0	0	0
0.954993	0	0	0
1.096478	0	0	0
1.258925	0	0	0

1.44544	0	0	0
1.659587	0	0	0
1.905461	0	0	0
2	0	0	0
2.187762	0	0	0
2.511886	0	0	0
2.884031	0	0	0
3.311311	0	0	0
3.801894	0	0	0
4.365158	0	0	0
5.011872	0	0	0
5.754399	0	0	0
6.606934	0	0	0
7.585776	0	0	0
8.709636	0	0	0
10	0	0	0
11.48154	0	0	0
13.18257	0	0	0
15.13561	0	0	0
17.37801	0	0	0
19.95262	0	0	0
22.90868	0	0	0
26.30268	0	0	0
30.19952	0	0	0
34.67369	0	0	0
39.81072	0	0	0
45.70882	0	0	0
52.48075	0	0	0
60.25596	0	0	0
69.1831	0	0	0
79.43282	0	0	0
91.20108	0	0	0
104.7129	0	0	0
120.2264	0	0	0
138.0384	0	0	0
158.4893	0	0	0
181.9701	0	0	0
208.9296	0	0	0
239.8833	0	0	0
275.4229	0	0	0
316.2278	0	0	0
363.0781	0	0	0
416.8694	0.42	0.51	0.657981
478.6301	2.27	2.78	3.476142
549.5409	6.08	7.32	8.923075

630.9573	12.49	14.7	17.52372
724.436	21.72	24.95	29.094015
831.7638	33.52	37.58	42.857024
954.9926	47.11	51.56	57.470973
1096.478	61.27	65.52	71.345908
1258.925	74.6	78.07	83.053229
1445.44	85.86	88.16	91.736348
1659.587	94.22	95.28	97.369061
1905.461	98.9	99.12	99.672082
2000	100	100	100

8.4.2 Particles Size distribution data for varying the number of impacts

Table A 1.7 (b): Energy intensity data for number of Impact variation

Size (µm)	Feed	10mm- 300 drops	30mm- 11 drops
0.01	0	0	0
0.011482	0	0	0
0.013183	0	0	0
0.015136	0	0	0
0.017378	0	0	0
0.019953	0	0	0
0.022909	0	0	0
0.026303	0	0	0
0.0302	0	0	0
0.034674	0	0	0
0.039811	0	0	0
0.045709	0	0	0
0.052481	0	0	0
0.060256	0	0	0
0.069183	0	0	0
0.079433	0	0	0
0.091201	0	0	0
0.104713	0	0	0
0.120226	0	0	0
0.138038	0	0	0
0.158489	0	0	0

0.18197	0	0	0
0.20893	0	0	0
0.239883	0	0	0
0.275423	0	0	0
0.316228	0	0	0
0.363078	0	0	0
0.416869	0	0	0
0.47863	0	0	0
0.549541	0	0	0
0.630957	0	0	0
0.724436	0	0	0
0.831764	0	0	0
0.954993	0	0	0
1.096478	0	0	0
1.258925	0	0	0
1.44544	0	0	0
1.659587	0	0	0
1.905461	0	0	0
2	0	0	0
2.187762	0	0	0
2.511886	0	0	0
2.884031	0	0	0
3.311311	0	0	0
3.801894	0	0	0
4.365158	0	0	0
5.011872	0	0	0

5.754399	0	0	0
6.606934	0	0	0
7.585776	0	0	0
8.709636	0	0	0
10	0	0	0
11.48154	0	0	0
13.18257	0	0	0
15.13561	0	0	0
17.37801	0	0	0
19.95262	0	0.03	0
22.90868	0	0.1	0
26.30268	0	0.16	0
30.19952	0	0.23	0
34.67369	0	0.3	0
39.81072	0	0.36	0
45.70882	0	0.42	0
52.48075	0	0.48	0
60.25596	0	0.55	0
69.1831	0	0.66	0
79.43282	0	0.82	0
91.20108	0	1.08	0
104.7129	0	1.46	0
120.2264	0	1.98	0
138.0384	0	2.61	0
158.4893	0	3.31	0
181.9701	0	3.98	0

208.9296	0	4.55	0
239.8833	0	4.96	0
275.4229	0	5.23	0
316.2278	0	5.52	0
363.0781	0	6.17	0.35
416.8694	0.47	7.65	1.88
478.6301	2.7	10.53	5.26
549.5409	7.32	15.36	11.18
630.9573	14.87	22.5	19.94
724.436	25.35	31.96	31.38
831.7638	38.23	43.33	44.73
954.9926	52.39	55.8	58.76
1096.478	66.41	68.25	71.99
1258.925	78.86	79.56	83.13
1445.44	88.72	88.8	91.42
1659.587	95.56	95.48	96.77
1905.461	99.18	99.15	99.42
2000	100	100	100

9.5 APPENDIX A 5: Mass fraction data as a function of drop height

8.5.1 Mass fraction vs. drop height for 10 mm ball size data

Table 1.8 (a) Data for 10 mm ball size for varying drop height as a function of mass fraction of size classes

10mm ball size					
Height	**M_1**	**M_2**	**M_3**	**Etotal**	**Es**
0	0.96734	0.03266	0	0	0
0.55	0.969926	0.030074	0	1.061297	0.10613
1.2	0.967777	0.032223	0	2.315556	0.231556
1.75	0.962793	0.037207	0	3.376853	0.337685

8.5.2 Mass fraction vs. drop height for 20 mm ball size data

Table 1.8 (b) Data for 20 mm ball size for varying drop height as a function of mass fraction of size classes

20mm ball size					
Height	**M_1**	**M_2**	**M_3**	**Etotal**	**Es**
0	0.96734	0.03266	0	0	0
0.55	0.944829	0.055171	0	15.48737	1.548737
1.2	0.833745	0.139337	0.026919	33.79062	3.379062
1.75	0.831051	0.142158	0.026791	49.27799	4.927799

8.5.3 Mass fraction vs. drop height for 30 mm ball size data

Table 1.8 (c) Data for 30 mm ball size for varying drop height as a function of mass fraction of size classes.

30mm ball size					
Height	**M_1**	**M_2**	**M_3**	**Etotal**	**Es**
0	0.96734	0.03266	0	0	0
0.55	0.860335	0.119725	0.01994	26.68364	2.668364
1.2	0.802066	0.153309	0.044625	58.21885	5.821885
1.75	0.766125	0.187074	0.046801	84.90249	8.490249

9.6 APPENDIX A 5: Mass fraction data for varying the impact and specific energy

8.6.1 Mass fraction vs. input energy for 10 mm ball size data

Table 1.9 (a) Number of impacts variation as a function of impact and specific energy for 10 mm ball size

10mm ball size					
N	M_1	M_2	M_3	Impact Energy (Et)	Specific Energy (Es)
0	0.96734	0.03266	0	0	0
50	0.962793	0.037207	0	2.313198	0.2313198
100	0.95978	0.04022	0	4.626396	0.4626396
150	0.956868	0.043132	0	6.939594	0.6939594
200	0.94787	0.05213	0	9.252792	0.9252792
250	0.925538	0.061841	0.012621	11.56599	1.156599
300	0.866468	0.104344	0.029189	13.879188	1.3879188
400	0.830543	0.115979	0.053478	18.505584	1.8505584
500	0.800868	0.1239	0.075232	23.13198	2.313198
600	0.694741	0.125245	0.180014	27.758376	2.7758376

8.6.2 Mass fraction vs. input energy for 20 mm ball size data

Table 1.9 (b) Number of impacts variations as a function of impact and specific energy for 20 mm ball size

20mm ball size					
N	M_1	M_2	M_3	Impact Energy (Et)	Specific Energy (Es)
0	0.96734	0.03266	0	0	0
50	0.833745	0.139337	0.026919	33.79062	3.379062
100	0.745916	0.196388	0.057696	67.58124	6.758124
150	0.716601	0.22097	0.06243	101.37186	10.137186
200	0.675094	0.236224	0.088682	135.16248	13.516248
300	0.650631	0.262576	0.086792	202.74372	20.274372

8.6.3 Mass fraction vs. input energy for 30 mm ball size data

Table 1.9 (c) Number of impacts variation as a function of impact and specific energy for 10 mm ball size

30mm ball size					
N	M_1	M_2	M_3	Impact Energy (Et)	Specific Energy (Es)
0	0.96734	0.03266	0	0	0
50	0.802066	0.153309	0.044625	58.159566	5.8159566
100	0.718391	0.211943	0.069666	116.319132	11.6319132
150	0.677397	0.227916	0.094687	174.478698	17.4478698
200	0.640682	0.259243	0.100075	232.638264	23.2638264
300	0.578341	0.29539	0.126269	348.957396	34.8957396
400	0.457998	0.308996	0.233007	465.276528	46.5276528
500	0.364583	0.296637	0.33878	581.59566	58.159566
600	0.312462	0.280344	0.407194	697.914792	69.7914792

9.7 APPENDIX A 6: Attainable Region Analysis Data

9.7.1 Mass fraction of size class one vs. size class two for 10 mm ball size data

Table A 2.1: Attainable Region data for 10 mm ball size

10mm				
N	Size Class One	Size Class Two	Size Class Three	Σ(Size Classes)
0	0.967340041	0.032659959	0	1
50	0.962793091	0.037206909	0	1
100	0.959779963	0.040220037	0	1
150	0.956868026	0.043131974	0	1
200	0.947869807	0.052130193	0	1
250	0.925537989	0.061840754	0.012621257	1
300	0.866467604	0.104343535	0.029188861	1
400	0.830542906	0.115979165	0.053477929	1
500	0.800868214	0.123899568	0.075232218	1
600	0.69474082	0.125244758	0.180014422	1

9.7.2 Mass fraction of size class one vs. size class two for 20 mm ball size data

Table A 2.2: Attainable Region data for 20 mm ball size

20mm				
N	**Size Class One**	**Size Class Two**	**Size Class Three**	**Σ(Size Classes)**
0	0.967340041	0.032659959	0	1
50	0.833744538	0.139336786	0.026918677	1
100	0.745916144	0.196388296	0.05769556	1
150	0.716600595	0.220969542	0.062429863	1
200	0.675094118	0.236224015	0.088681866	1
300	0.650631486	0.262576214	0.0867923	1

9.7.1 Mass fraction of size class one vs. size class two for 30 mm ball size data

Table A 2.3: Attainable Region data for 30 mm ball size

30mm				
N	**Size Class One**	**Size Class Two**	**Size Class Three**	**Σ(Size Classes)**
0	0.967340041	0.032659959	0	1
50	0.802066007	0.153309113	0.04462488	1
100	0.718390703	0.211943255	0.069666042	1
150	0.677397445	0.227915845	0.09468671	1
200	0.640682053	0.259243367	0.100074579	1
300	0.578341458	0.295389864	0.126268678	1
400	0.457997744	0.308995595	0.233006661	1
500	0.364583128	0.296637075	0.338779797	1
600	0.312461919	0.280343958	0.407194123	1

9.8 APPENDIX B: Energy intensity calculations

The input energy (J) was calculated as follows:

$$E_b = m_b g h \quad \text{(B.1)}$$

where m_b is the mass of the drop weight (ball) in g , g is the gravitational accelerations in m/s^2 and h is the drop height in metres. The total impact energy (J) and the specific energy (J/g) are calculated according to equation B.2 and B.3 respectively as shown below

$$E_T = N E_b \quad \text{(B.2)}$$

$$E_s = \frac{E_T}{M_p} \quad \text{(B.3)}$$

where N is the number of impacts, M_p is the mass of the particles in g.

The density and volume of the media can be determined by using equations 1.4 and 1.5 respectively

$$\rho = \frac{m_b}{V} \quad \text{(B.4)}$$

$$V = \frac{\pi\, d^3}{3} \quad \text{(B.5)}$$

By manipulating the above equations, the mass of the ball can be determined as shown in equation B.6 below

$$m_b = \rho . V = \rho . \frac{\pi d^3}{3} \quad \text{(B.6)}$$

Once the mass of the ball is known, it can then be replaced into equation B.1 and B.2 as shown below:

$$E_b = m_b g h$$

$$= \rho \frac{\pi d^3}{3} g h \quad \text{(B.7)}$$

$$E_T = N . \rho \frac{\pi d^3}{3} g h \quad \text{(B.8)}$$

Assuming total impact energy to be the same, then

$$m_{10} g h N = m_{30} g h N$$

Keeping the number of impacts the same at 50, the height at which one of the media sizes (either 10 mm or 30 mm) can be calculated. For this particular experiment, using 10 mm ball size at its highest impact energy and a drop height of 1.75 m, the height at which 30 mm ball size should be dropped at can be calculated as follow:

$$h_{new} = \frac{m_{10} g h_{1.75} N}{m_{30} g N}$$

$$h_{new} = \frac{m_{10} h_{1.75}}{m_{30}}$$

$$h_{new} = \frac{\rho . \frac{\pi (d_{10})^3}{3} h_{1.75}}{\rho . \frac{\pi (d_{30})^3}{3}}$$

$$h_{new} = \frac{(d_{10})^3}{(d_{30})^3} \quad h_{1.75}$$

$$h_{new} = \frac{(10mm)^3}{(30mm)^3} \quad 1.75m$$

$$h_{new} = 0.065m = 6.5cm$$

Keeping the height constant at 1.2 m, the number of drops required can be determined as follows:

Using the 10 mm ball size, one can determine its impact energy. Once the impact energy is determined, the total impact energy can then be calculated and assumed to be the same for the bigger ball size.

From equation B.7

$$E_b = \rho \frac{\pi d^3}{3} gh$$

$$= 7850 \frac{kg}{m^3} . \frac{\pi}{3} . \left(\frac{10mm}{0.001}\right)^3 . 9.82 \frac{m}{s^2} . 1.2m$$

$$= 8.878 \times 10^{16} J$$

Where 0.001 is the conversion factors from mm to m.

Therefore

$$E_T = E_b . N$$

$$= 8.878 \times 10^{16} J . 300$$

$$= 2.6634 \times 10^{19}\ J$$

Assuming constant energy (E_T), the number of drops required for the 30 mm ball size can be determined as follows:

$$N_{30} = \frac{E_T}{E_{30}} = \frac{E_T}{\rho . \frac{\pi (d_{30})^3}{3} . gh}$$

$$= \frac{2.6634 \times 10^{19} J}{7850 \frac{kg}{m^3} . \frac{\pi \left({}^{30mm}/_{0.001} \right)^3}{3} . 9.82 \frac{m}{s^2} . 1.2m}$$

$$= \frac{7.99032 \times 10^{19} J}{7.1912 \times 10^{18} J.}$$

$$= 11\ drops$$

Therefore, 30 mm ball size needs to be dropped 11 times at a height of 1.2 metres.

9.9 APPENDIX C: Particle Size Distribution plots

Figure C.1 below shows the cumulative % distribution as a function of particle size. It can be seen that using the small grinding media at 100 drops produced similar particle size distributions. This shows that the results are reproducible.

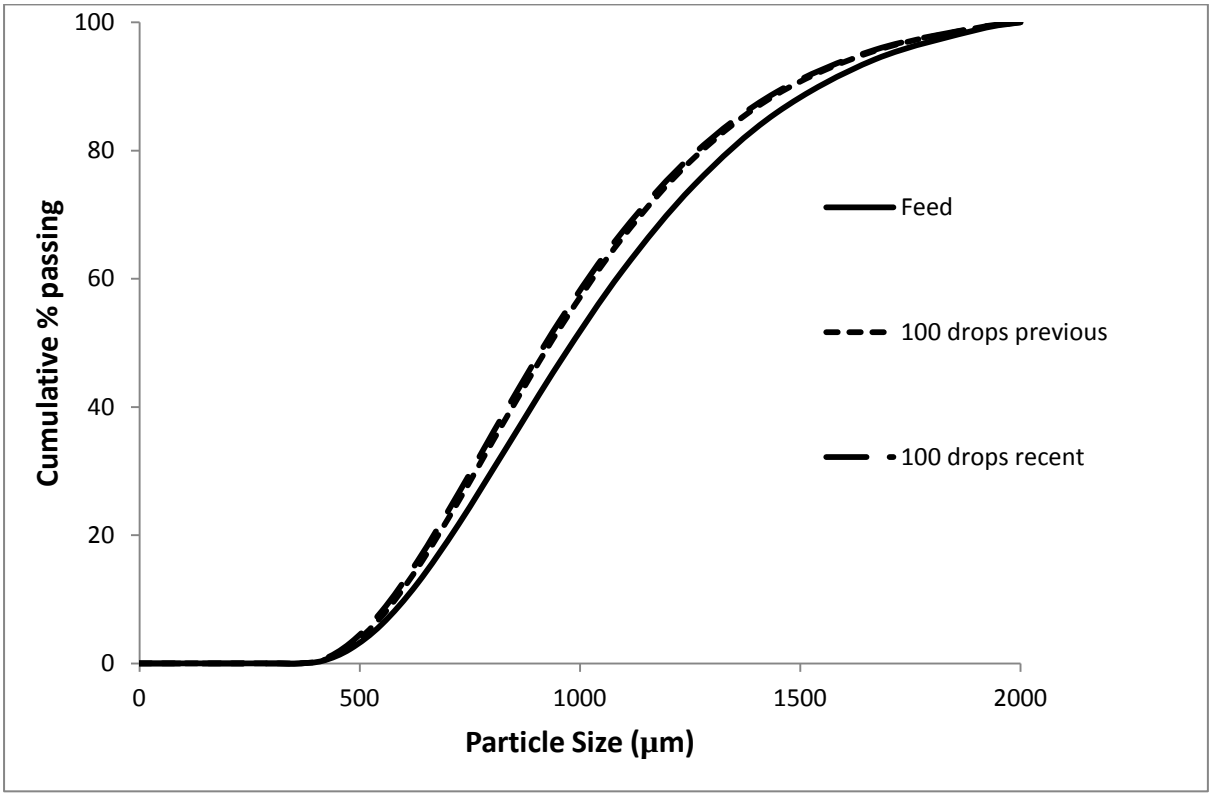

Figure C1 (a)**:** Cumulative distribution plots for smaller media size (10 mm) for varying number of impacts (N).

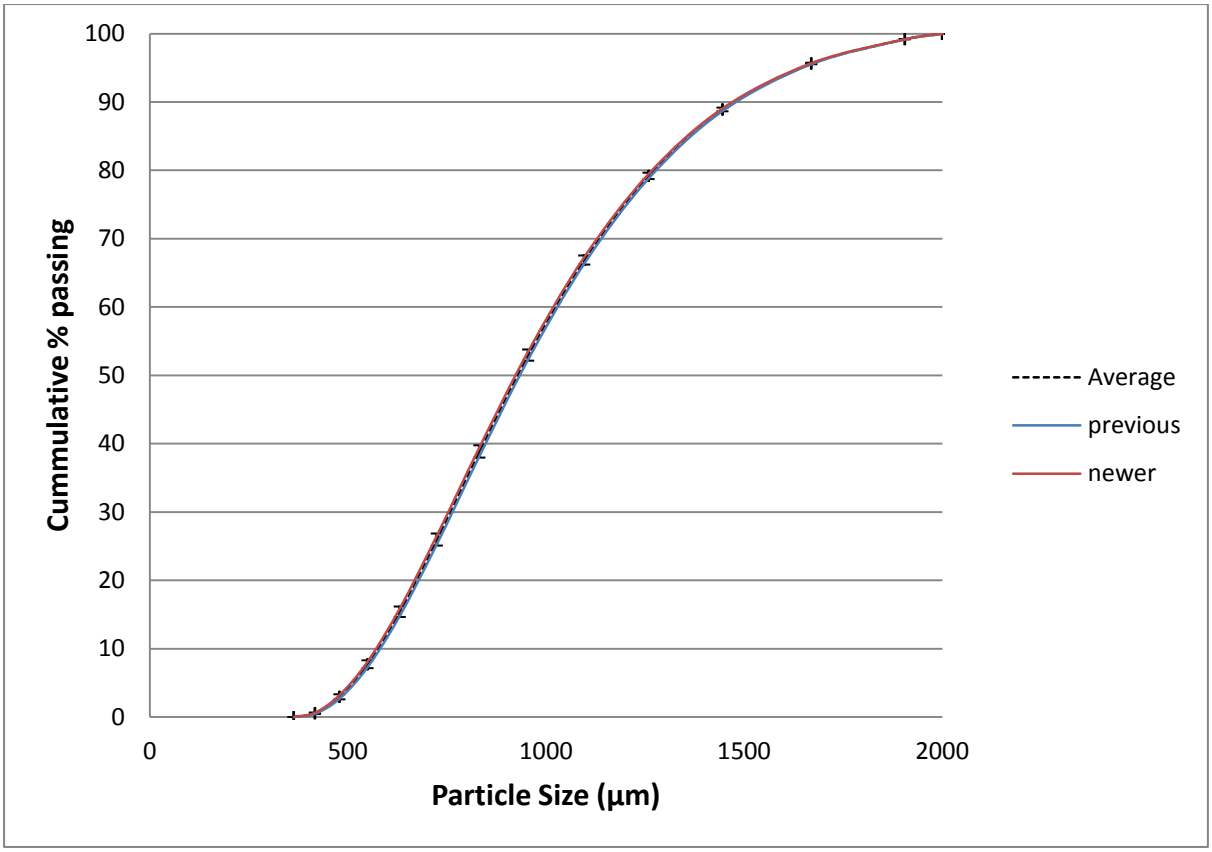

Figure C1 (b)**:** Cumulative distribution plots for smaller media size (10 mm) for varying number of impacts (N) comparing the accuracy of the data.

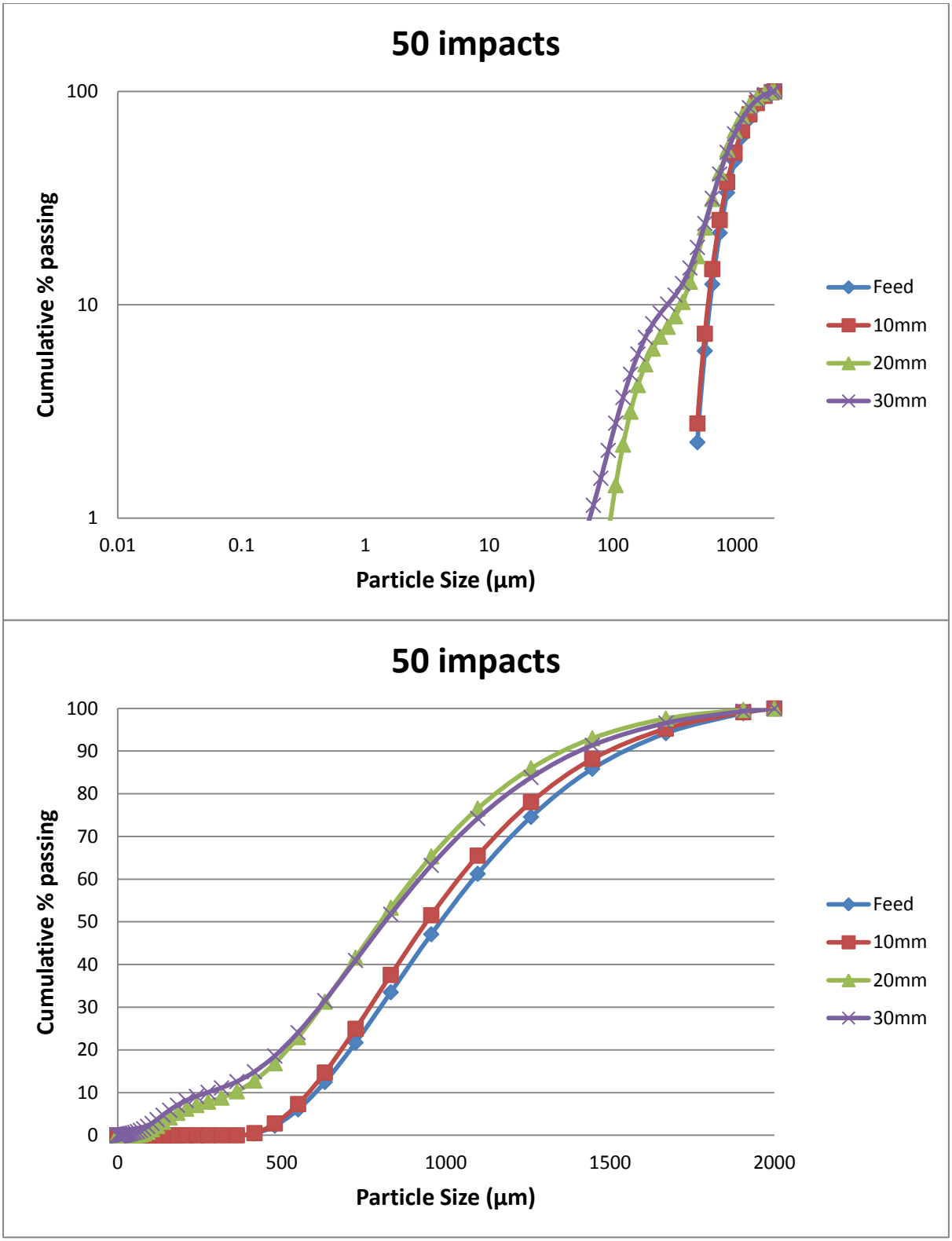

Figure C2**:** Cumulative distribution plots for three media sizes, at a constant drop height and number of impacts of 1.2 m and 50 respectively.

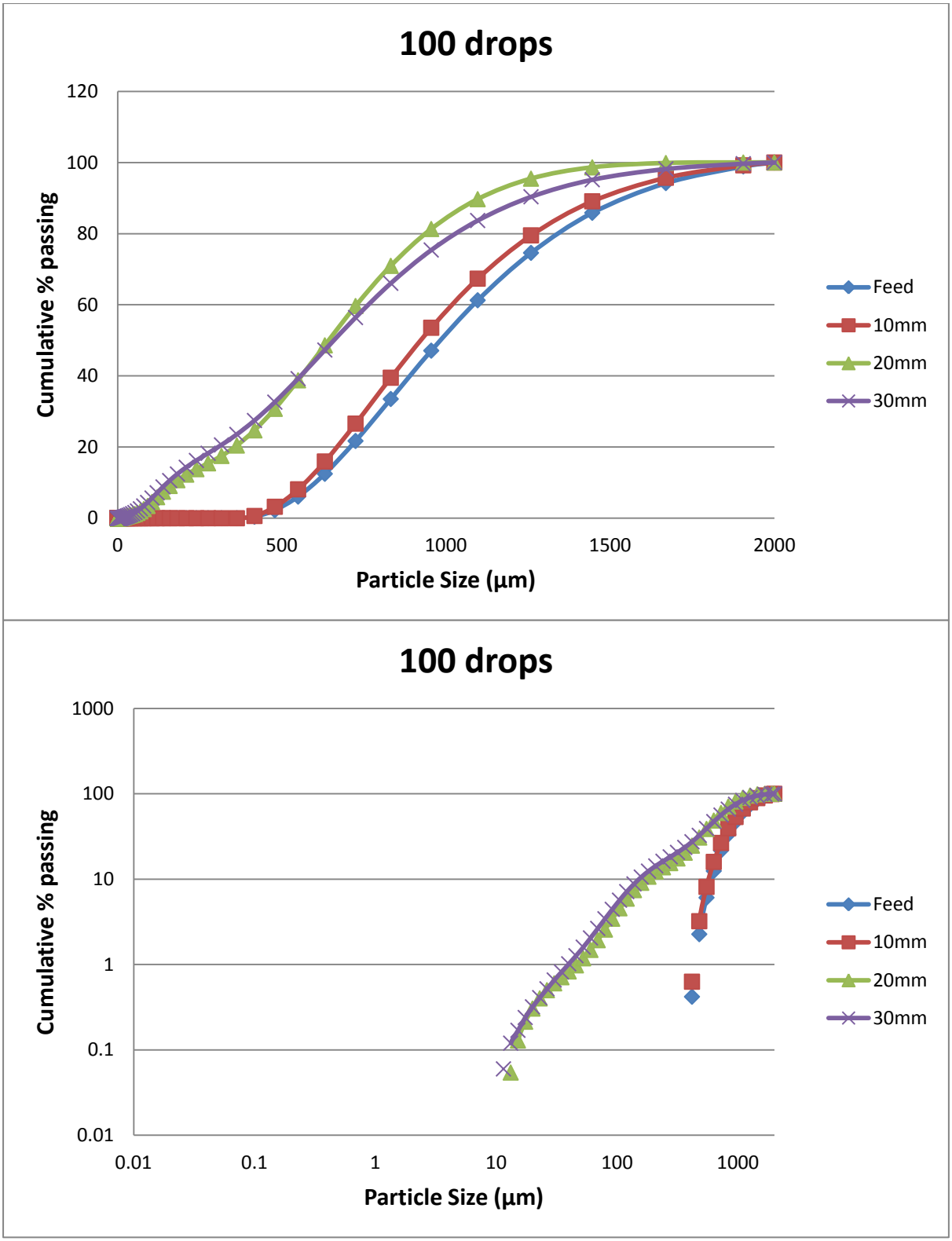

Figure C3**:** Cumulative distribution plots for three media sizes, at a constant drop height and number of impacts of 1.2 m and 100 respectively.

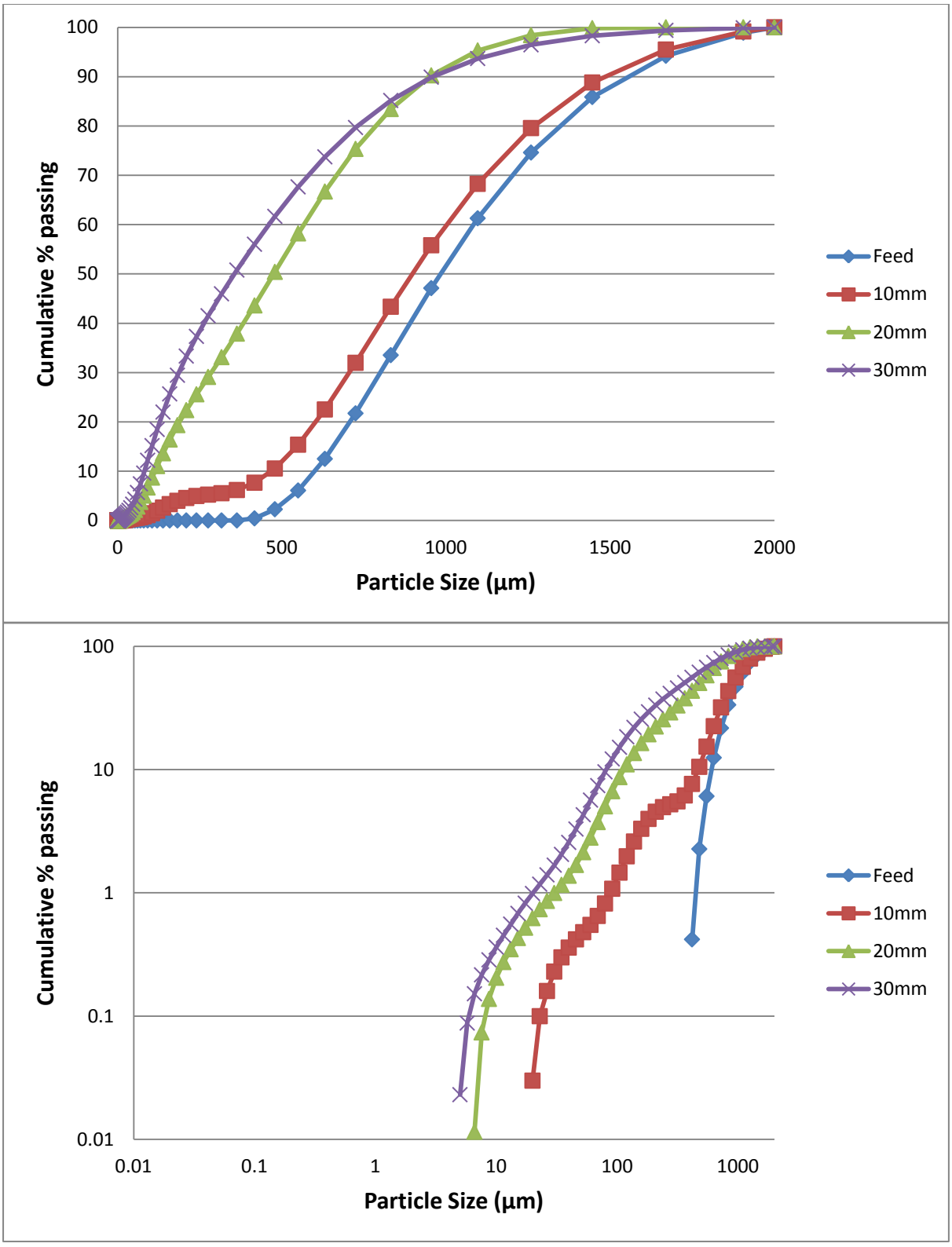

Figure C4**:** Cumulative distribution plots for three media sizes, at a constant drop height and number of impacts of 1.2 m and 300 respectively.

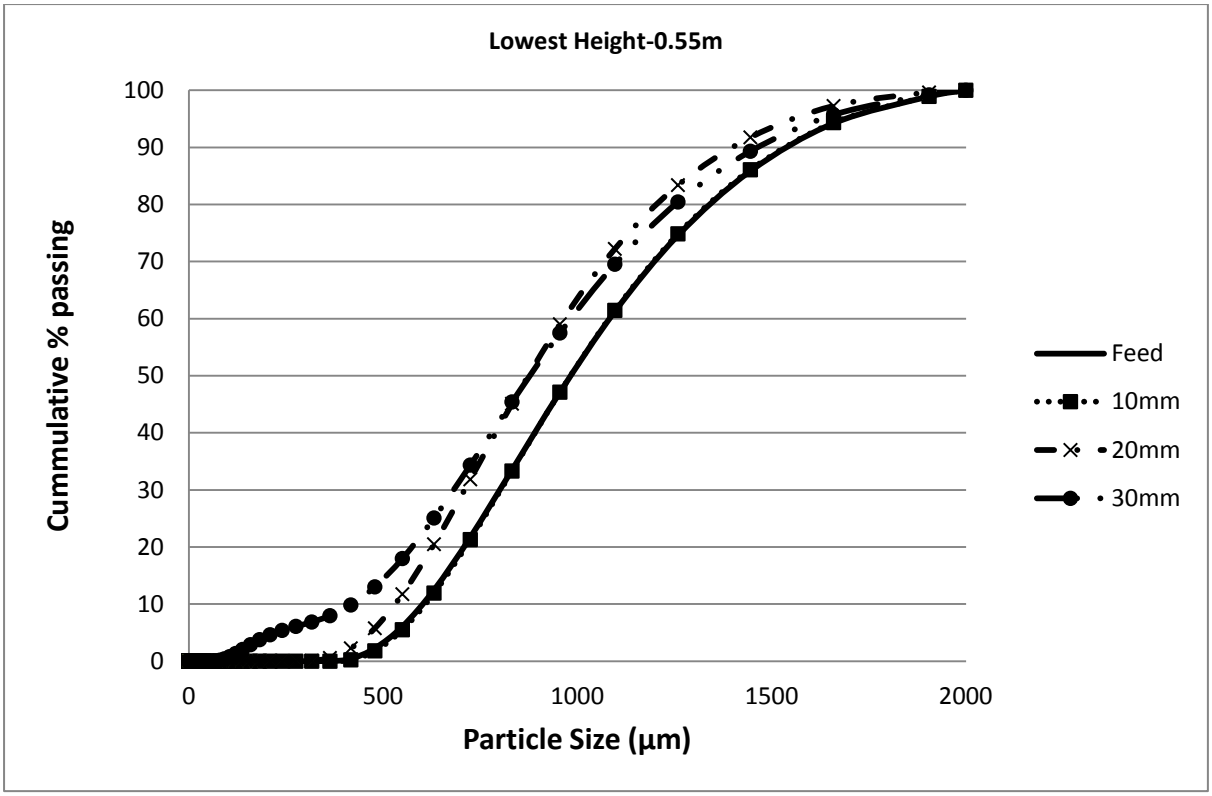

Figure C5**:** Cumulative distribution plots for three media sizes, at a constant number of impacts and drop height of 50 and 0.55 m respectively.

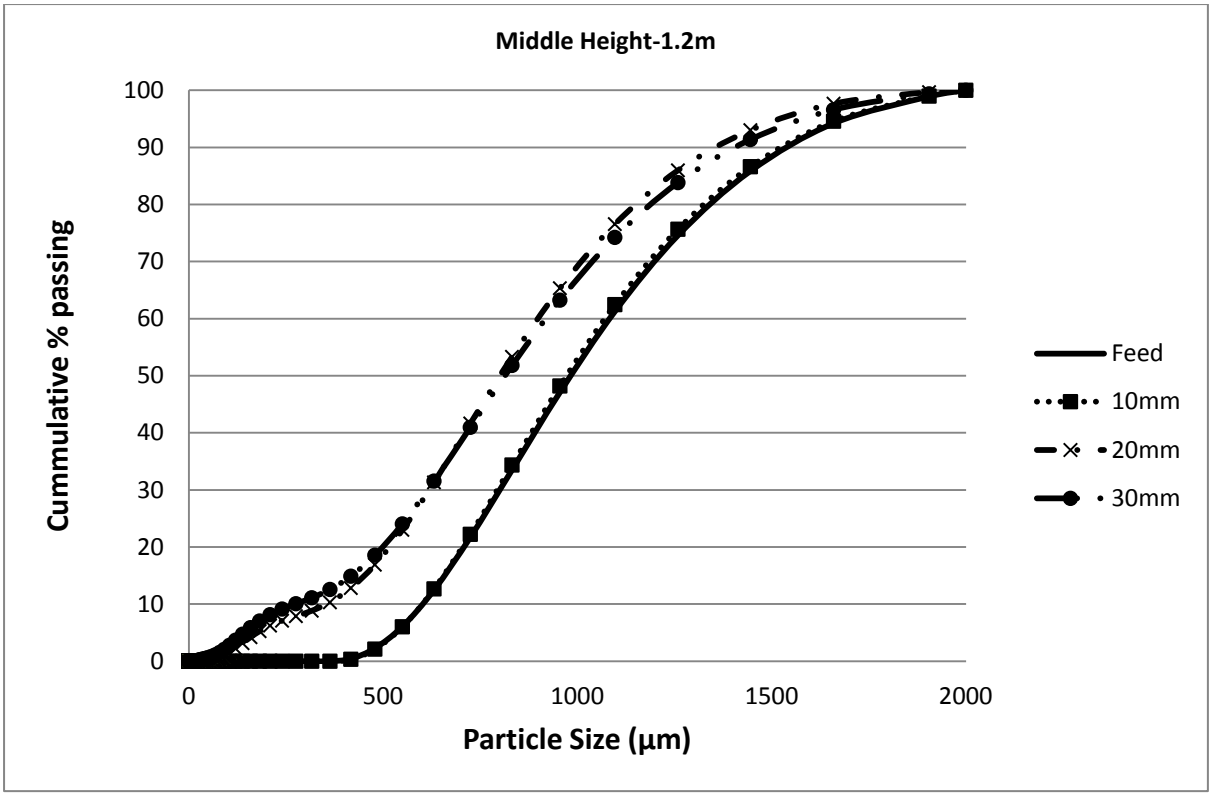

Figure C6**:** Cumulative distribution plots for three media sizes, at a constant number of impacts and drop height of 50 and 1.2 m respectively.

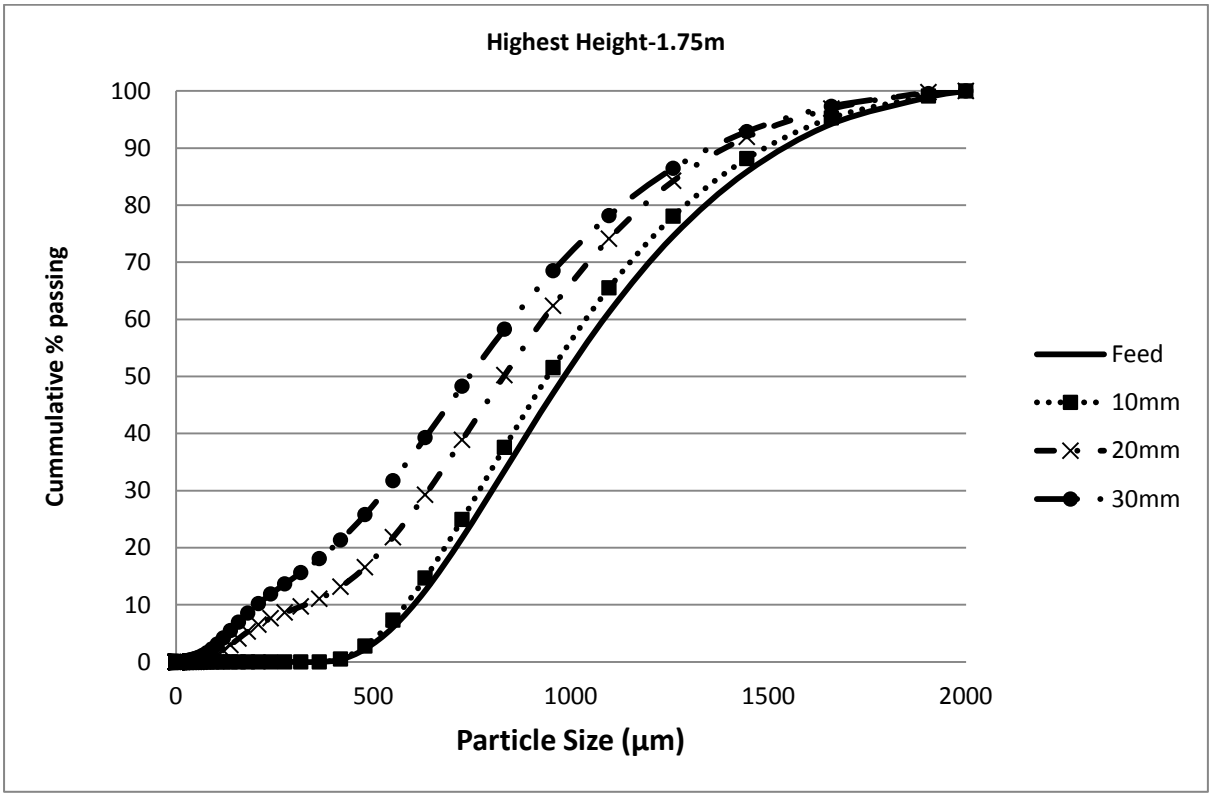

Figure C7**:** Cumulative distribution plots for three media sizes, at a constant number of impacts and drop height of 50 and 1.75 m respectively.

9.10 APPENDIX D: Mass fraction plots as a function of Number of impacts, Drop Height, Input energy and Specific Energy Plots

9.10.1 Appendix D1: Mass Fraction of each size class vs. Number of impacts

9.8.1.1 10mm ball size plots

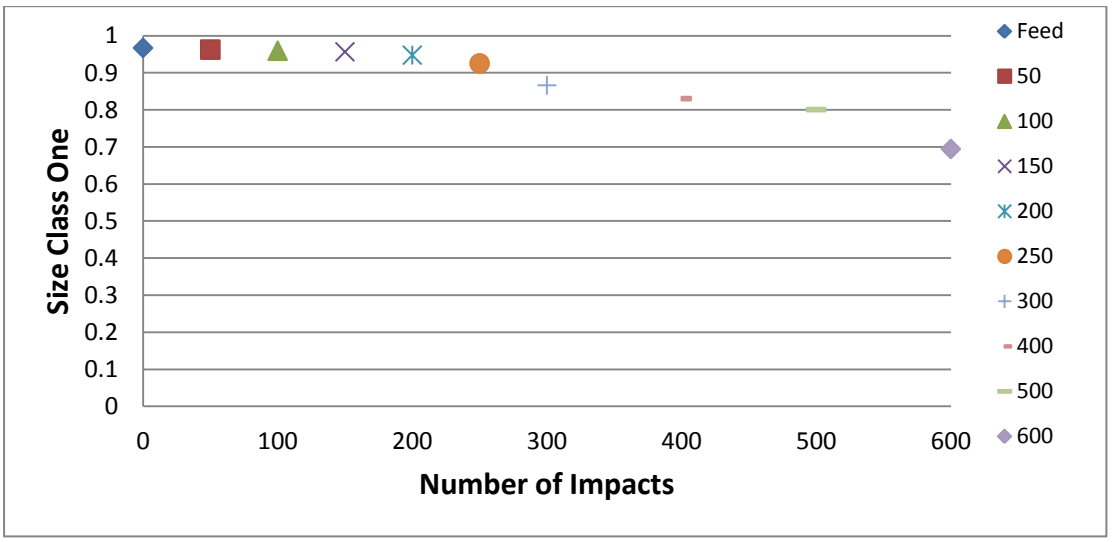

Figure D1.1 (a): Mass fraction of Size Class One vs. Number of Impacts

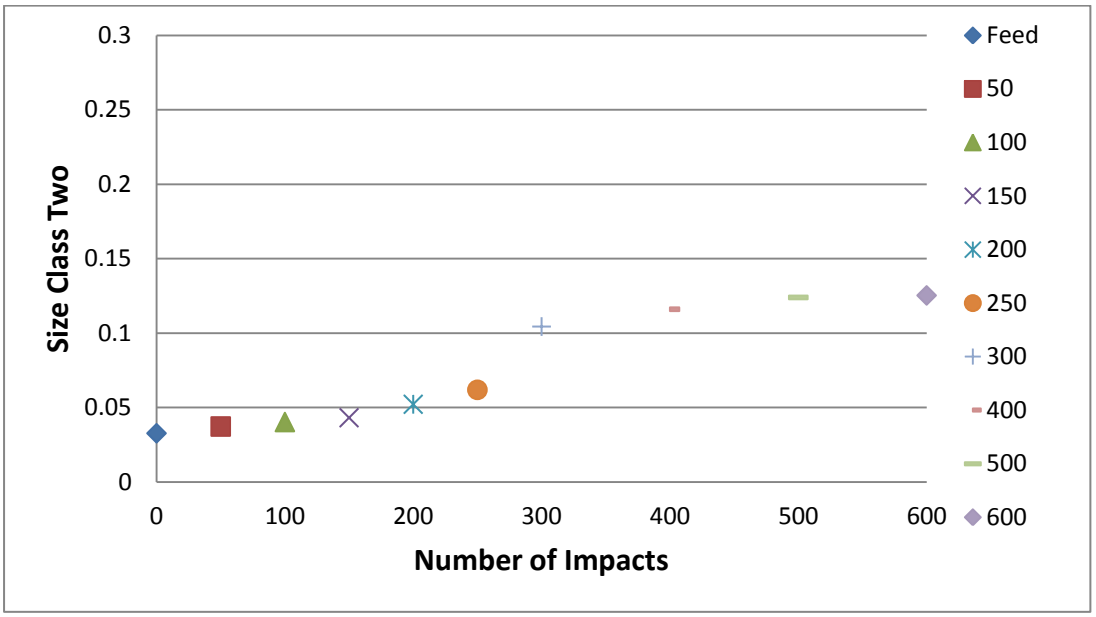

Figure D1. (b): Mass fraction of Size Class Two vs. Number of Impacts

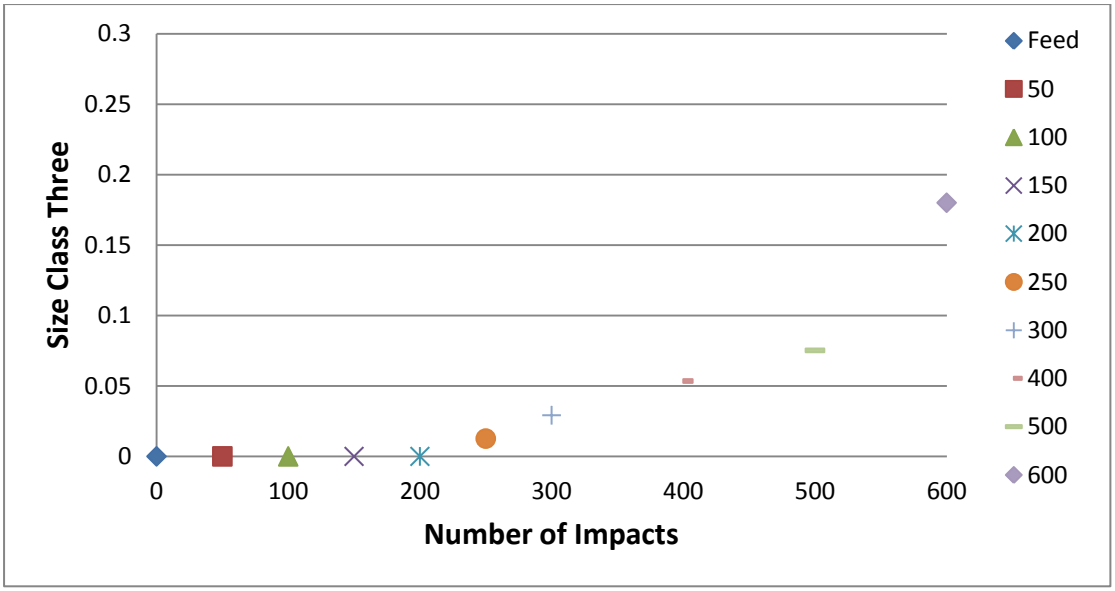

Figure D1.1 (c): Mass fraction of Size Class Three vs. Number of Impacts

9.8.1.2 20mm ball size plots

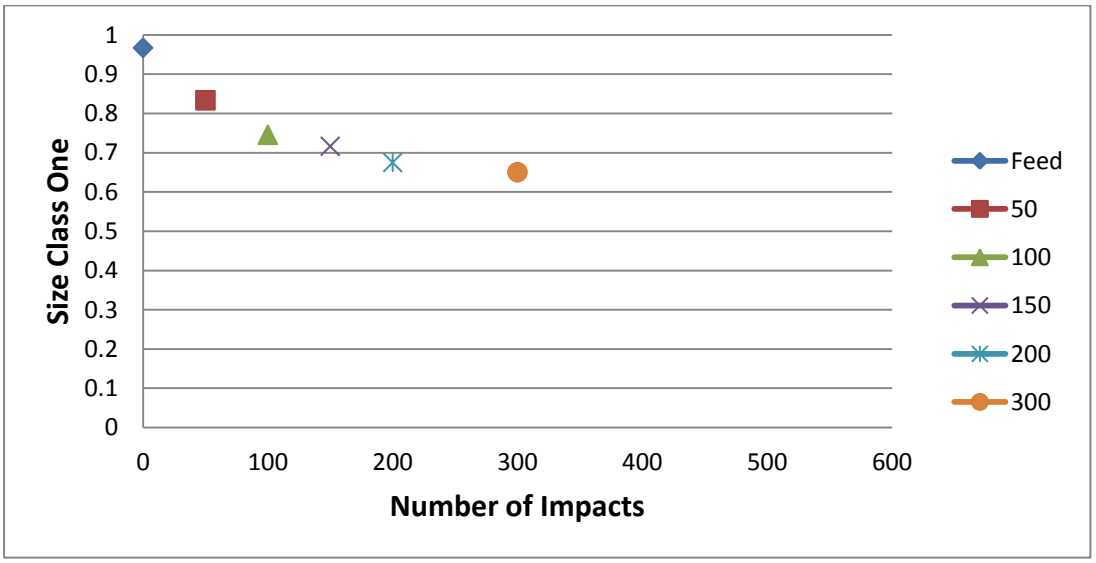

Figure D1.2 (a): Mass fraction of Size Class One vs. Number of Impacts

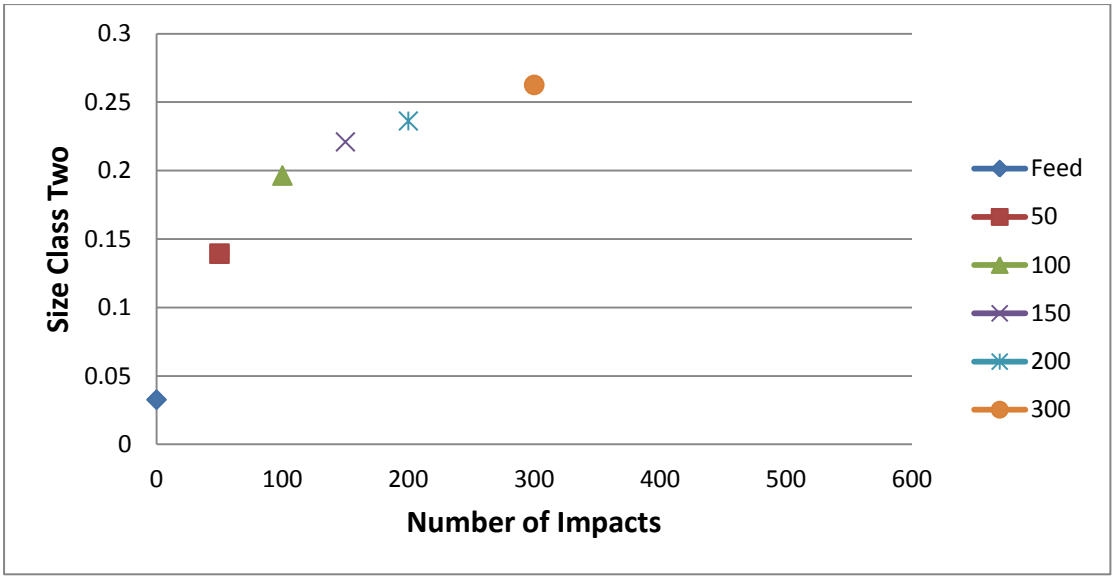

Figure D1.2 (b): Mass fraction of Size Class Two vs. Number of Impacts

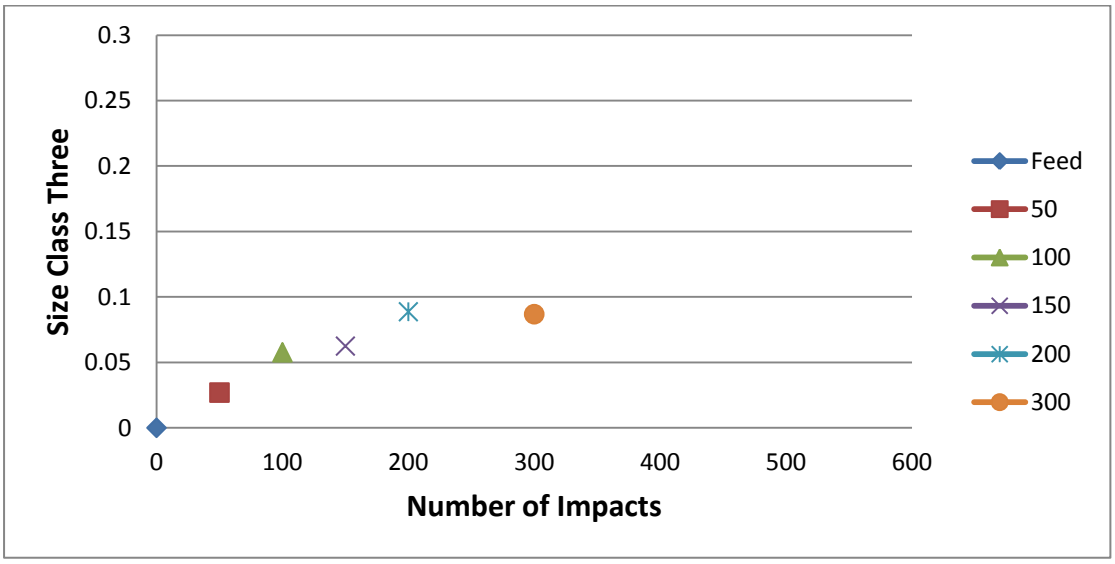

Figure D1.2 (c): Mass fraction of Size Class Three vs. Number of Impacts

9.8.1.3 30mm ball size plots

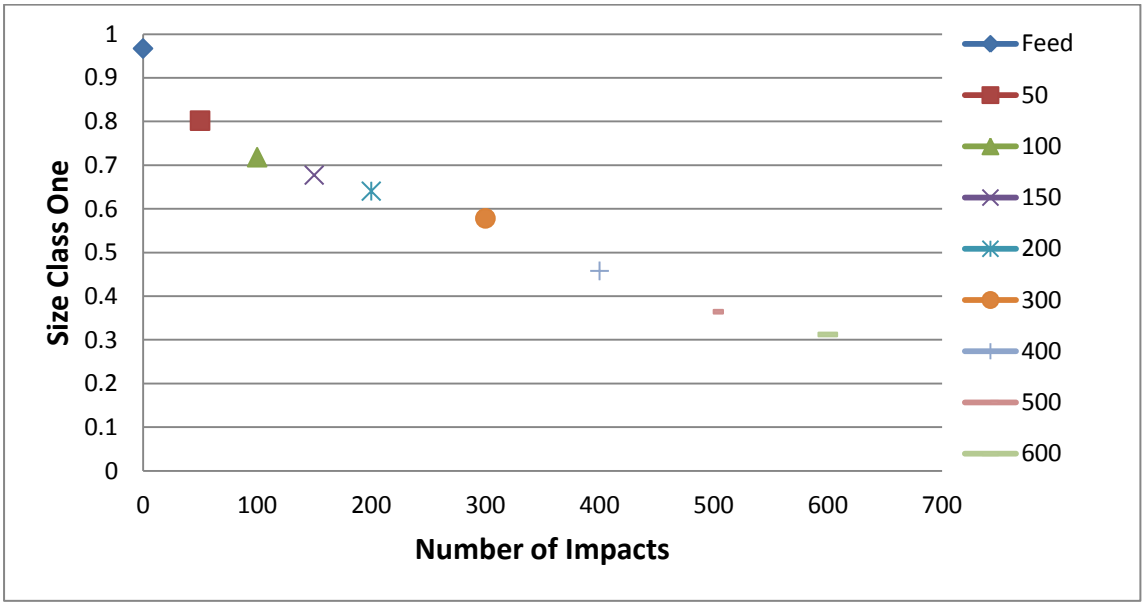

Figure D1.3 (a): Mass fraction of Size Class One vs. Number of Impacts

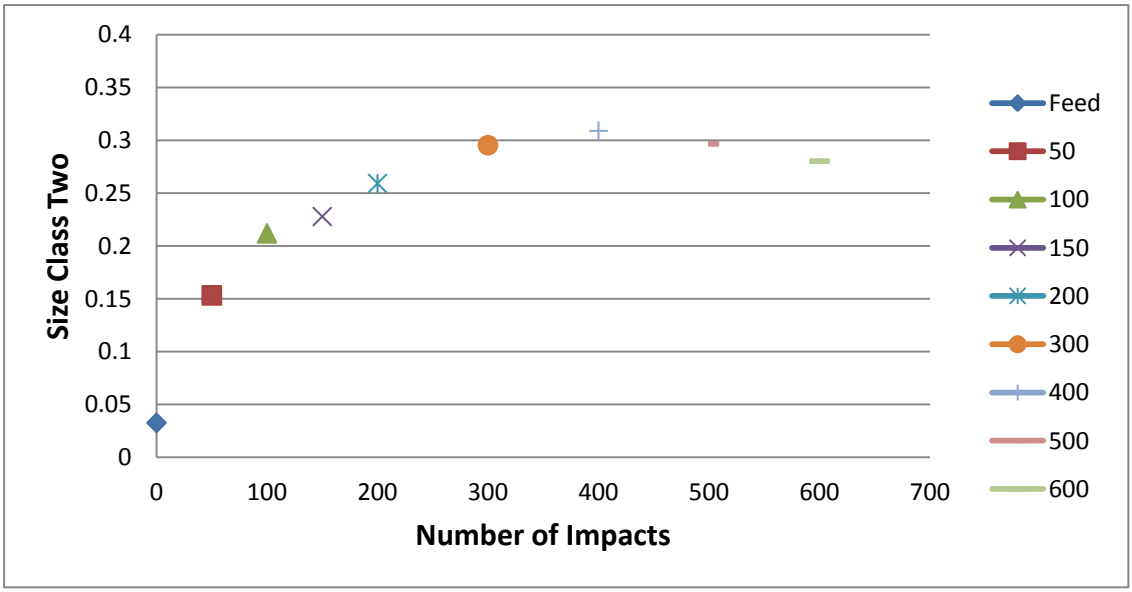

Figure D1.3 (b): Mass fraction of Size Class Two vs. Number of Impacts

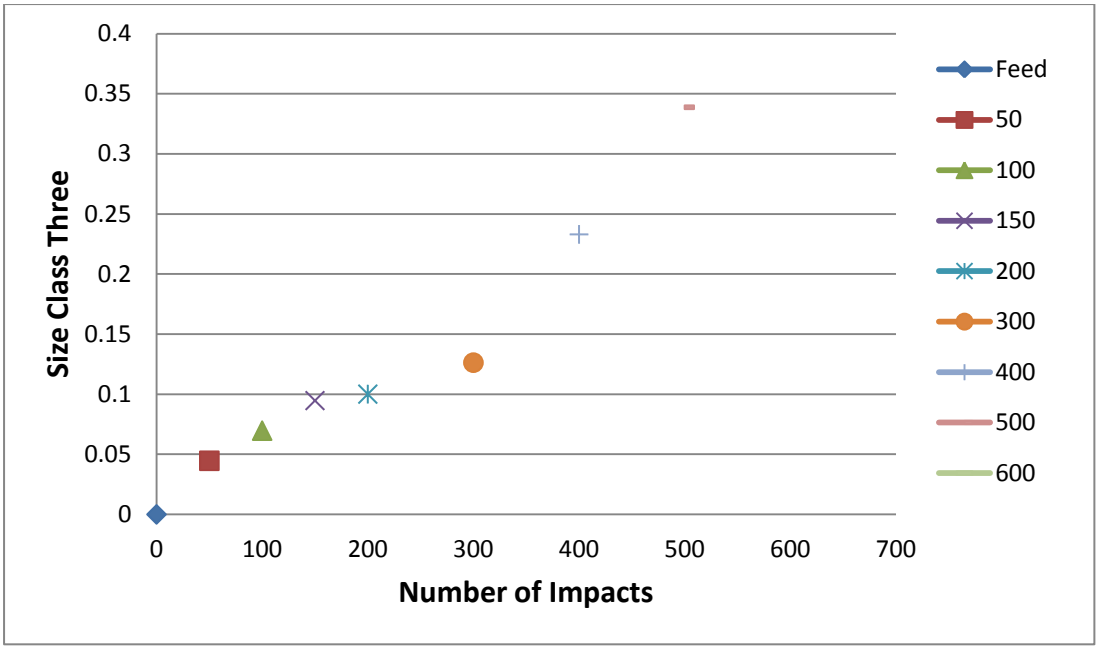

Figure D1.3 (c): Mass fraction of Size Class Three vs. Number of Impacts

9.10.2 Appendix D2: Mass Fraction of each size class vs. Drop height plots

9.10.2.1 Appendix D2: Mass Fraction vs. Drop Height plots

9.10.2.1.1 10mm ball size plots

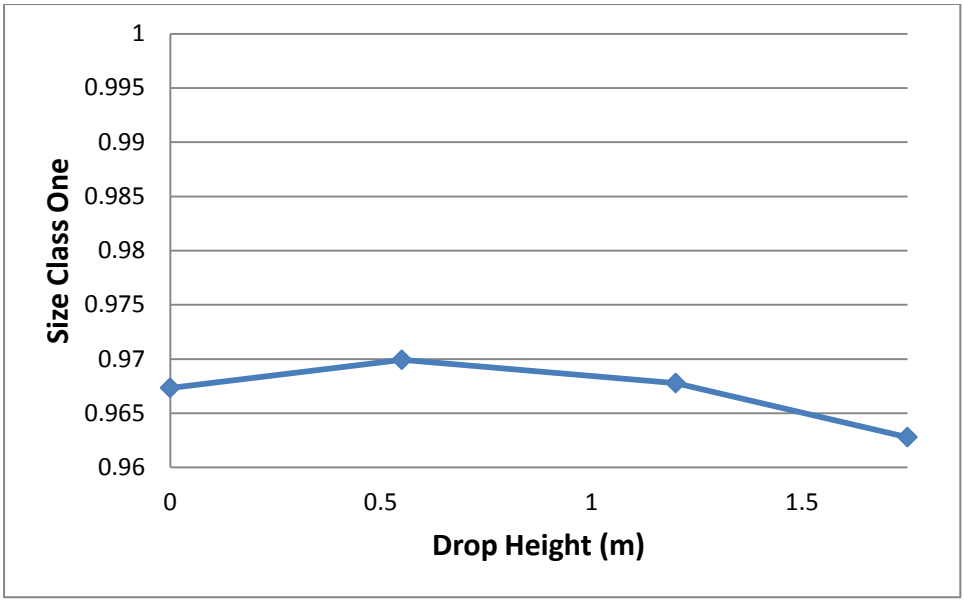

Figure D2.1 (a): Mass fraction of Size Class One vs. Drop Height

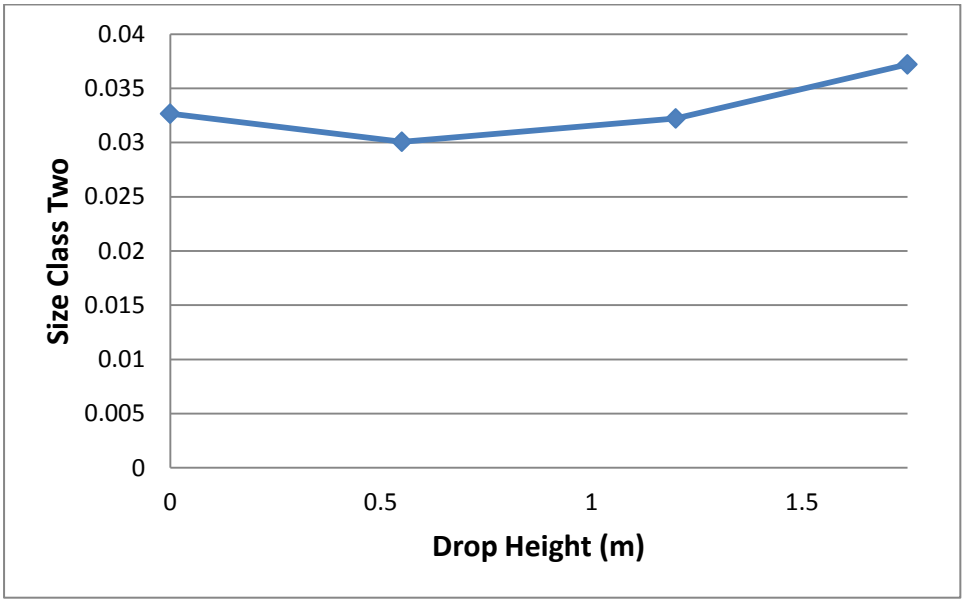

Figure D2.1 (b): Mass fraction of Size Class Two vs. Drop Height

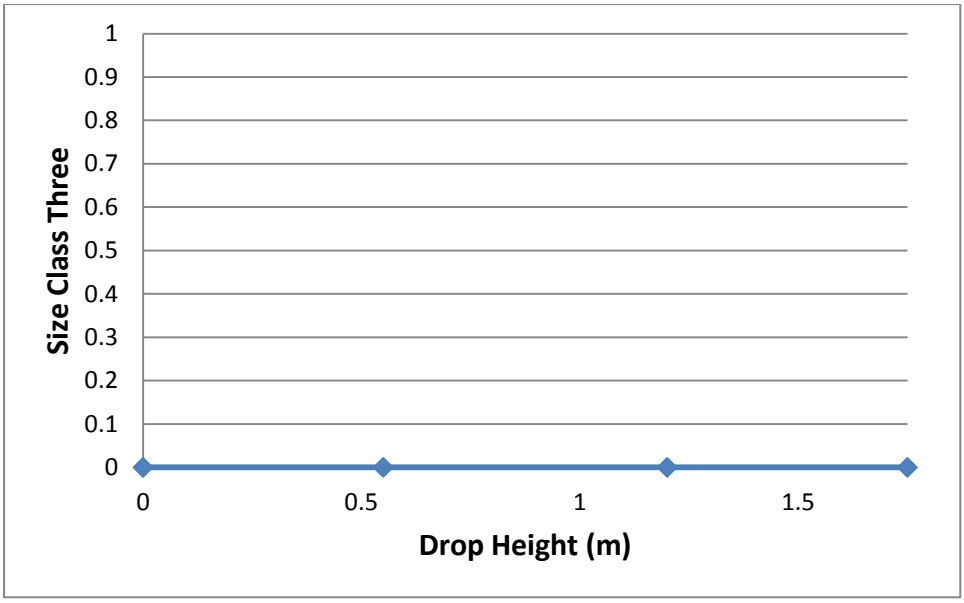

Figure D2.1 (c): Mass fraction of Size Class Three vs. Drop Height

9.10.2.1.2 20mm ball size plots

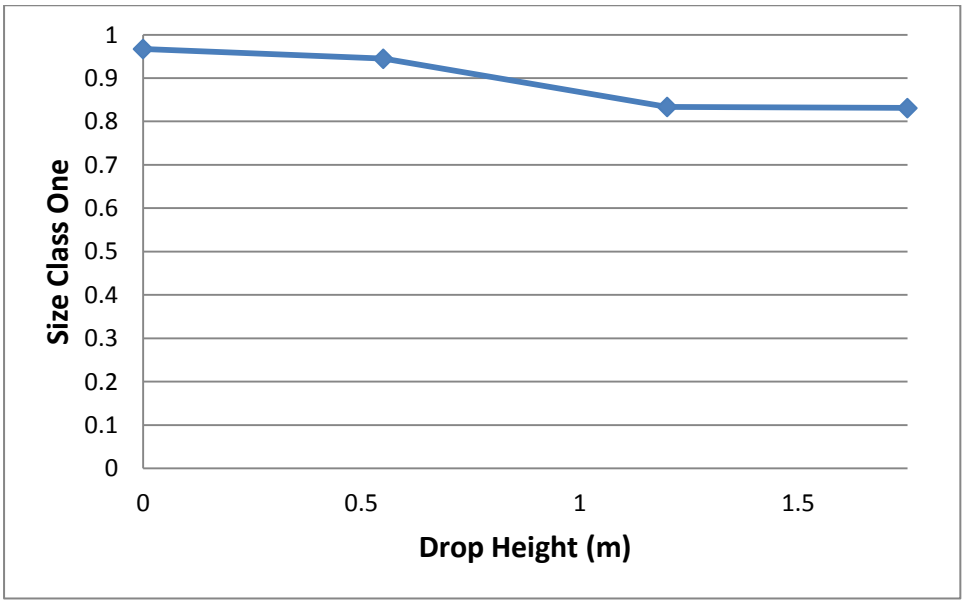

Figure D2.2 (a): Mass fraction of Size Class One vs. Drop Height

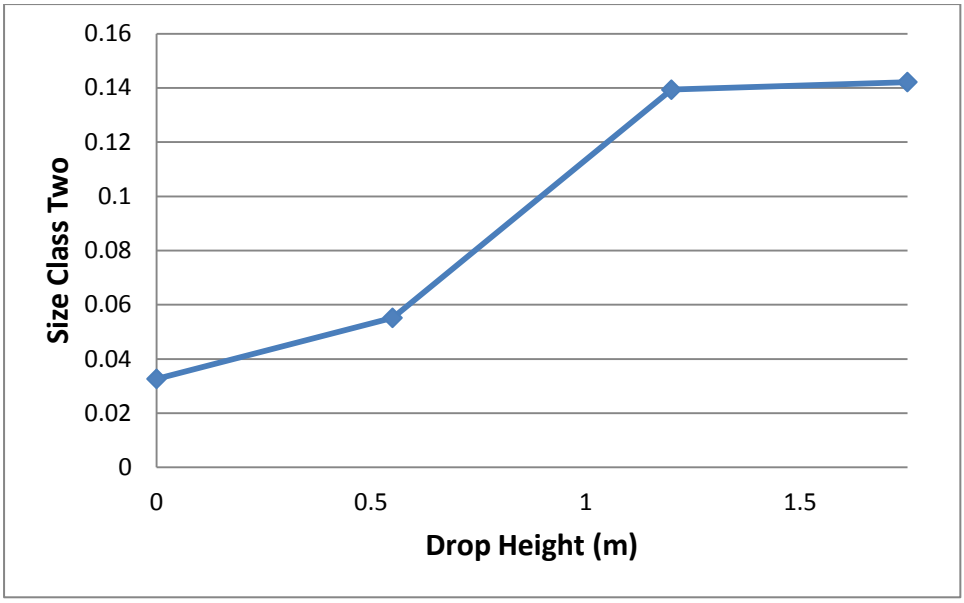

Figure D2.2 (b): Mass fraction of Size Class Two vs. Drop Height

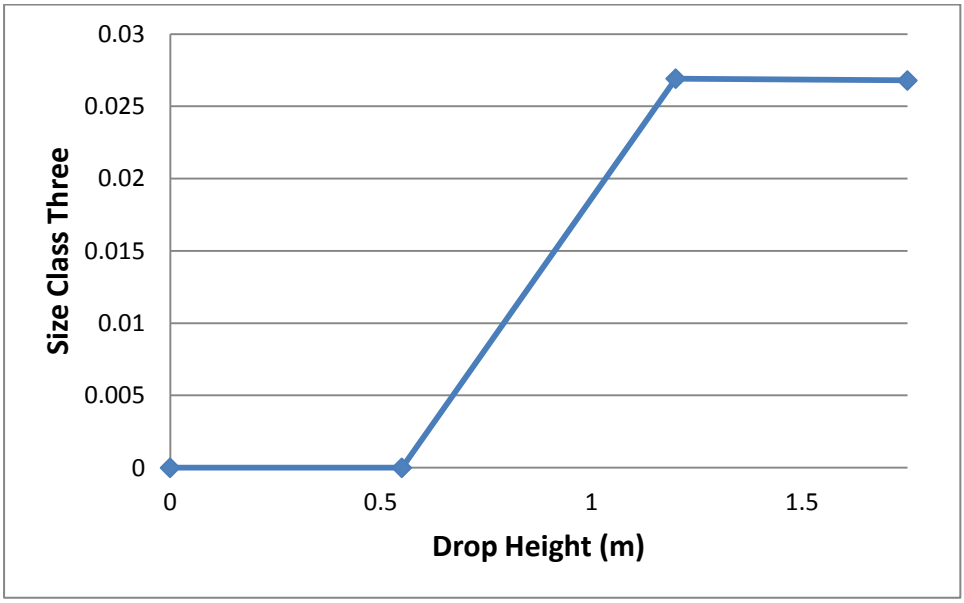

Figure D2.2 (c): Mass fraction of Size Class Three vs. Drop Height

9.10.2.1.3 30mm ball size plots

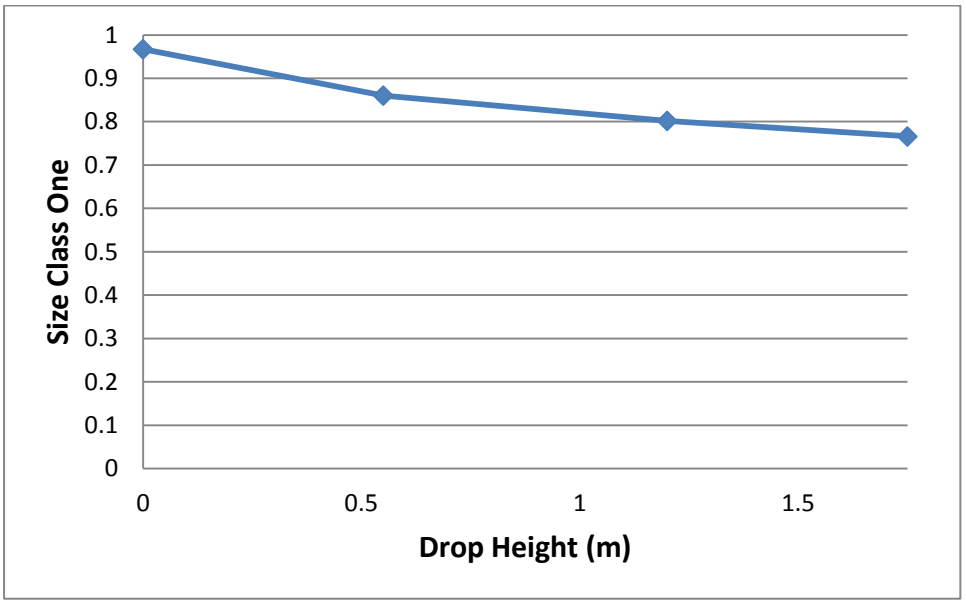

Figure D2.3 (a): Mass fraction of Size Class One vs. Drop Height

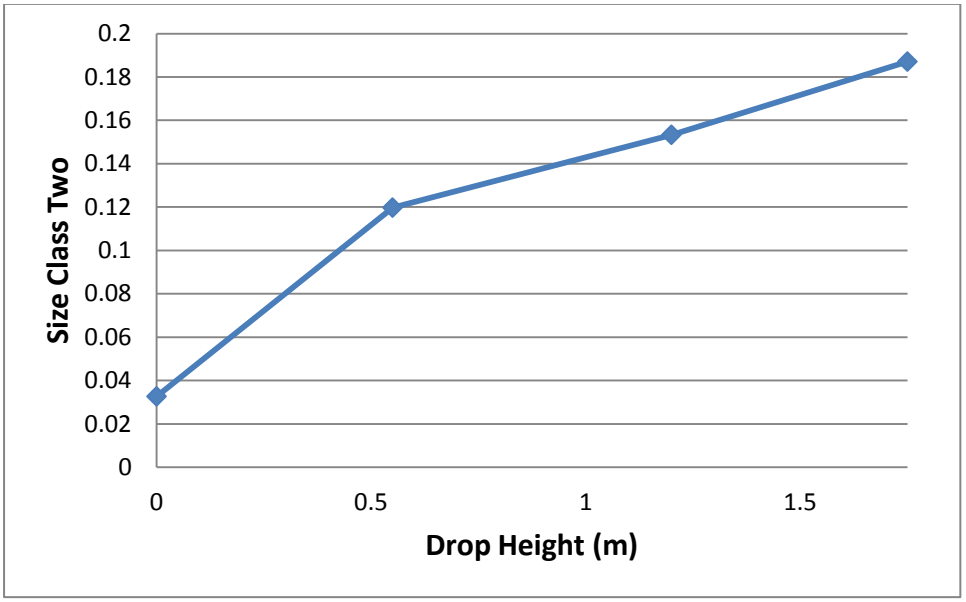

Figure D2.3 (b): Mass fraction of Size Class Two vs. Drop Height

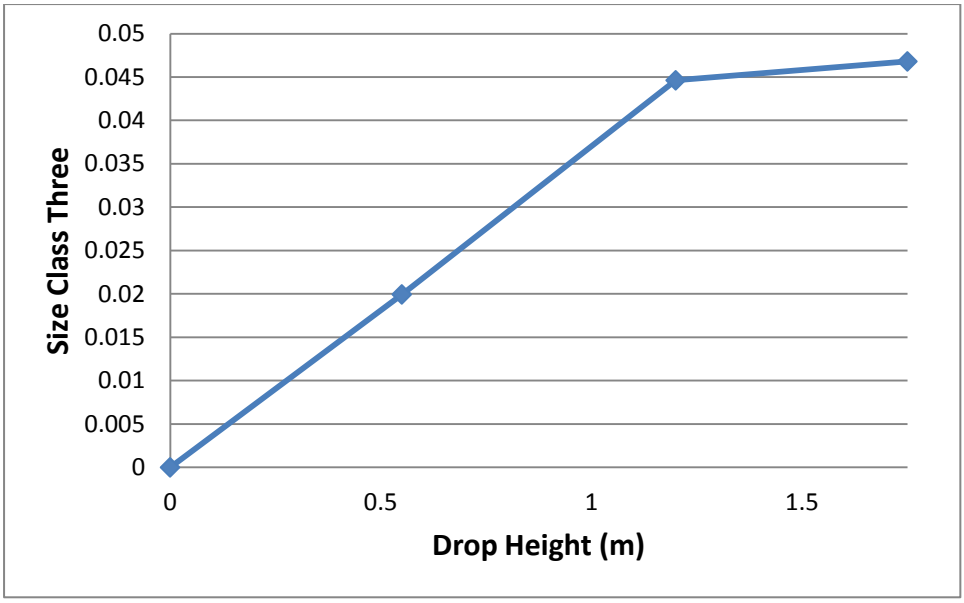

Figure D2.3 (c): Mass fraction of Size Class Three vs. Drop Height

9.10.3 Appendix D3: Mass Fraction of each size class vs. Input Energy plots

9.10.3.1 Appendix D3: Mass Fraction vs. Input Energy

9.10.3.1.1 10mm ball size plots

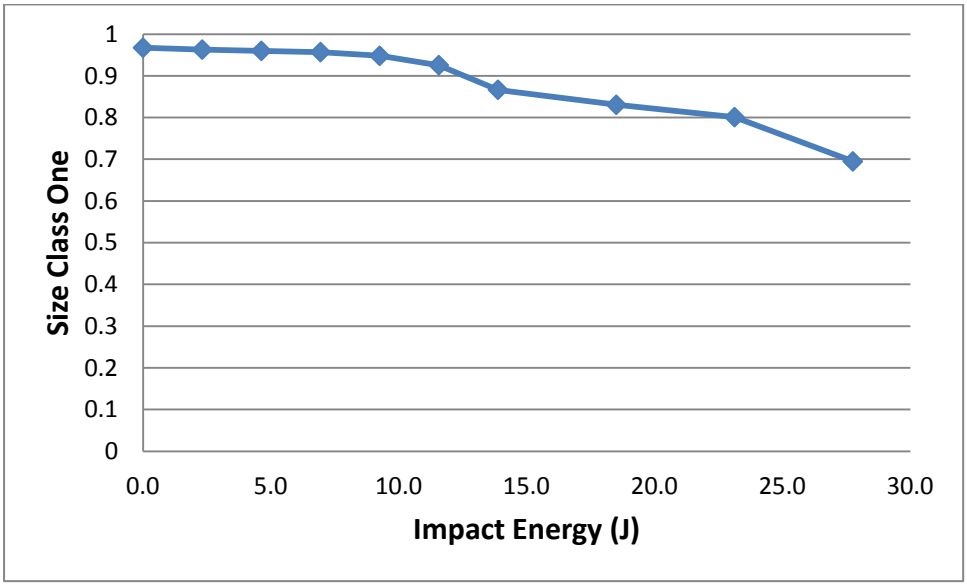

Figure D3.1 (a): Mass fraction of Size Class One vs. Impact Energy

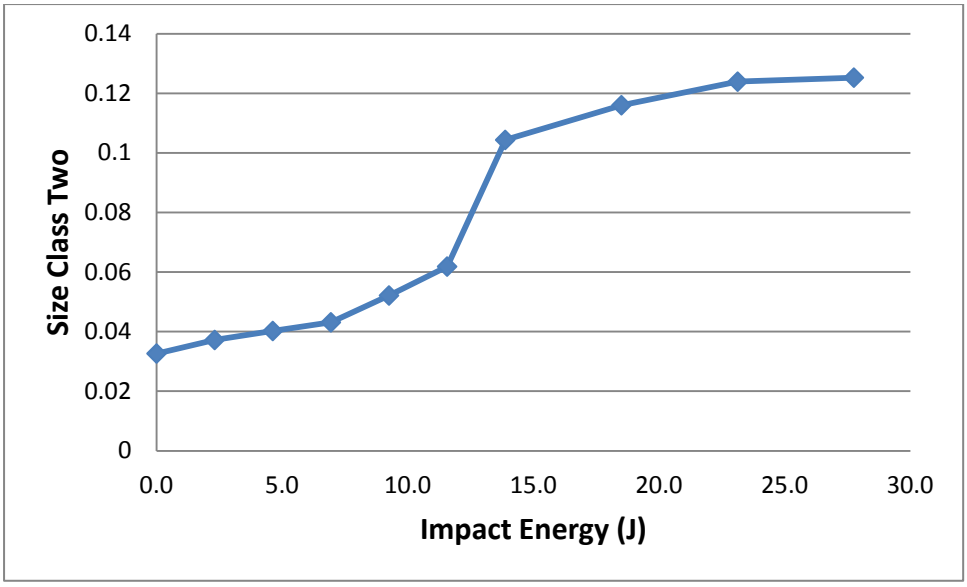

Figure D3.1 (b): Mass fraction of Size Class One vs. Impact Energy

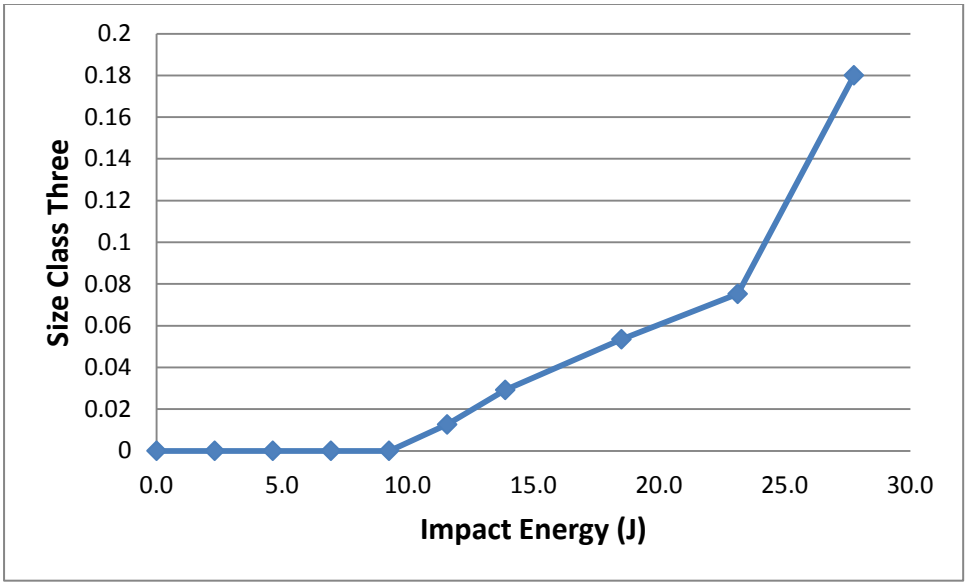

Figure D3.1 (c): Mass fraction of Size Class One vs. Impact Energy

9.10.3.1.2 20mm ball size plots

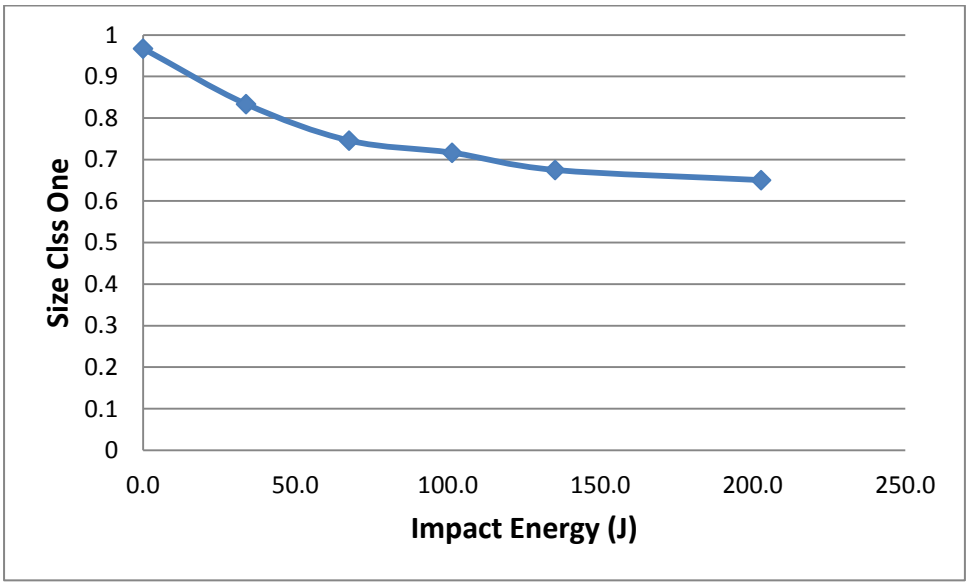

Figure D3.2 (a): Mass fraction of Size Class One vs. Impact Energy

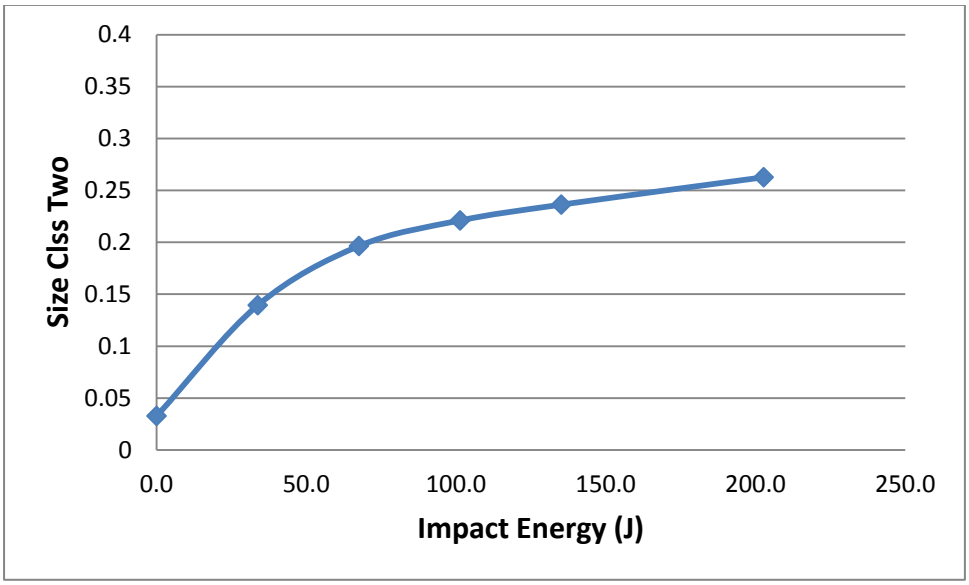

Figure D3.2 (b): Mass fraction of Size Class Two vs. Impact Energy

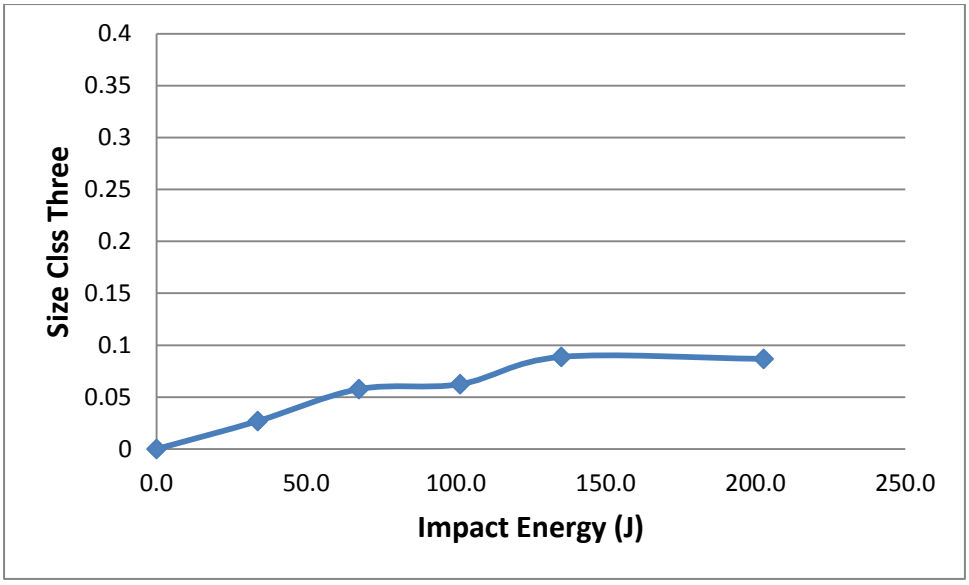

Figure D3.2 (c): Mass fraction of Size Class Two vs. Impact Energy

9.10.3.1.3 30mm ball size plots

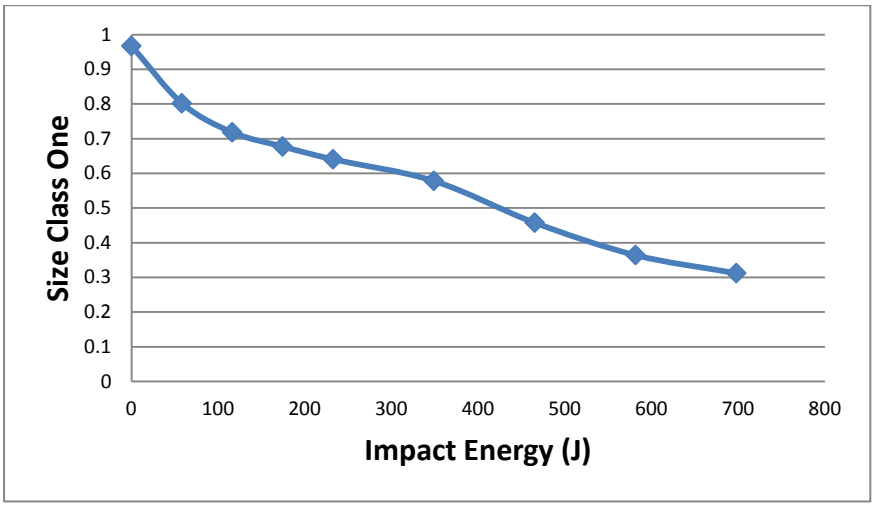

Figure D3.3 (a): Mass fraction of Size Class Three vs. Impact Energy

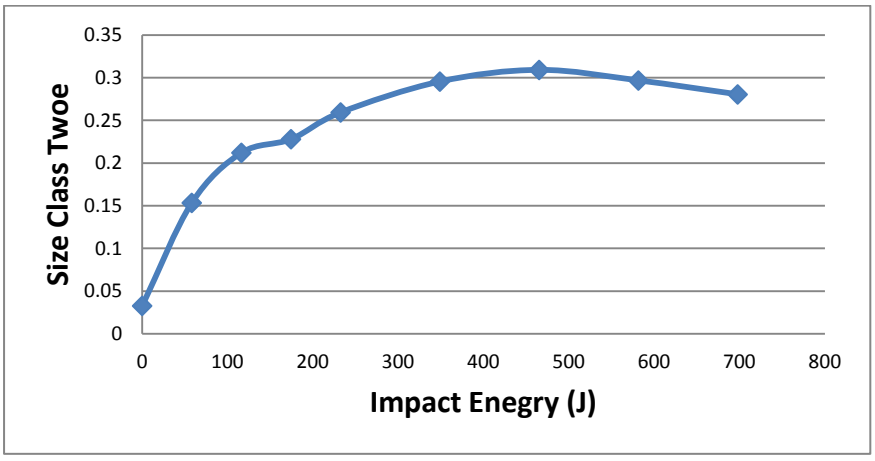

Figure D3.3 (b): Mass fraction of Size Class Three vs. Impact Energy

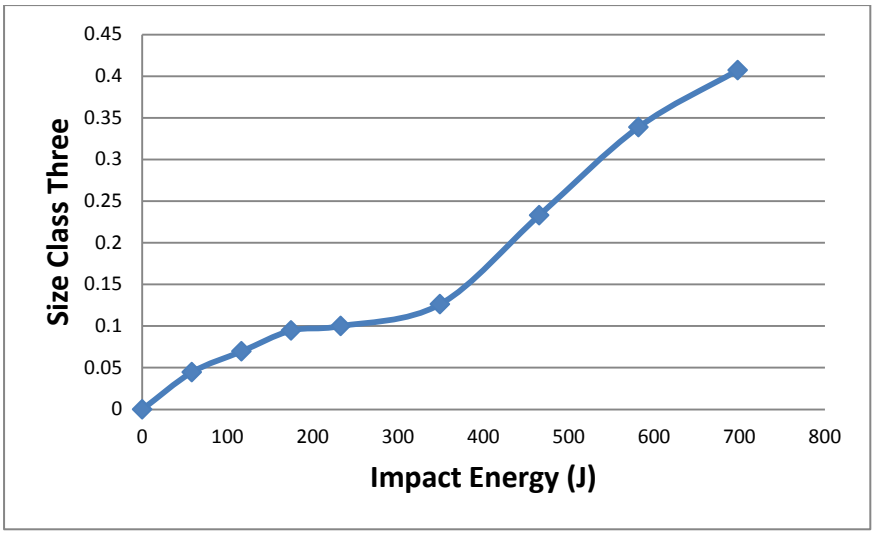

Figure D3.3 (c): Mass fraction of Size Class Three vs. Impact Energy

9.10.3.1.4 Comparison plot for all three grinding media sizes

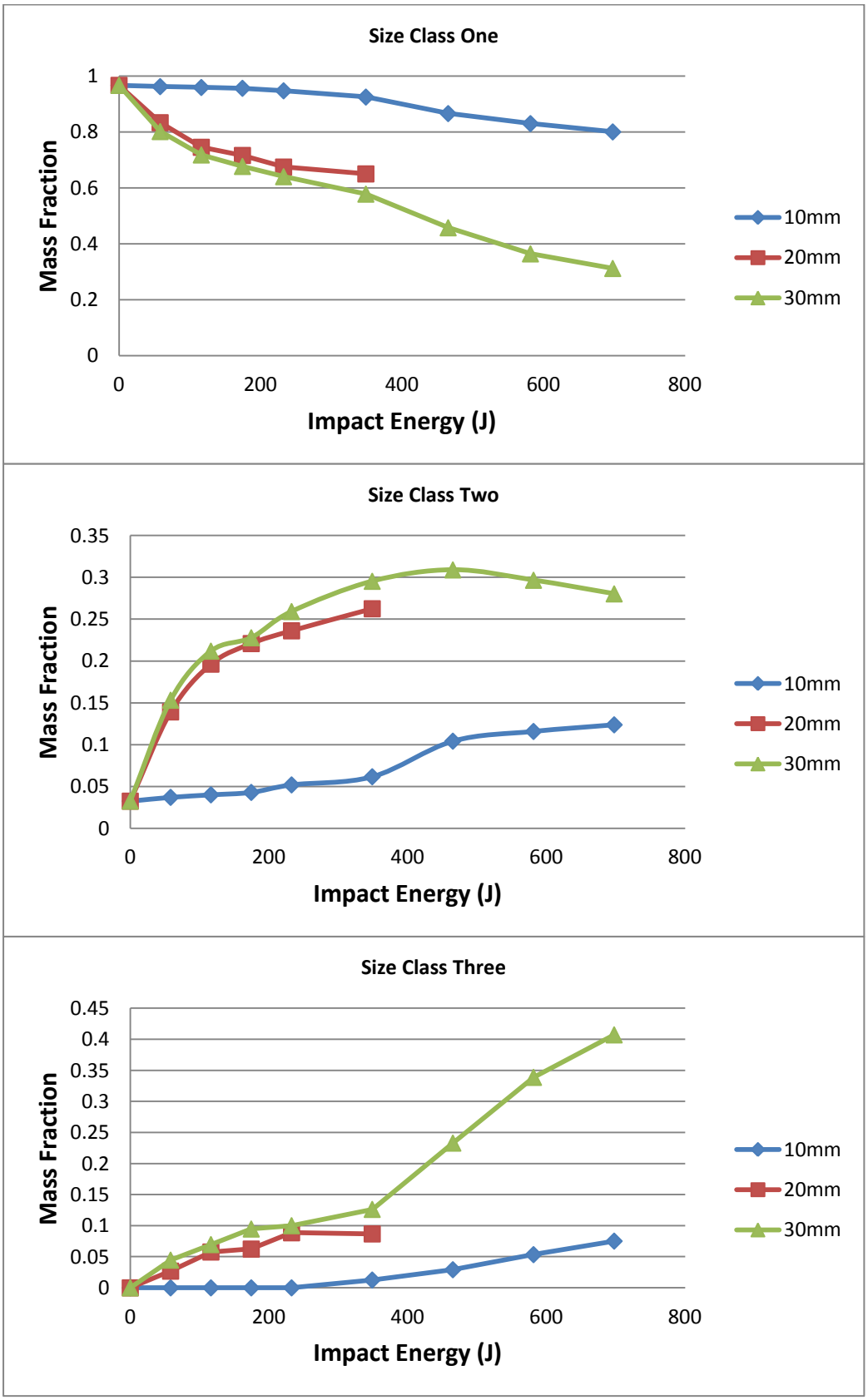

Figure D3.4**:** Comparison of Mass fraction vs. Impact Energy for three ball sizes.

9.10.4 Appendix D4: Mass Fraction of each size class vs. Specific Energy plots

9.10.4.1 Appendix D4: Mass Fraction vs. Specific Energy

9.10.4.1.1 10mm ball size plots

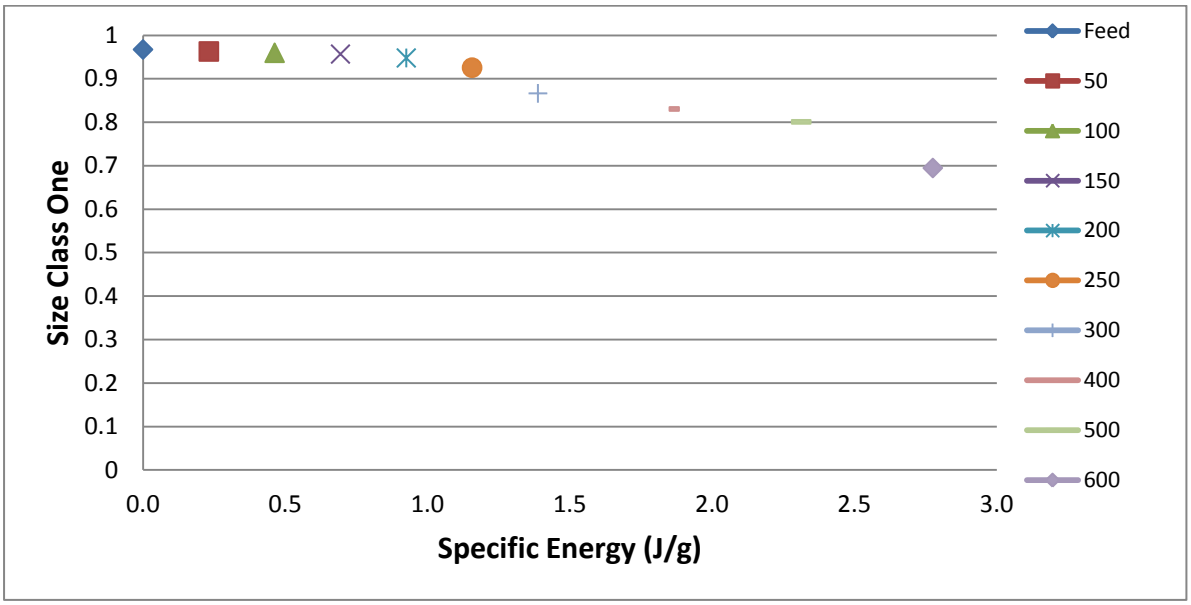

Figure D4.1 (a): Size Class One vs. Specific Energy

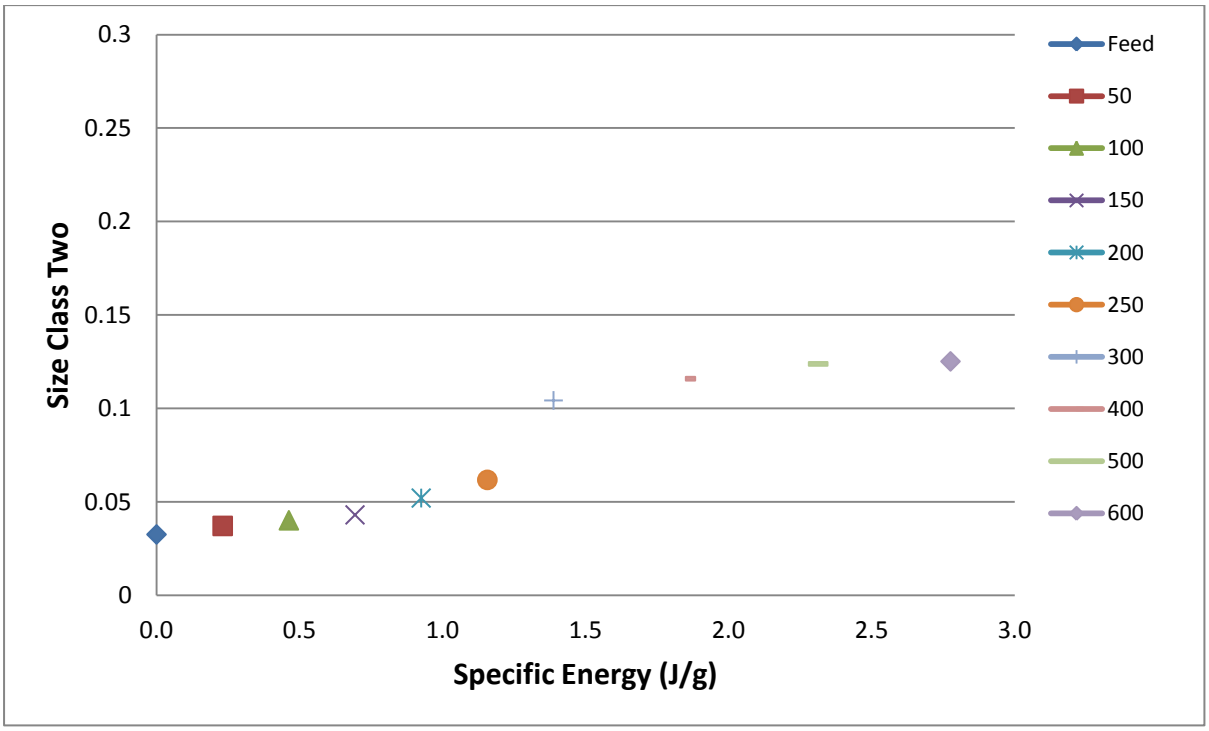

Figure D4.1 (b): Size Class Two vs. Specific Energy

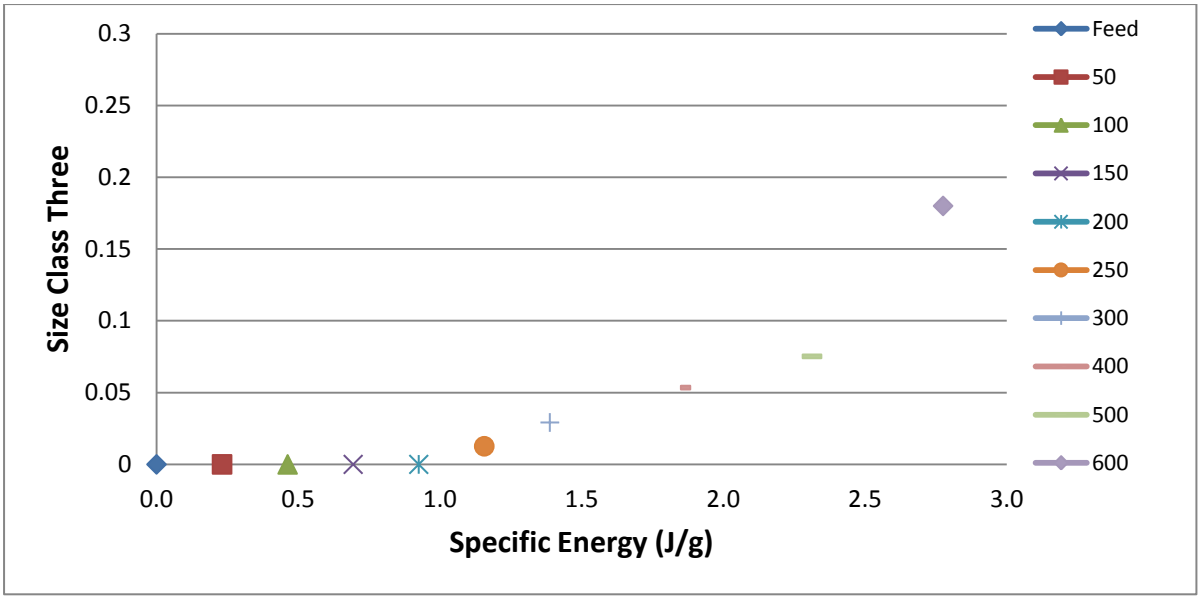

Figure D4.1 (c): Size Class Three vs. Specific Energy

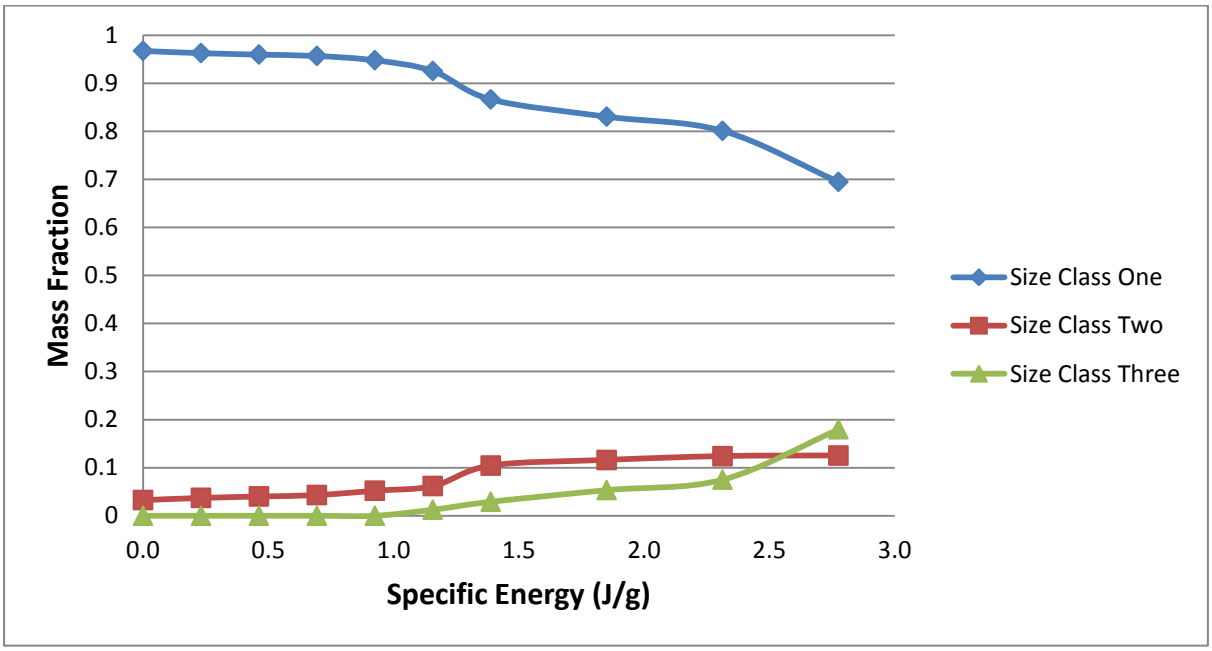

Figure D4.1 (d): Mass fraction of all size classes vs. Specific Energy

9.10.4.1.2 20mm ball size plots

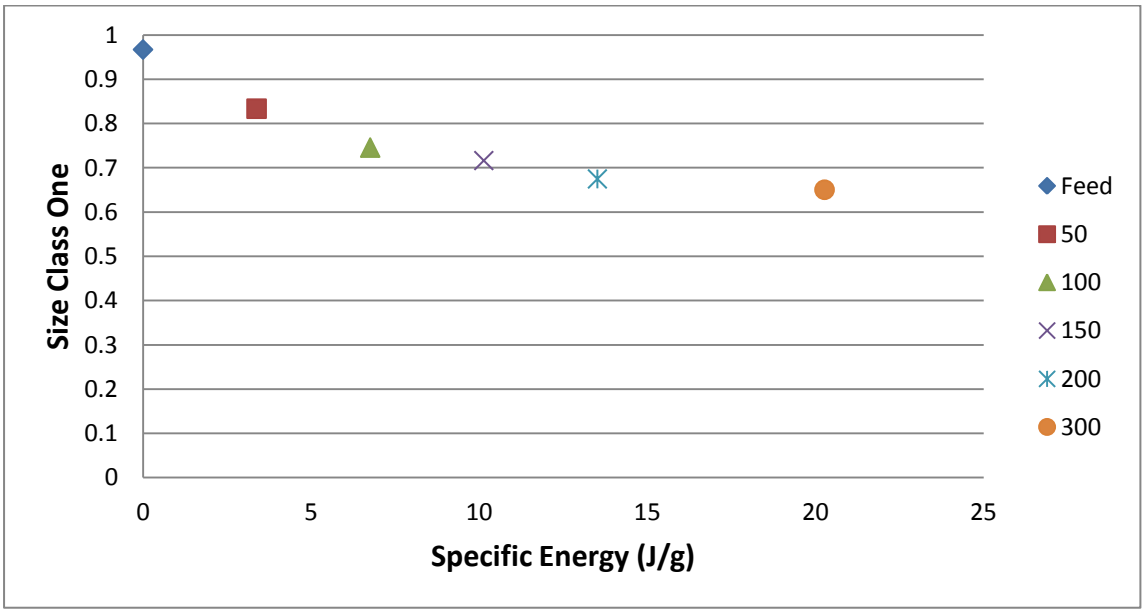

Figure D4.2 (a): Size Class Two vs. Specific Energy

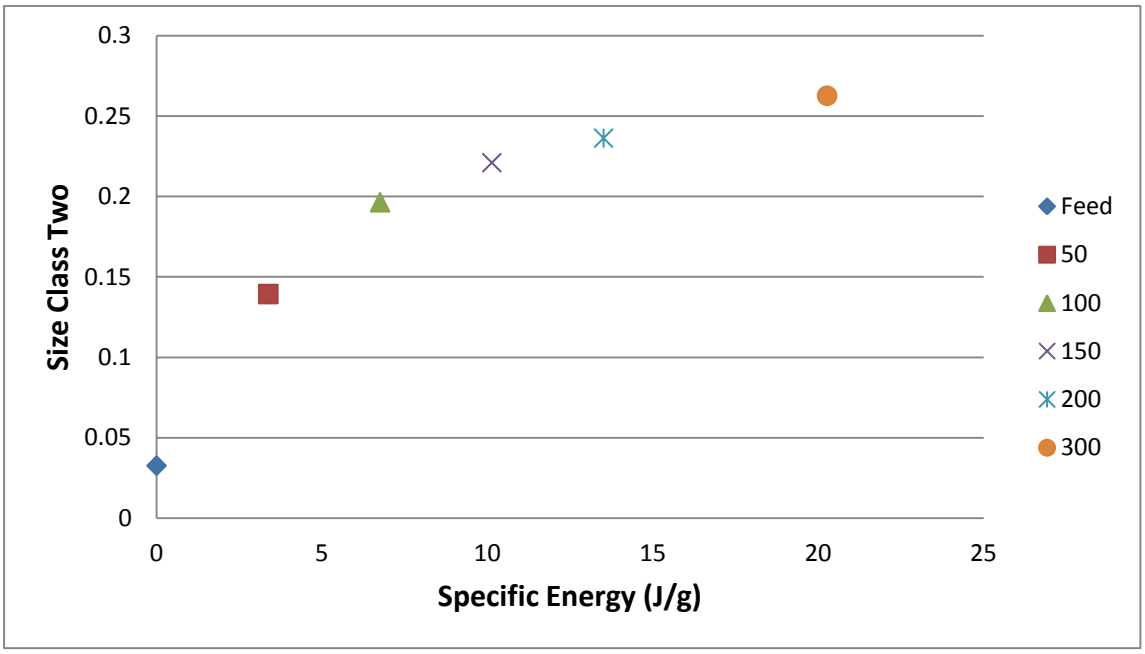

Figure D4.2 (b): Size Class Two vs. Specific Energy

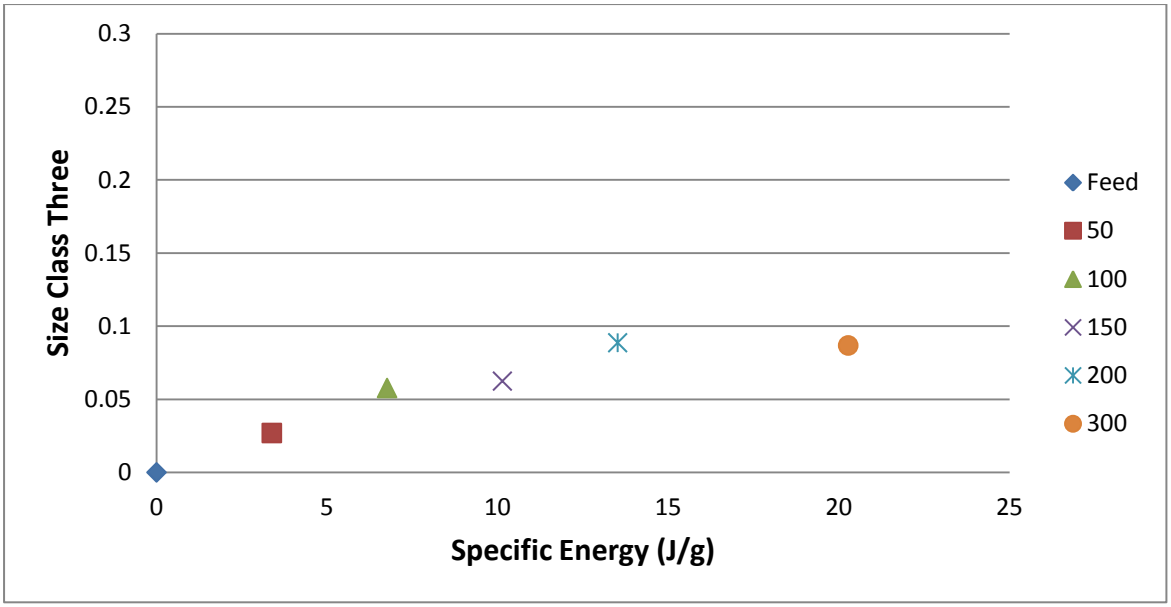

Figure D4.2 (c): Size Class Two vs. Specific Energy

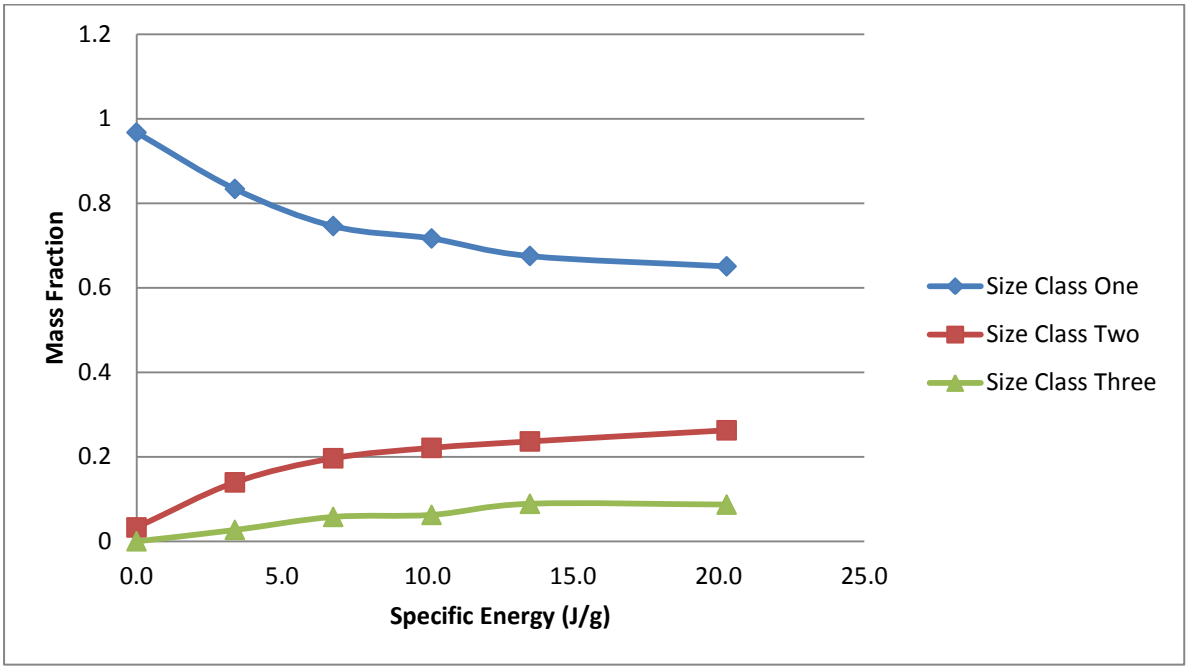

Figure D4.2 (d): Mass fraction of all size classes vs. Specific Energy

9.10.4.1.3 30mm ball size plots

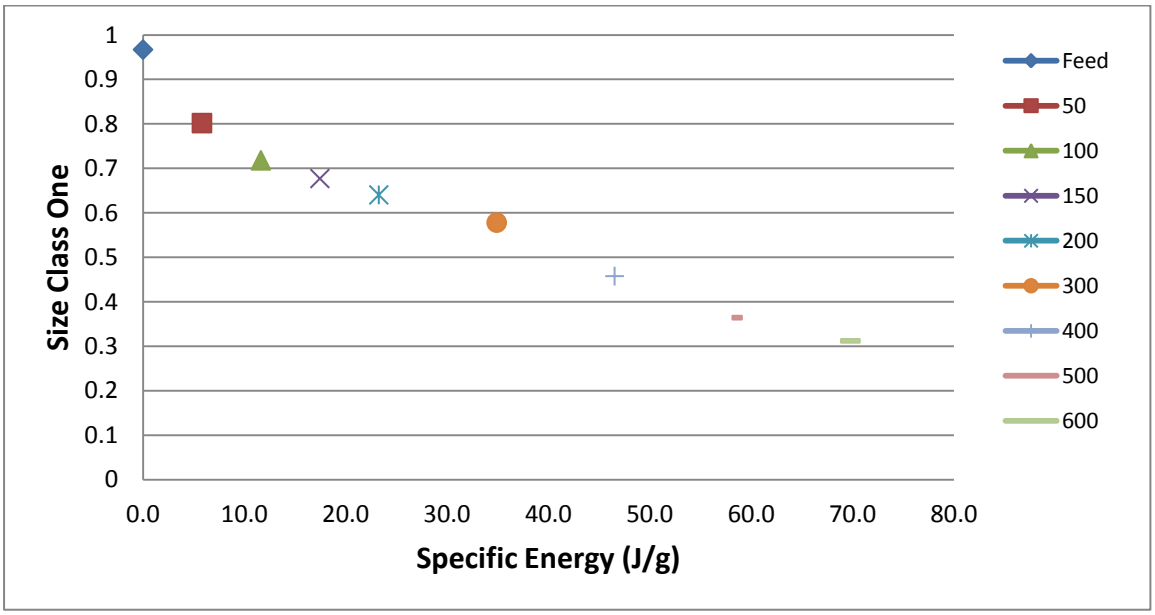

Figure D4.3 (a): Size Class One vs. Specific Energy

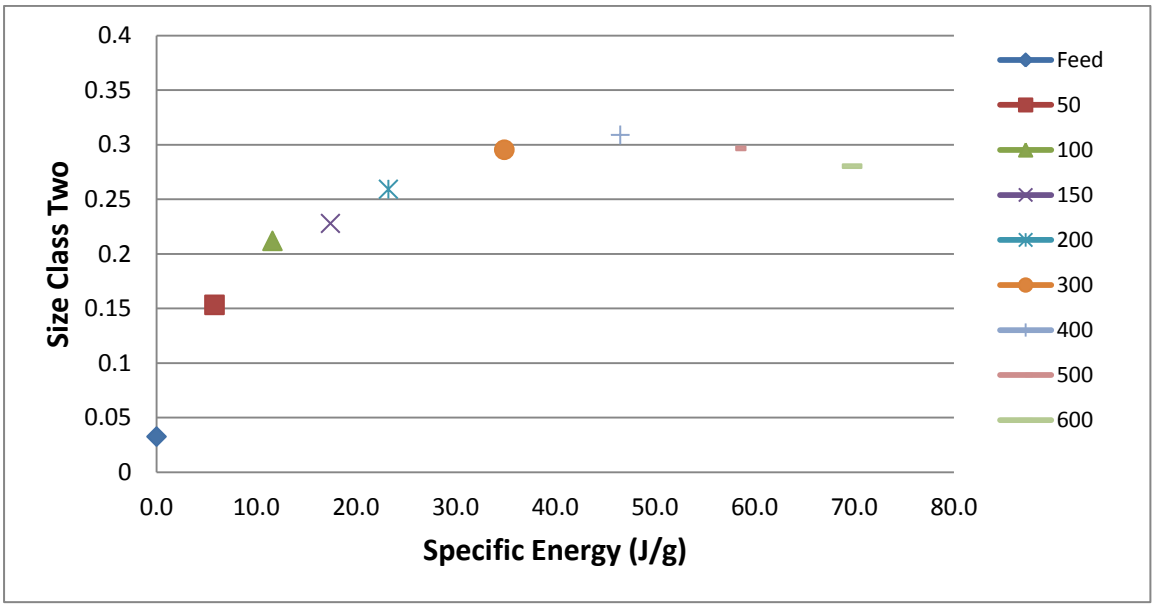

Figure D4.3 (b): Size Class Two vs. Specific Energy

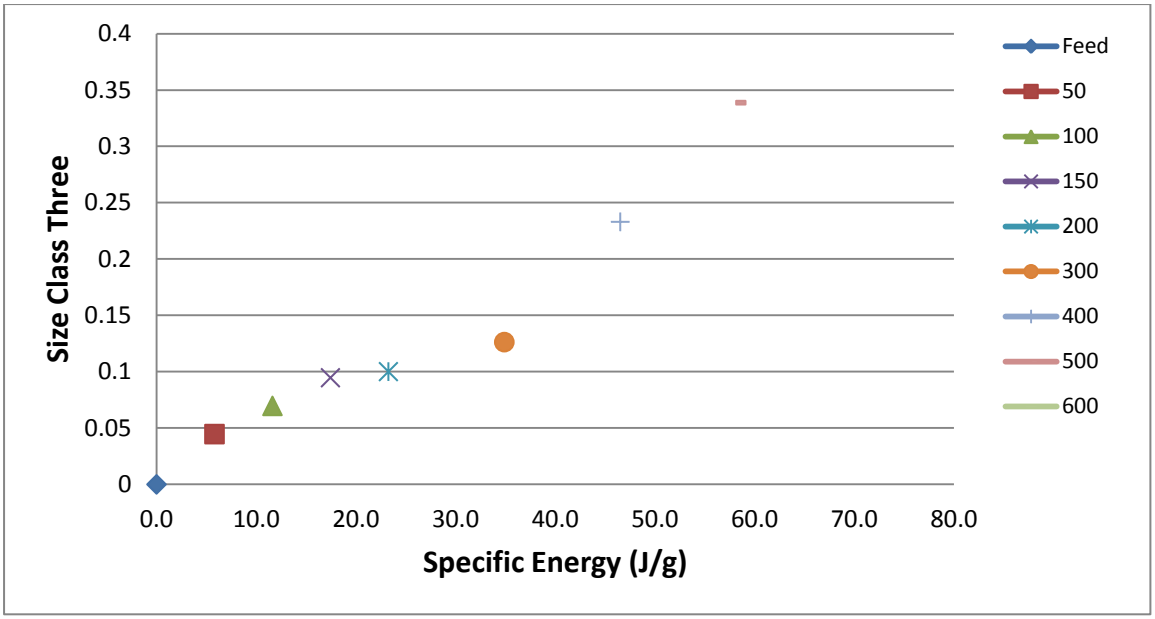

Figure D4.3 (c): Size Class Three vs. Specific Energy

9.10.4.1.4 Comparison plot for all three grinding media sizes

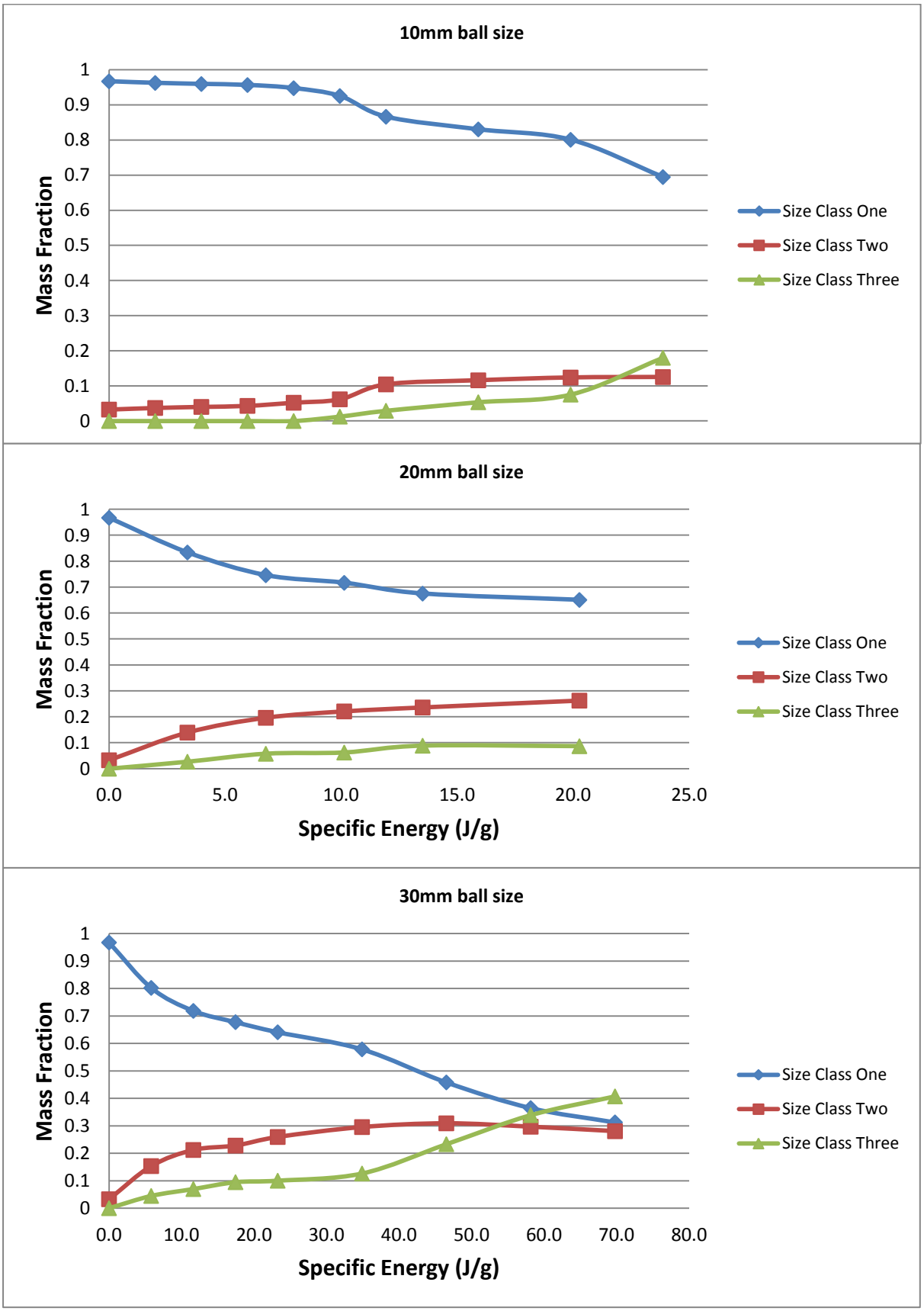

Fig D 4.4: Mass fraction vs. Specific Energy for three ball sizes.

10 APPENDIX E: Attainable Region Analysis Plots

10.1 Appendix E1: 10mm ball size plots

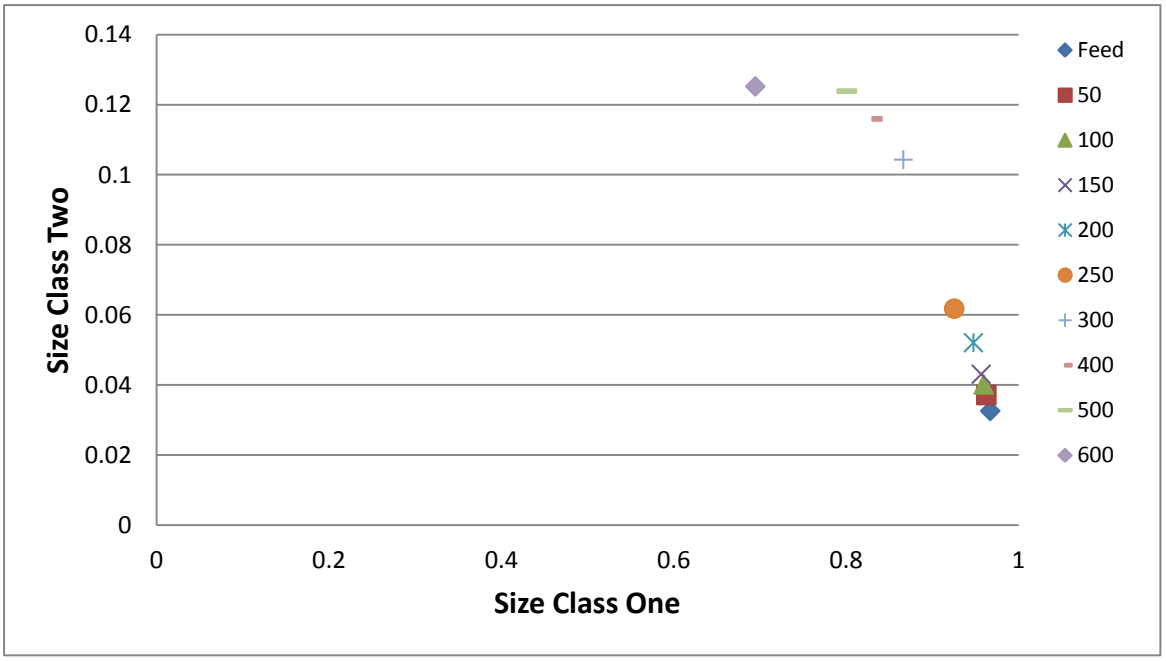

Figure E1.1 (a): Mass fraction of Size Class One vs. Size Class Two

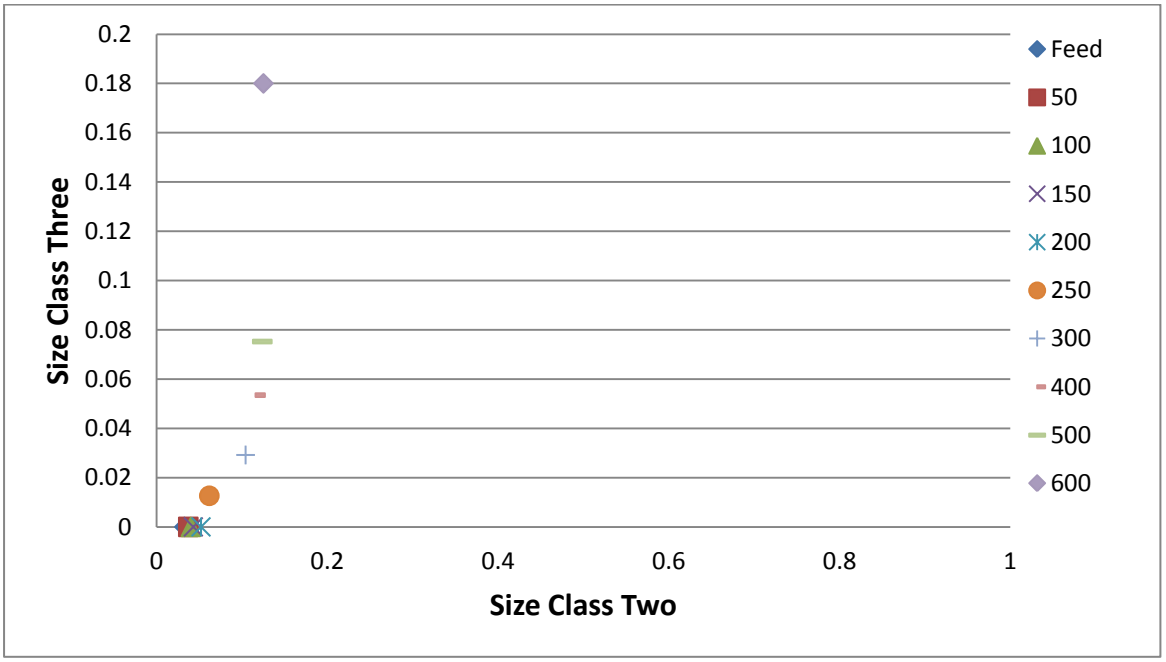

Figure E.1 (b): Mass fraction of Size Class Two vs. Size Class Three

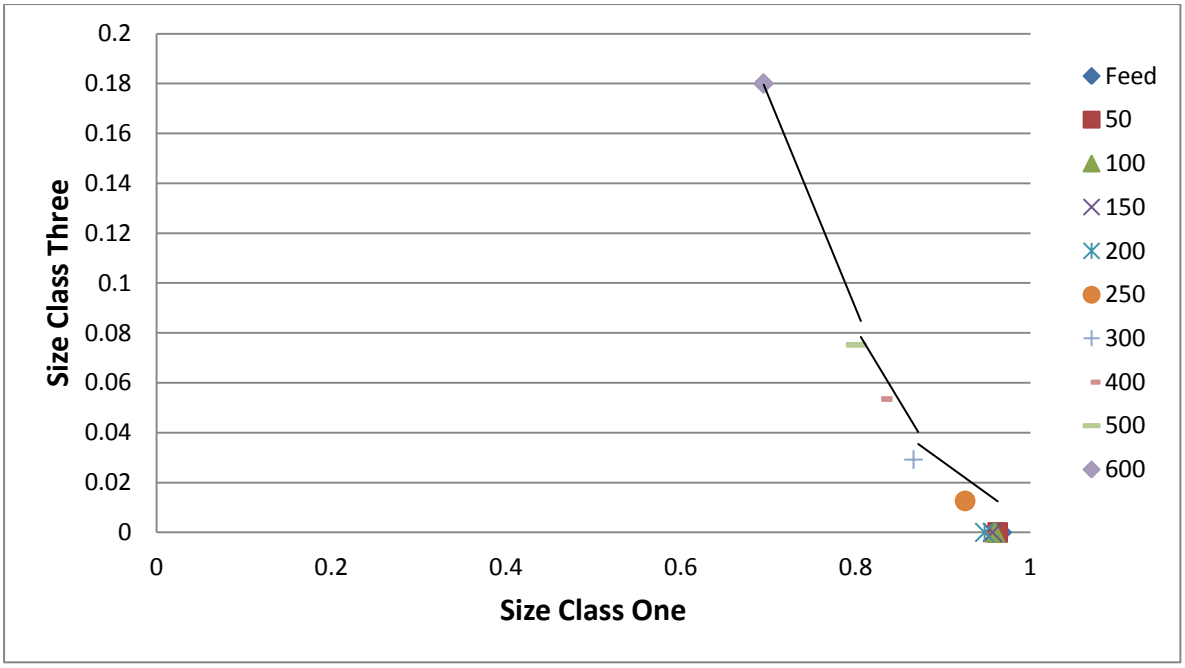

Figure E.1 (c): Mass fraction of Size Class One vs. Size Class Three

10.2 Appendix E2: 20mm ball size plots

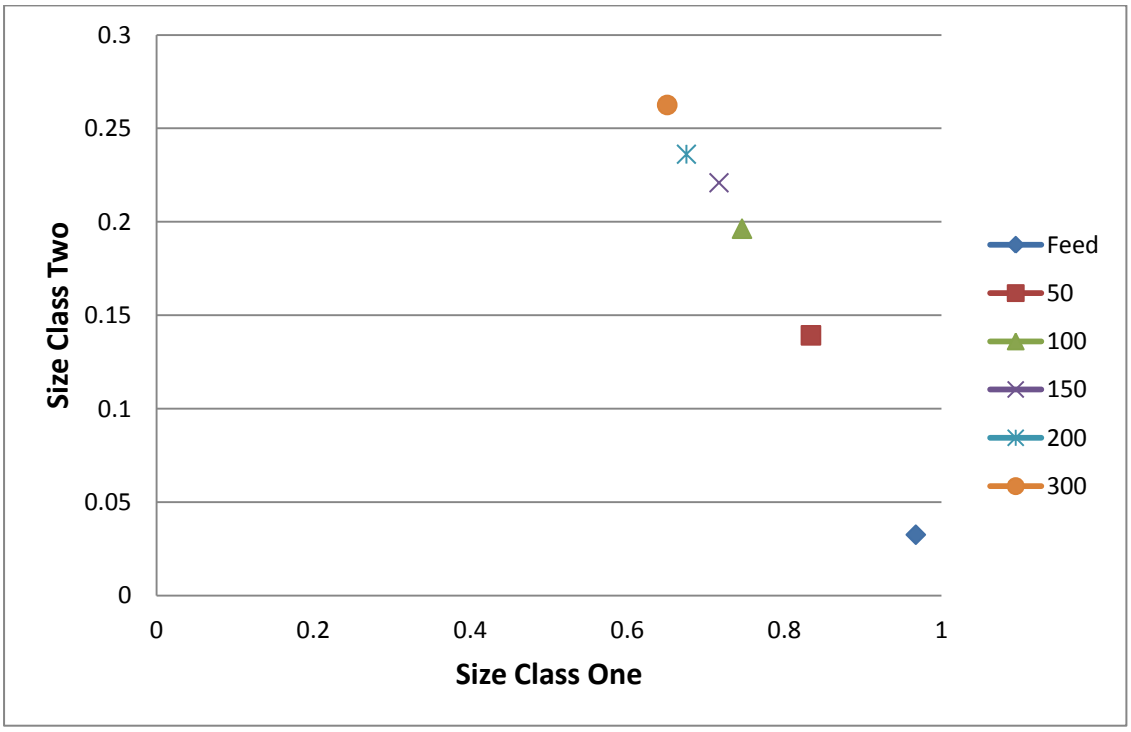

Figure E.2 (a): Mass fraction of Size Class One vs. Size Class Two

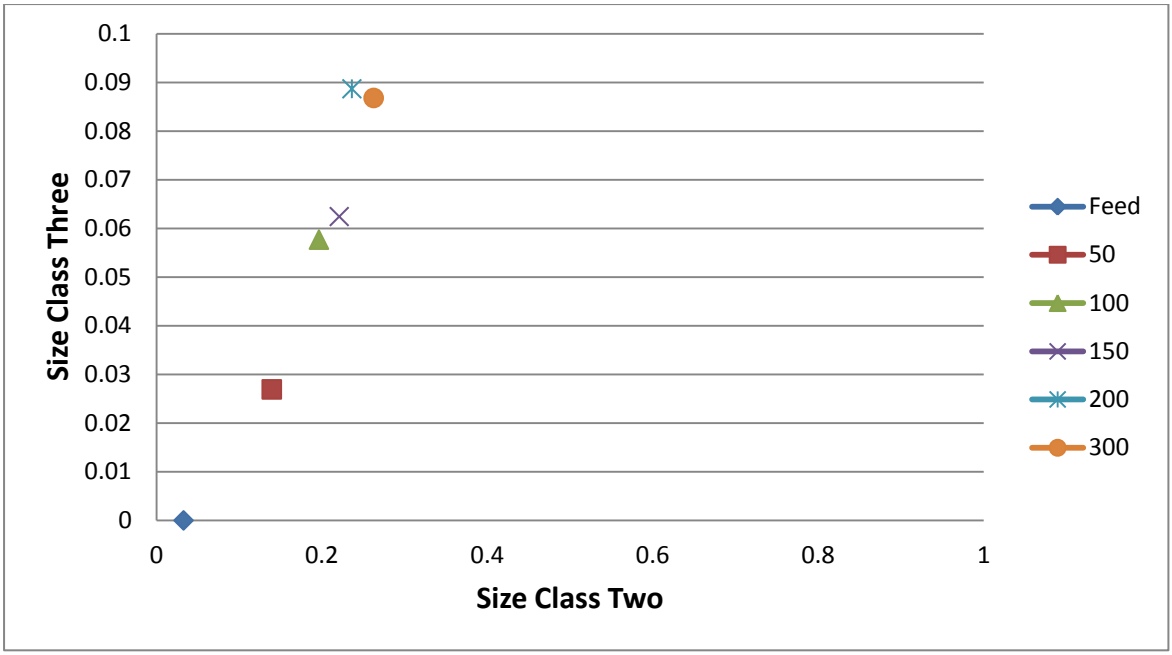

Figure E.2 (b): Mass fraction of Size Class Three vs. Size Class Two

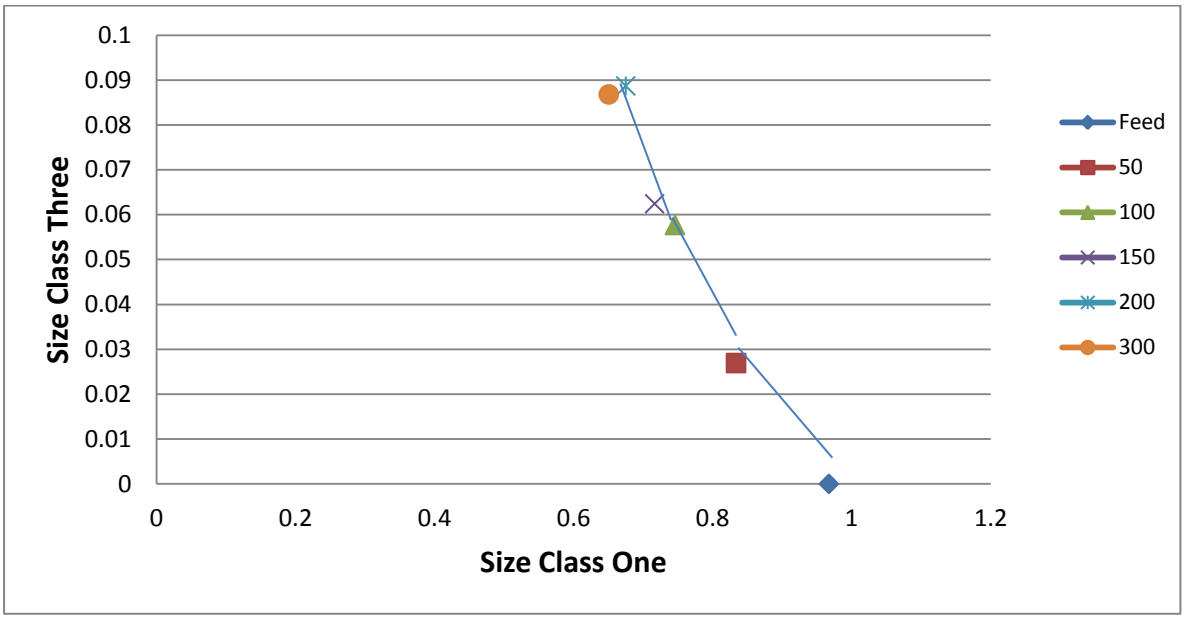

Figure E.2 (c): Mass fraction of Size Class One vs. Size Class Three.

10.3 Appendix E3: 30mm ball size plots

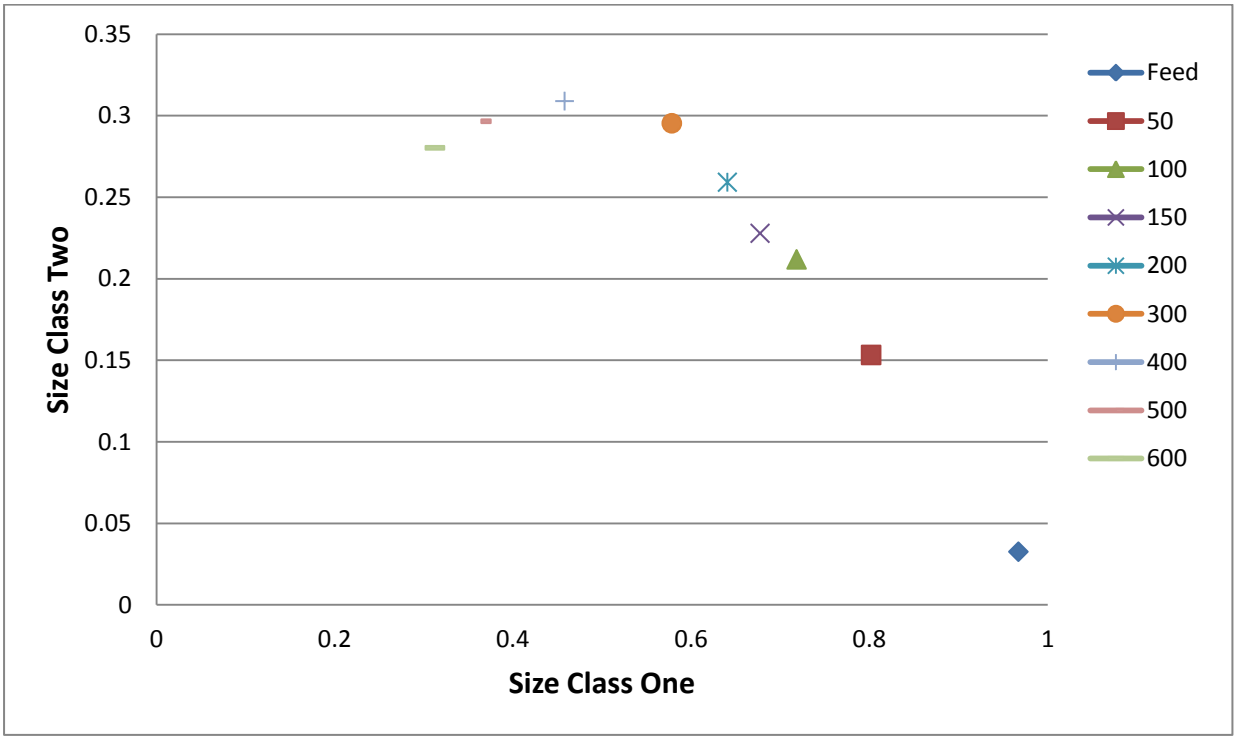

Figure E.3 (a): Mass fraction of Size Class One vs. Size Class Two

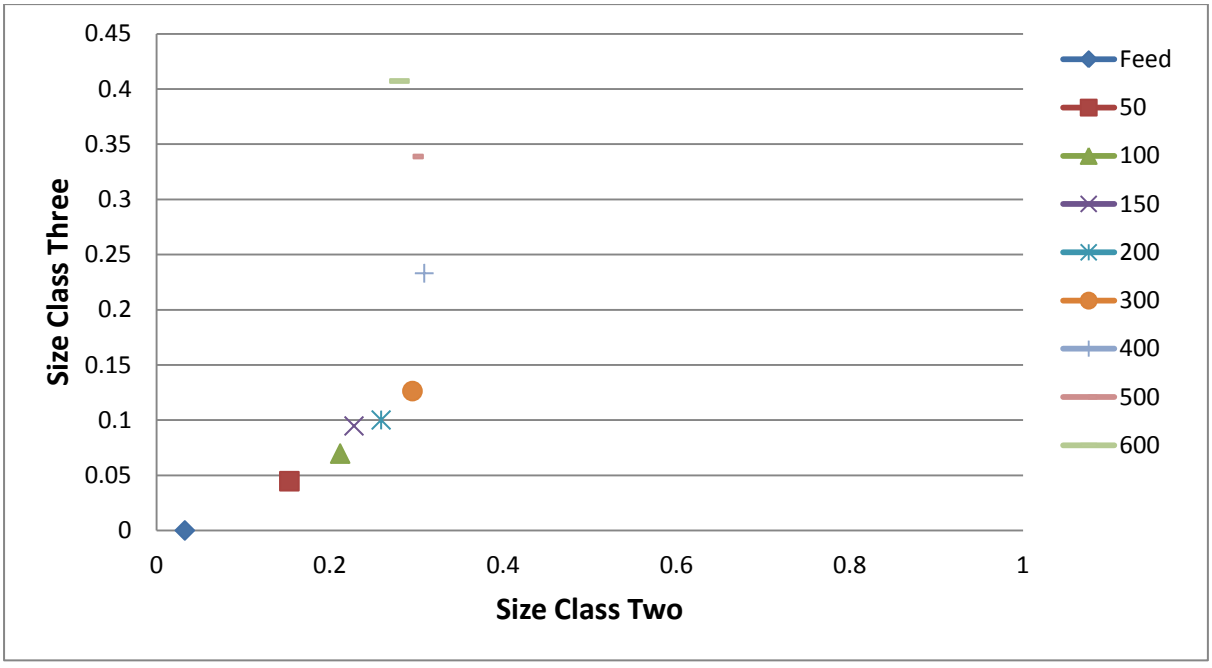

Figure E.3 (b): Mass fraction of Size Class Three vs. Size Class Two

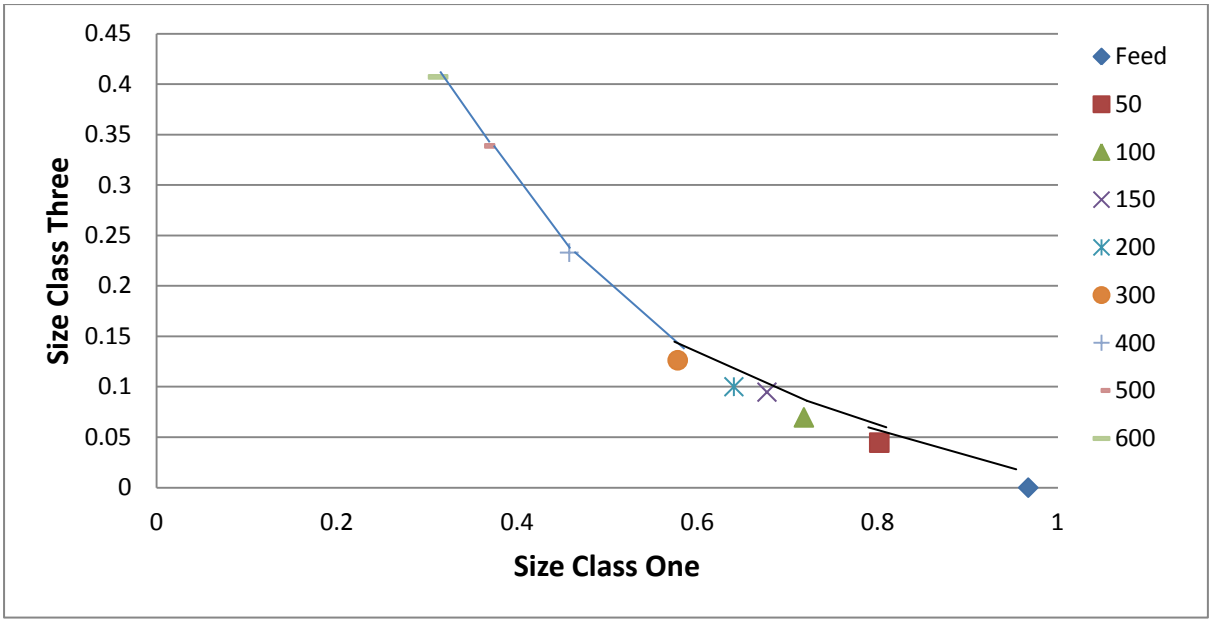

Figure E.3 (c): Mass fraction of Size Class Three vs. Size Class One for 30 mm ball size

11 APPENDIX F: Specific Energy vs Overall Size Class One Plots after 50 impacts

11.1 Appendix F1: 10 mm ball size plot

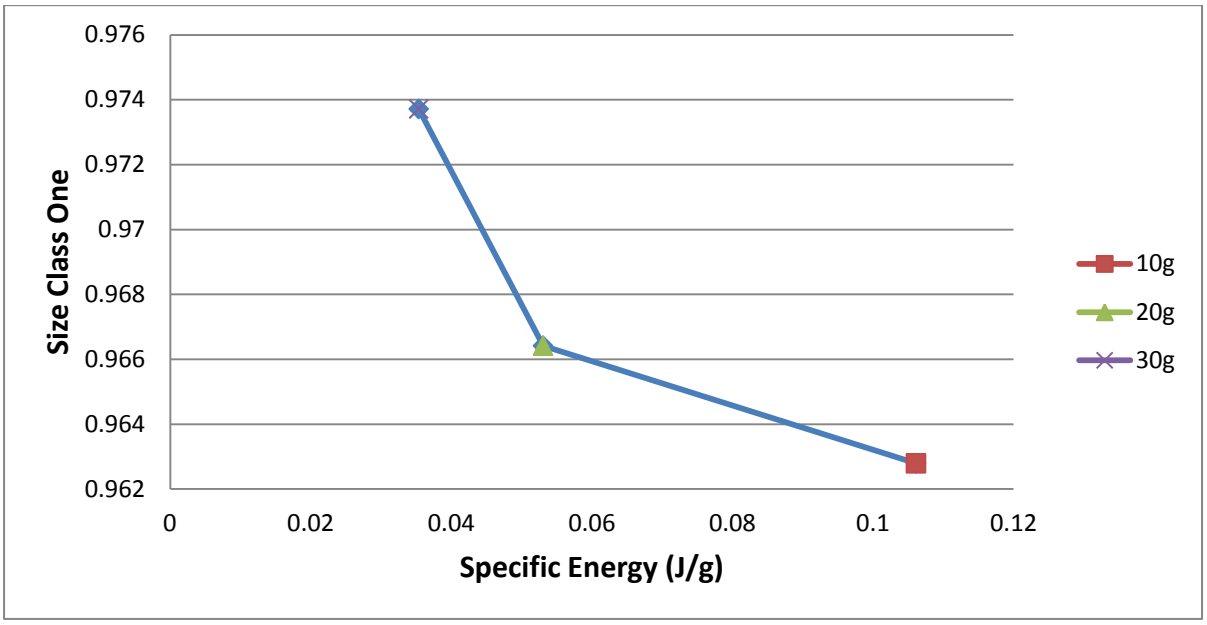

11.2 Appendix F2: 20 mm ball size plot

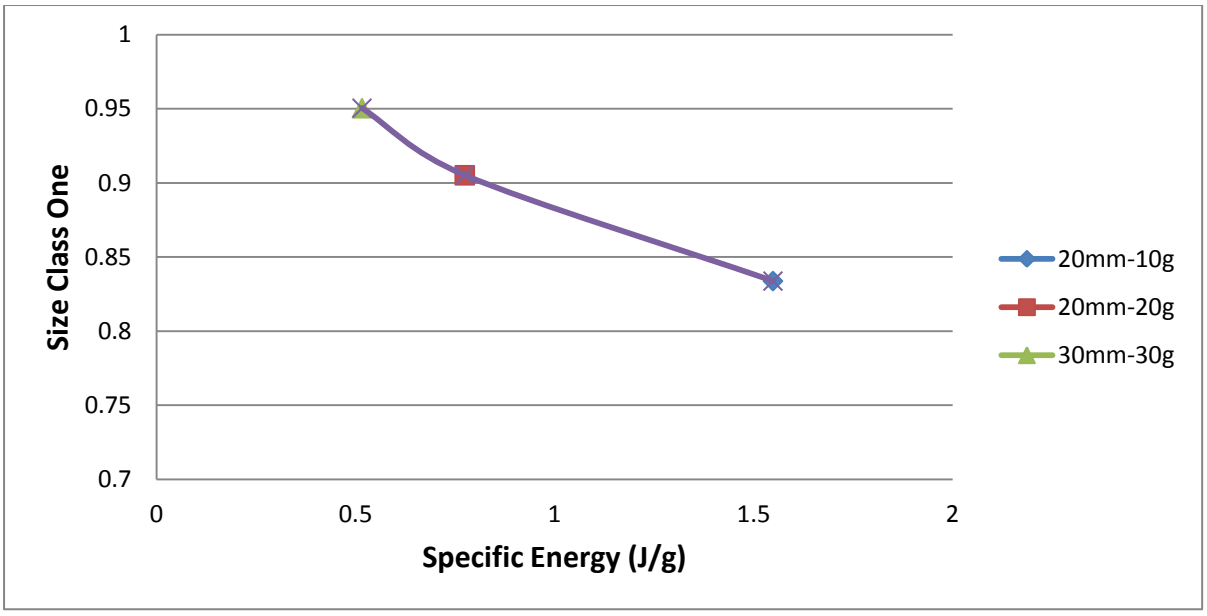

11.3 Appendix F3: 30 mm ball size plot

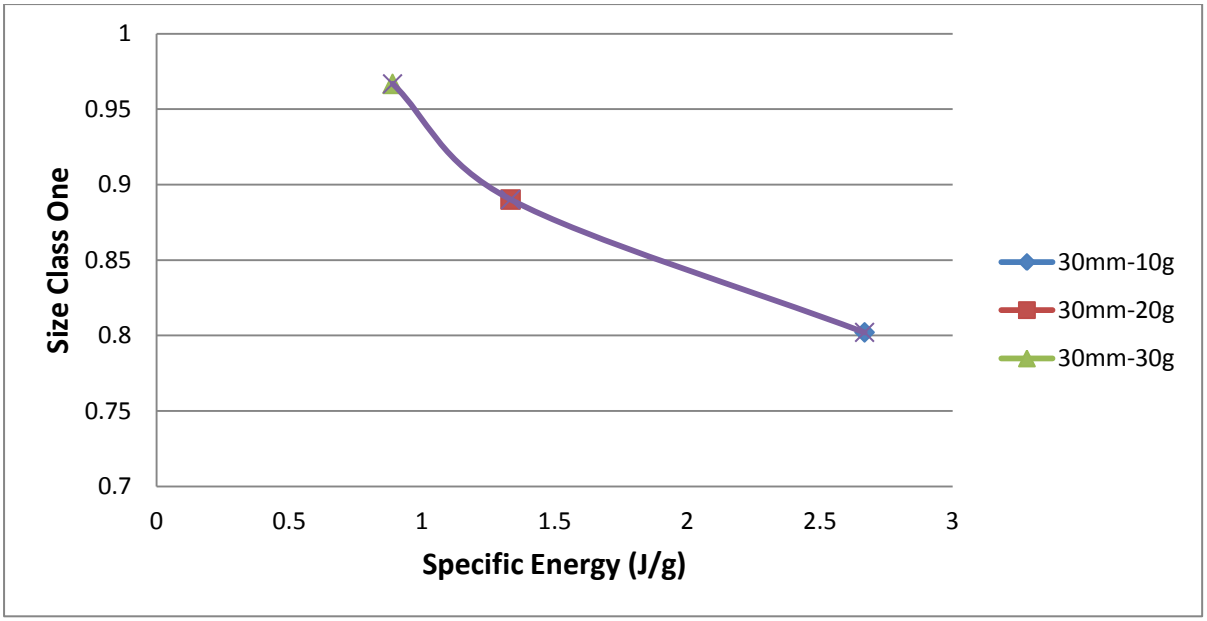

11.4 Appendix F4: Combined plot for three different grinding media sizes